«ELECTRICAL ENGINEERING & ELECTROMECHANICS»

SCIENTIFIC & PRACTICAL JOURNAL

Journal was founded in 2002 by

National Technical University «Kharkiv Polytechnic Institute»

Co-Founder – State Institution «Institute of Technical Problems of Magnetism of the NAS of Ukraine»

Адреса редакції / Editorial office address:
Кафедра "Електричні апарати", НТУ "ХПІ", вул. Кирпичова, 21, м. Харків, 61002, Україна
Dept. of Electrical Apparatus, NTU "KhPI", Kyrpychova Str., 21, Kharkiv, 61002, Ukraine
тел. / phone: +380 57 7076281, +380 67 3594696, e-mail: a.m.grechko@mail.ru (**Гречко Олександр Михайлович** / **Grechko O.M.)**

ISSN (print) 2074-272X
ISSN (online) 2309-3404

Printed 25.04.2016. Format 60 x 90 ⅛. Paper – offset. Laser printing.
Edition 200 copies. Order no.66/172-02-2016.
Design of cover by Vyrovets L.P. e-mail: vsv_2007@ukr.net
Printed by Printing house «Madrid Ltd» (11, Maksymilianivska Str., Kharkiv, 61024, Ukraine)

ELECTRICAL ENGINEERING & ELECTROMECHANICS

Scientific and practical journal

2016/2

TABLE OF CONTENTS

Electrical Engineering. Great Events. Famous Names

Electrotechnical Complexes and Systems. Power Electronics

Theoretical Electrical Engineering and Electrophysics

High Electric and Magnetic Field Engineering. Cable Engineering

Power Stations, Grids and Systems

Discussions

UDC 621.3:537.311:910.4 **doi: 10.20998/2074-272X.2016.2.01**

M.I. Baranov

AN ANTOLOGY OF THE DISTINGUISHED ACHIEVEMENTS IN SCIENCE AND TECHNIQUE. PART 31: PORTRAIT OF THE KHARKIV PHYSICIST ALEXANDER ILYICH AKHIEZER

Purpose. Description in the short form of the basic distinguished scientific achievements, features of personality and way of life of the known Kharkiv theoretical physicist A.I. Akhiezer. Methodology. Existent scientific approaches for treatment and systematization of physical knowledges. Methods of historical method at research of development in human society of basic sections of theoretical physics. Results. Short information is resulted about the basic creative and vital stages, and also fundamental scientific achievements of the indicated prominent physicist of the 20th century. Some personal qualities of this Kharkiv theoretical physicist, becoming a founder known in the world of physical school are described. Originality. First the Kharkiv scientist-electrophysicist for the wide circle of readers imagined a short scientifically-historical essay the known physicist of contemporaneity, being based on his scientific works and published materials about him. Practical value. Scientific popularization of creative activity of the known Kharkov physicist and his achievements in area of theoretical physics. Next reminder a wide reader on the example of creative life in science and got prominent scientific results of works of one human personality known in the scientific world about incessant in modern society connection of times and generations. References 33, figures 10.
Key words: **history, physics, Kharkiv region, distinguished scientific achievements.**

Приведен краткий научно-исторический очерк об известном физике-теоретике Харьковщины − академике АН УССР (НАН Украины) Ахиезере А.И. и его выдающемся вкладе в мировую физическую науку. Библ. 33, рис. 10.
Ключевые слова: **история, физика, Харьковщина, выдающиеся научные достижения.**

Introduction. In [1] the author has described portraits of eminent physicists of the «high-brigade» of the Ukrainian Physico-Technical Institute (UPTI) – A.K. Walter, K.D. Sinelnikov, A.I. Leypunsky and G.D. Latyshev, which largely can be called experimental physicists, rather than theoretical physicists. Of course, such a highly conditional approach to the division of experimental physicists, theorists and commentators not diminish the role of the aforementioned legendary Kharkiv scientists in the development of many theoretical problems in the field of nuclear physics, accelerator technology, high-energy physics and plasma technology. To achieve at the UPTI world-class scientific results from the beginning of the organization in our country, this new generation of this Physics Institute (1928) in its structure for the first time in the Soviet Union was specifically highlighted the theoretical division or structurally organized during the craze in the 1930s the so-called «theoretical brigade». The credit for the structural formation of such a purely theoretical division in UPTI belongs to its first director, the future Academician of the Academy of Sciences of the USSR (1958), Ivan Vasilyevich Obreimov (1894-1981). Thefirst head of the theoretical division of the UPTI in the period 1928-1931 was the famous Soviet physicist Dmitri Dmitrievich Ivanenko (1904-1994), the world's first proposed in 1932 by the proton-neutron model of the nucleus of an atom of matter [2, 3]. In the period 1932-1937 theoretical department of the UPTI was headed by talented Soviet physicist and future Nobel Prize winner in Physics (for 1962) Lev Davidovich Landau (1908-1968) [2, 4, 5]. After moving L.D. Landau to Moscow (1937), where he became head of the Theoretical Department of the Institute of Physical Problems (IFP) of the USSR Academy of Sciences (director of the IPP - the world-famous scientist, Academician of the Academy of Sciences of the USSR and the future winner of the Nobel Prize in Physics (1978) Petr Leonidovich Kapitsa (1894-1984) [4]), the theoretical department of the UPTI since 1938 was headed by his pupil, Ph.D. and the future Academician of the Ukrainian SSR Academy of Sciences Alexander Ilyich Akhiezer [2]. Note that at the UPTI in 1941 and the second theoretical department was created, headed by a Prof. and future Academician of the USSR Academy of Sciences Ilya Mihailovich Lifshitz (1917-1982) [2]. Employees of these theoretical divisions «shoulder to shoulder» in close scientific and industrial contacts with employees of all other departments UPTI effectively solved defined by on their decision-making bodies of the Soviet country complex scientific and technical problems in domains of priority areas of nuclear and experimental physics having mostly special (secret) character. «Pure» science staff of the UPTI theoretical departments were engaged only after the decision of the immediate tasks for the scientific support of the Institute carried out design development and manufacturing on their basis in the «metal» planned legislative solutions products. Using the form of a brief historical sketch of scientific and, to the best of their knowledge and physical abilities epistolary try to «draw» a multi-faceted portrait of the outstanding domestic theoretical physicist A.I. Akhiezer (Fig. 1) which became one of the brightest legends of Kharkiv.

Fig. 1. Outstanding Soviet and Ukrainian physicist, Doctor of Physical and Mathematical Sciences, Prof., Academician of the Ukrainian Academy of Sciences (NASU), Honored Scientist of Ukraine, laureate of State Prize of Ukraine in the field of science and technology Alexander Ilyich Akhiezer (1911-2000) [7]

The main stages of the life and career of the Kharkiv physicist. Born Akhiezer A.I. on October 31, 1911 in the city of Cherikov, Mogilev province (now Belarus), then part of the co-becoming of the Russian Empire, the son of a country doctor Ilya Alexandrovich and Natalia Grigirievna Akhiesers [6]. In 1934 he graduated from the energy department of the Kiev Polytechnic Institute, and after examination of interview on the knowledge of physics and mathematics at the captious L.D. Landau began working at the Theoretical Department of the UPTI. In 1936, A.I. Akhiezer (Fig. 2) successfully defended his PhD thesis on the study of the scattering of photons on photons at high frequencies (low frequencies for the physical event on the scattering «of light in the world» was considered much earlier prominent German physicists Leonard Euler (1707-1783) and Werner Heisenberg (1901-1976) [8]), and became Candidate of Physical and Mathematical Sciences. This scientific task in front of him was placed by his supervisor, the head of the Theoretical Division of the UPTI, Prof. L.D. Landau. By the way, A.I. Akhiezer was the third physicist, who passed to L.D. Landau «Theoretical minimum» (two examinations at special mathematics and seven examinations in the main sections of theoretical physics [4, 5]). The first physicist who passed to L.D. Landau «Theoretical minimum» was Kompaneets Alexander Solomonovich (1914-1974), and the second one - Eugene Mikhailovich Lifshitz (1915-1985) which in the future became famous Soviet theoretical physicists [6, 9]. Next, the reader's attention should be paid to worked in the 1930s at the same with A.I. Akhiezer Theoretical Department of the UPTI (period 1935-1937) Hungarian Laszlo Tisza (see Fig. 2), graduated in 1928 from the Göttingen University voluntarily come to work in one of the best in Europe at the physical science centers - UPTI and became in 1960 a professor of physics at the Massachusetts Institute of Technology (USA). Namely American survivor, Prof. L. Tisza turned to the history of development in science and technology UPTI the last of the witnesses of the turbulent time for UPTI 1930s and acting in it scientific, historical persons [7, 10].

Fig. 2. Candidate of Physical and Mathematical Sciences A.I. Akhiezer (left) and in the future the famous American physicist Laszlo Tisza (1907-2009) - employees of the theoretical department of the UPTI led by talented theoretical physicist Doctor of Physical and Mathematical Sciences, Prof. Landau (Laboratory building of the UPTI at the old institute site on the Tchaikovsky Street, 1936, Kharkiv) [7, 10]

At the end of the 1930s at the center of scientific interest of Akhiezer A.I. is the interaction of ultrasound with crystals. In 1938 he obtained a kinetic equation for a gas of quasiparticles in crystals. He developed the kinetic energy theory of sound absorption in dielectrics and metals. Designed they sound energy absorption mechanism in the crystals obtained in physics called «*Akhiezer absorption mechanism*» [6, 8, 11]. In 1940, A.I. Akhiezer on this subject successfully defended his doctoral thesis, and in 1941 became a Professor at Kharkiv State University (KSU) named after V.N. Karazin [11]. In the period 1936-1990 he taught at the Kharkiv State University named after V.N. Karazin, and in the period 1951-1964 – at the Military Radio Engineering Academy [11] In 1940 he founded the Department of Theoretical Nuclear Physics at the Physics and Mathematics Faculty of KSU named after V.N. Karazin and headed it until 1975. In the period of the military evacuation of the UPTI (1941-1943) to Alma-Ata (Kazakhstan) in parallel with the main work as the head of the Theoretical Division of the UPTI-FTI (the period 1938-1988) he was a part-time teacher at the Kazakh Mining Institute [11]. In the period 1944-1952 he was at the invitation of Academician Igor Vasilievich Kurchatov as a seconded by UPTI-PTI worked in Moscow in a special laboratory №2 (now RRC «Kurchatov Institute») to solve physical problems in the framework of the Atomic Project of the USSR [12]. As we can see, he, unlike his older brother, mathematician Naum Ilyich Akhiezer (1901-1980) [13], did not refused from the incoming suggestions from his scientific leader of this grand-scale problems to be solved and the investment of scientific and technological project, the outstanding Soviet scientist and organizer of science I.V. Kurchatov. In view of the come declassification in Russia and

Ukraine many works of the period 1940-1950s. by this secret superproject [3] and the appearance in the press and on the Internet a lot of information about them, now we can say that one of the important tasks of problem that can be solved in the «Moscow period» of work of Akhiezer A.I. (Fig. 3), was the problem of the scattering of «slow» neutrons in crystals [14]. This task Akhiezer A.I. has solved together with the talented Soviet theoretical physicist and future academician of the Academy of Sciences of the USSR Isaak Jakovlevich Pomeranchuk (1913-1966), also worked in the 1930s at the Theoretical Department of the UPTI under the leadership of the legendary Soviet theoretical physicist L.D. Landau [4]. The importance of the physical problem, successfully solved by Akhiezer A.I. and Pomeranchuk I.Ja., may indicate that it was impossible without the solution to develop and create a right to the USSR as a well-functioning nuclear reactor to produce plutonium-239 (nuclear explosives №1), and the use of uranium-235 nuclear technology (nuclear explosives №2) for the first Soviet atomic bomb [3, 14]. In addition, they (A.I. Akhiezer, I.Ja. Pomeranchuk) regardless of the outstanding Italian theoretical physicist, Nobel Prize winner in Physics (for 1938) Enrico Fermi [4] established the possibility of using certain crystalline materials (e.g., ultrapure graphite [4, 8]) «cold» neutrons, developed the theory of neutron refraction (the term «*refraction*» comes from the Latin word «*refractus*» – «*refracted*» [15]) and the neutron absorption theory in homogeneous solid media [14]. Some of the results of these studies included in their joint scientific monograph «*Some problems of the theory of the nucleus*» (1948) awarded in 1949 of the prize named after L.I. Mandelshtam of the USSR Academy of Sciences [14].

Fig. 3. Doctor of Physical and Mathematical Sciences, Prof. A.I. Akhiezer at his office of the Head of Department of Theoretical Physics of the UPTI (in the short days of arrival from Moscow to «furlough» with family and the staff of the Institute), resumed his permanent work after the difficult years of war and military evacuation in Alma-Ata (1946, UPTI-PTI, Kharkiv) [7]

Combining up to 1952 work at the UPTI-PTI (in its theoretical department and organized in 1945 on the initiative of the supervisor of the Atomic Project of the USSR, Academician of the USSR Academy of Sciences I.V. Kurchatov, under the supervision of the director of the institute, Doctor of Physical and Mathematical Sciences, Prof. Kirill Dmitrievich Sinelnikov [1] special Laboratory №1, existed in UPTI-PTI to 1950) and the Moscow special laboratory №2, led by the legendary I.V. Kurchatov and dedicated exclusively to the problems of the Soviet Atomic Project, A.I. Akhiezer extends the «field» of his scientific activity. It was to include quantum electrodynamics and elementary particle physics, nuclear physics and the theory of linear accelerators, solid state physics and magnetism, plasma physics, magnetic hydrodynamics and the theory of the interaction of charged particles with crystals [14]. Using materials of current Internet communications [6, 9-12, 16] and a number of scientific papers by Akhiezer A.I. [17-27] indicate some of them received personally and together with his favorite pupil (Fig. 4) the fundamental results in the specified areas of physics for many years during their theoretical studies.

Main scientific achievements of the Kharkiv Physics. Scientifically known in the USSR and abroad to Doctor of Physical and Mathematical Sciences, Prof., Academician of the Ukrainian Academy of Sciences A.I. Akhiezer brought his theoretical developments in the fields of physics mentioned above. Formulate in a compressed form based on published material [6, 9-12, 16-27] basic scientific achievements he received during the 1930-1990s in the field of modern physics:

- The problems of the scattering of high-energy photons on photons (quantum-physical scattering of «light on light» for the high frequencies) and coherent scattering of photons on atomic nuclei are strictly solved (co-jointly with I.Ja. Pomeranchuk, 1936-1938);
- He developed basics of a new kinetic theory of sound absorption in solids («*Akhiezer absorption mechanism*», 1938);
- The processes of dispersion and absorption of the «slow» neutrons crystal substances are investigated (co-jointly with I.Ja. Pomeranchuk, 1944-1947);
- He predicted (regardless of the unknown to him then results by E. Fermi) the possibility of obtaining stable nuclear experiments in nuclear reactors and «cold» neutrons (1944-1947);
- He introduced a new concept of magnons (spin-wave quanta) in ferrodielectrics and considered their interaction with phonons and with each other (1946);
- He predicted by calculations the electron cyclotron resonance, which is important in physics (co-jointly with L.E. Pargamanik, 1947);
- He developed the theory of resonant nuclear reactions and the theory of diffraction of the scattering of charged particles by atomic nuclei (co-jointly with I.Ja. Pomeranchuk, «*Akhiezer – Pomeranchuk model*», 1948-1949);
- He determined the terms of evolutionary and sustainability criteria of MHD waves in the medium (together with G.Ja. Lyubarskii and R.V. Polovin 1948);
- He theoretically predicted exponential growth of the

fluctuations in the plasma by an electron beam (together with Y.B. Feinberg, «*beam plasma instability*», 1949);

- He has made a significant contribution to the development of the theory of electromagnetic shock waves in plasma (1949);
- He theoretically predicted splitting diffraction deuteron (nucleus of heavy hydrogen - deuterium contains one proton and one neutron [8, 15]) (together with A.G. Sitenko, 1955);
- He predicted theoretically effect of the magnet acoustic resonance in the material recognized in the USSR as a scientific discovery №46 with priority of 1956 and confirmed experimentally (together with V.G. Baryakhtar, S.V. Peletminskii, 1956);
- He Initiated research in the Soviet Union in the new Soviet scientists to the field of physical problem tasks by electronic acoustics (1956);
- He developed the theory of absorption of ultrasound energy in metals, insulators, and magnetic crystal substance (together with GY. Lyubarskii and M.I. Kaganov, 1957);
- He studied by calculations the scattering of electromagnetic waves on plasma fluctuations (together with A.G. Sitenko and I.G. Prokhoda, 1957);
- He built a refined theory of relaxation and kinetic processes in magnetically ordered crystals of substances (1959);
- He has made significant scientific contributions to the theory of linear accelerators of electrons and heavier particles - protons and ions (co-jointly with Y.B. Feinberg, N.A. Khizhnyak, G.Y. Lyubarskii, K.D. Sinelnikov and A.K. Walter, 1950-1960-s);
- He has developed a number of theories of quantum electrodynamics, and based on these calculated radiative corrections for a number of quantum electrodynamic effects in the interaction of elementary particles of high energy (together with R.V. Polovin, 1963);
- He calculated the number of the electromagnetic characteristics of hadrons (elementary particles subject to strong physical impact - baryons and mesons [8, 15]), and summarized the quark model of the structure of elementary particles based on electromagnetic processes (together with M.P. Rekalo, 1964);
- He developed the theory of scattering of pions (elementary particles that have a mass of about 270 electron masses of peace and non-carriers of nuclear forces of interaction in the material [8, 15]) in the matter of nuclear material (jointly with I.A. Akhiezer, 1964);
- He studied theoretically the radiation processes of channeled electrons and positrons in crystals of a substance (with N.F. Shul'ga and V.F. Boldyshev, 1974-1982);
- He developed the theory of quantum electrodynamic effects of interaction of particles in crystals of a substance (with N.F. Shul'ga).

Fig. 4. Academician of the Ukrainian Academy of Sciences A.I. Akhiezer (second from left) with his students, Doctors of Science and future Ukrainian academics in the field of theoretical physics during a discussion of obtained solution of important physical problem (from left to right: V.G. Baryakhtar, S.V. Peletminskii and K.N. Stepanov) (1960, UPTI-PTI, Kharkiv) [28]

That is the main course, and not quite complete list of significant physical achievements to the world-society scientific results of academician of Ukrainian Academy of Sciences (NASU) Akhiezer A.I. for many decades his active creative work in relevant areas of modern physics mentioned above. Formulated here in a concentrated form of outstanding scientific achievements and merits of Prof. A.I. Akhiezer (Fig. 5) to our countries, the national science and higher education were awarded the following honorable marks of distinction and high state awards [6, 9, 14]:

- Medal «For Valiant Labor in the Great Patriotic War of 1941-1945» (1945);
- Prize named after L.I. Mandelshtam of the USSR Academy of Sciences (for the book «*Some Problems in Nuclear Theory*», 1949);
- Order «Badge of Honor» (1954);
- Election of Corresponding Member (1958) and Academician of the Academy of Sciences of the Ukrainian SSR (1964);
- Two Orders of Red Banner of Labor (1971 and 1981);
- Prize named after K.D. of the Academy of Sciences of the Ukrainian SSR (for a cycle of works «*High-frequency relaxation processes in magnetic materials*», 1978);
- USSR State Prize in Science and Technology (for the work «*The discovery and study of dynamic phenomena associated with phonon interactions in magnetic crystals*», 1986);
- Honorary title «Honored Worker of Science and Technology of Ukraine» (1986);
- Diploma of the Presidium of the Supreme Soviet of the Ukrainian SSR (1991);
- Prize named after N.N. Bogolyubov of the NAS of Ukraine (for the series of works «*The quantum and stochastic evolutionary system in perturbation theory*», 1995);
- Order of Ukraine «For Merits» III-rd (1996) and II-nd (1999) degrees;
- International ITEP prize named after I.Ja. Pomeranchuk of the Russian Academy of Sciences (1998);

- Prize named after A.S. Davydov of the NAS of Ukraine (for the series of works «*The interaction of high-energy particles with nuclei and crystals*», 2000);
- State Prize of Ukraine in the field of science and technology (2002, posthumously).

Fig. 5. Academician of the Ukrainian Academy of Sciences A.I. Akhiezer in thoughts on the complex issues of domestic physical science, ways of its survival and future development in the current conditions (1970, KhPTI, Kharkiv) [7]

Kharkiv scientific school of theoretical physics. Academician of the Ukrainian Academy of Sciences (NASU) Akhiezer A.I. became the founder of the Kharkiv school of physics internationally recognized [11, 14, 28]. He paid great attention to the preparation of highly qualified personnel. As part of this scientific school under the scientific guidance of Akhiezer A.I. theoretical physicists have been successfully protected more than 72 Candidate and 33 Doctor theses [9, 11]. Representatives of this famous law school have been published in leading scientific journals of the USSR, Ukraine and abroad hundreds of scientific articles and dozens of monographs. Let us discuss some of these publications. So, the first scientific monograph published by A.I. Akhiezer in 1948 at the insistence of Academician I.V. Kurchatov, was the book «*Some Problems in Nuclear Theory*» (co-authored with I.Ja. Pomeranchuk). In 1953, by A.I. Akhiezer important book «*Quantum Electrodynamics*» (co-written with V.B. Berestetskii) was published. It was the first monograph, summarized the lessons in this experience of the world The cutting area of physical science. It has been translated into many languages and reprinted many times. In addition, A.I. Akhiezer personally and co-authored with his students and colleagues published the following monographs on current topics [6, 9, 11]: «*Spin Waves*» (together with V.G. Baryakhtar and S.., Peletminskii, 1968); «*Electrodynamics of plasma*» (co-authored with I.A. Akhiezer, R.V. Polovin, A.G. Sitenko and K.N. Stepanov, 1974); «*The course of general physics. Mechanics and molecular physics*» (co-authored by L.D. Landau and E.M. Lifshitz, 1969); «*Methods of Statistical Physics*» (co-authored with S.V. Peletminskii, 1977); «*Electrodynamics of adrons*» (co-authored by M.P. Rekalo, 1977); «*Biography of elementary particles*» (co-authored by M.P. Rekalo, 1983); «*Electromagnetism and electromagnetic waves*» (co-authored with I.A. Akhiezer, 1985); «*Fields and fundamental interactions*» (jointly with S.V. Peletminskii, 1986); «*Nuclear Physics*» (1988); «*Electrodynamics of nuclei* « (co-authored with A.G Sitenko and V.K. Tartakovsky, 1989); «*The theory of fundamental interactions*» (in collaboration with S.V. Peletminskii, 1993); «*From the rays of light to the colored quarks*» (co-authored with J.P. Stepanovski, 1993); «*Electrodynamics of high-energy matter*» (co-authored with N.F. Shul'ga, 1993); «*Nuclear Theory*» (co-authored with Yu.A. Berezhnoj, 1995); «*Introduction to the theory of the multiplier systems (reactors)*» (co-authored with I.Ja. Pomeranchuk, 2002), and others.

A number of students of Akhiezer A.I. became academicians and corresponding members of the Ukrainian SSR Academy of Sciences (NASU) [2, 6, 11]: V.G. Baryakhtar, D.V. Volkov, E.A. Kuraev, S.V. Peletminskii, A.G. Sitenko, N.F. Shul'ga, Yu.B. Feinberg, P.I. Fomin, K.N. Stepanov, etc. We also point out the fact that at present Academician of the National Academy of Sciences of Ukraine Victor Grigirievich Baryakhtar (see Fig. 4) leads the Institute of Magnetism, National Academy of Sciences of Ukraine (Kyiv), Academician of the National Academy of Sciences of Ukraine Nikolai Fedorovich Shu'lga - Institute for Theoretical Physics named after A.I. Akhiezer of the NSC «KhPTI» NAS of Ukraine (Kharkiv), created on January 31 1996 on the basis of Presidential Decree of 23 June 1993 [2, 29]. The name of Academician of NASU A.I. Akhiezer to the Institute for Theoretical Physics - ITF) was awarded the corresponding resolution of the Cabinet of Ministers of Ukraine in 2003.

Numerous students, the scientific community of the KhPTI-UPTI and leading universities of Kharkov, which is one of the largest centers of education and science of Ukraine, warmly welcomed the outstanding theoretical physicist of our time, academician of Ukrainian Academy of Sciences (NASU) Akhiezer A.I. in the jubilee celebrations of its 60th, 70th and 80th birthday, continued to actively work in the workplace (Fig. 6, 7) [30, 31]. Fig. 8 sealed with friends on the life and work together, theoretical physicists KhPTI, Academy of Sciences of the Ukrainian SSR A.I. Akhiezer and D.V. Volkov, has done much for the formation of the Kharkov school of theoretical physics, the development of physical science in the USSR and Ukraine and to strengthen their defense capability [9].

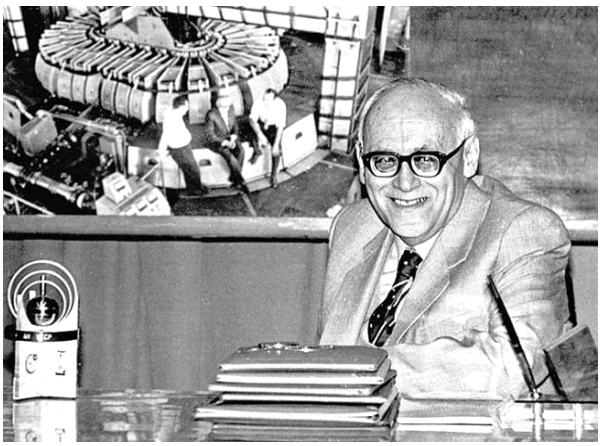

Fig. 6. Science master, Academician of the Academy of Sciences of the Ukrainian SSR A.I. Akhiezer accepting congratulations from colleagues on the day of celebration of its 70th anniversary and the solemn meeting on this important for the scientific community of the anniversary event of the Academic Council of the KhPTI (October 1981 KhPTI, Kharkiv) [7]

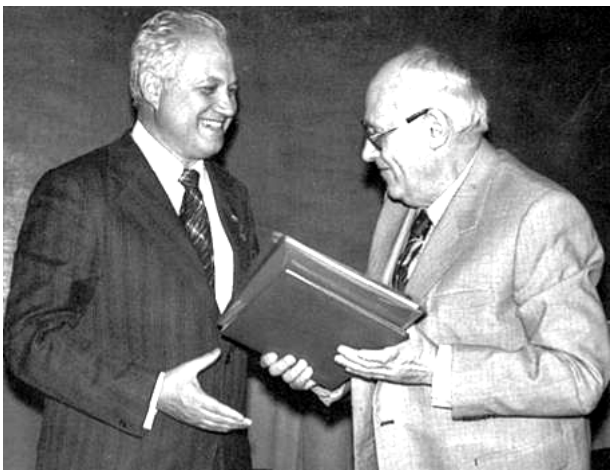

Fig. 7. Academician of the Ukrainian Academy of Sciences Akhiezer A.I. (right) at a meeting of the Academic Council of the KhPTI accepts congratulations on the occasion of his 70th birthday (anniversary address to his teacher presents his talented student-Academician of the Academy of Sciences of the Ukrainian SSR Baryakhtar V.G. (left), October 1981, KhPTI, Kharkiv) [28]

Fig. 8. Kharkiv theoretical physicists, academicians of the Academy of Sciences of the Ukrainian SSR Akhiezer A.I. (left) and Volkov D.V. (right) in their office at the KhPTI laboratory building on the old site of the Institute on the Tchaikovsky Street during discussion materials of a new problem task (1991, Kharkiv) [7]

After retiring to the well-deserved retirement home and rest, Alexander Ilyich, despite his practical blindness in the late 1990s (made surgery his vision is not saved), thanks to a clear mind, his technical secretary while her own daughter Zoya Alexandrovna Spolnik constantly supported human and scientific contacts with his native ITF NSC «KhPTI» of the National Academy of Sciences of Ukraine (above all, with his faithful disciples, and who became well-known scientists – S.V. Peletminskii, N.F. Shul'ga and K.N. Stepanov) [28, 32]. Fig. 9 shows one such case involving Academician of the NASU A.I. Akhiezer at the KhPTI in the celebrations on the occasion of the 90th anniversary of the birth of Lev Davidovich Landau [28].

Fig. 9. Academician of the National Academy of Sciences of Ukraine A.I. Akhiezer at a meeting of the Academic Council of the KhPTI shares his memories of the great theoretical physicist of our time, and his teacher Lev Davidovich Landau, 90-year anniversary of the birth of which were dedicated to the solemn gathering data Institute of scientific and technical community, universities and Kharkiv as a whole (January 1998, KhPTI, Kharkiv) [7]

Features of the personality and lifestyle of the Kharkiv physicist. American theoretical physicist, Prof. L. Tisza (1907-2009) who worked in the 1930s together with A.I. Akhiezer at the theoretical department of the UPTI, headed by then L.D. Landau, in his memoirs of 2001 as one of the «old» witness of our hero-scientist noted after-following [10]: *«... He has kept the tradition of LD Landau in both quality and breadth of applications in all areas of theoretical physics. L.D. Landau, obviously proud of them.* « Remembering his teacher, academician of Ukrainian Academy of Sciences (NASU) A.I. Akhiezer, its talented students, academicians of the NASU V.G. Baryakhtar (born in 1930) and S.V. Peletminskii (born in 1931) said [28, 33]: «*... He was a wonderful teacher, he was a teacher who knew all of physics, he was strict and demanding teacher, and he loved us as his children.*» Alexander Ilyich disciples often commemorated [28]: *«... We have to work as hard and very carefully considered presentation of the results. It is necessary to carefully choose the place of their publication. Must be able to listen to criticism of opponents.* « He was considerate to their employees (Fig. 10), defended their leading lights in all offices and able to appreciate them. He constantly planted them the

following principles of scientific research [28]: «*To master a new research technique. Have the courage to abandon their results, even if you have already received the approval of the classics of natural science. Be able to appreciate the discussions with colleagues.* « Teaching at KSU-KNU named after V.N. Karazin and the Military Radio Engineering Academy Alexander Ilyich was a holy thing throughout his life. By teaching activities and he drew his venerable pupils [28]. He loved the young student and loved to lecture for it [16, 28]. Communication of A.I. Akhiezer with students always gave him considerable pleasure. In the circle of colleagues, he stuck to the rigid position of principle [28]: *«... If you do not like students, you have to throw a teaching job immediately. It is impossible to assert itself on the students. It is immoral*». Alexander Ilyich was a demanding teacher of high school. It is extremely transparent and available to explain complex material to their students. He said that it is necessary to explain the material [16]: *«... In the workers and peasants, so that the proletariat was clear.*» He loved a good joke and humor. Jokes have been a part of his lectures. This scientist made his memorable lecture. He believed that «sometimes it is necessary to give a student a break from the note-taking, so you must do in the lecture breaks the story of a joke or a story of life» [16]. Used in its vocabulary a long time memorable utterances [16]: «*What field is quantized, still get ... zero!*» Too good for students and colleagues Alexander Ilyich was not.

Fig. 10. One of the last photos of lifetime of Academician of the NASU Akhiezer A.I. on his birthday, October 31, 1999, made in the work on the site of the old office of the scientist at the KhPTI, Tchaikovsky Street (from left to right: A.P. Rekalo, N.F. Shul'ga, A.A. Yatsenko, L.N. Davydov, A.I. Akhiezer, Z.A. Spolnik - daughter of Alexander Ilyich Akhiezer, L.G . Zazunov, S.V. Peletminskii, K.N. Stepanov and A.N. Akhiezer - son of mathematician Naum Ilyich Akhiezer) [7, 28]

He «*did not suffer any falsehood, sometimes he was ready to literally crush the interlocutor. Usually good-natured Akhiezer was able to demonstrate uncompromising-ness and stiffness* « [16]. Careerism Alexander Ilyich never differed. An important finishing touch to his portrait is that he «*never tried to be sure to enter themselves in the co-authors of the work and did not go on the necks of graduate students*» [16]. He was interested not only in physics. He was interested in any achievements of scholars of natural sciences. He showed great interest in the biographies of famous scientists around the scientific world. Alexander Ilyich knew Russian and foreign classical literature. He loved and highly appreciated classical music [16]. His favorite work in the field you specified earlier for the urgent and complex society for the study of modern physics sections was the main purpose of the whole of his long life and successful scientific work. According to the memoirs mentioned just above close to him in the human spirit of his favorite students, academics [28, 33]: *«... He never engaged in advertising their work, their results «never puffed out his cheeks», and could not stand people who «inflate» cheeks. He never betrayed the interests of science, education, interests, and, of course, friends.* « Friends, colleagues, relatives were with him - this outstanding Ukrainian scientist-physicist and a remarkable man to his last breath, and physical presence in our earthly life.

REFERENCES

1. Baranov M.I. An anthology of the distinguished achievements in science and technique. Part 28: Portraits of legendary physicists of «high-voltage brigade» of UPhTI. *Elektrotekhnika i elektromekhanika – Electrical engineering & electromechanics*, 2015, no.5, pp. 3-17. (Rus).

2. Available at: http://kipt.kharkov.ua/itp.html (accessed 21 May 2012). (Rus).

3. Baranov M.I. *Antologiia vydaiushchikhsia dostizhenii v nauke i tekhnike: Monografiia v 2-kh tomakh. Tom 1.* [An anthology of outstanding achievements in science and technology: Monographs in 2 vols. Vol.1]. Kharkov, NTMT Publ., 2011. 311 p. (Rus).

4. Baranov M.I. *Izbrannye voprosy elektrofiziki: Monografija v 2-h tomah. Tom 1: Elektrofizika i vydajushhiesja fiziki mira* [Selected topics electrophysics: Monographs in 2 vols. Vol.1: Electrophysics and outstanding physics of the world]. Kharkov, NTU «KhPI» Publ., 2008. 252 p. (Rus).

5. Baranov M.I. Lev Davidovich Landau (1908-1968 yy.). *Gazeta* «*Politekhnik*» − *Newspaper* «*Politekhnik*», 2008, no.1-2, pp. 3-4. (Rus).

6. *Akhiezer Aleksandr Il'ich* (Akhiezer Aleksandr Il'ich) Available at: https://ru.wikipedia.org/wiki/Akhiezer,_Aleksandr_Il'ich (accessed 15 June 2012). (Rus).

7. Available at: http://www.kipt.kharkov.ua/itp/akhiezer/ru/photo (accessed 10 April 2014). (Rus).

8. Kuz'michev V.E. *Zakony i formuly fiziki* [Laws and formulas of physics]. Kiev, Naukova Dumka Publ., 1989. 864 p. (Rus).

9. Available at: http://www.quickiwiki.com/ru/Aleksandr_Il'ich Akhiezer (accessed 21 May 2012). (Rus).

10. Available at: http://www.kipt.kharkov.ua/itp/akhiezer/ru/about/tisza (accessed 10 May 2013). (Rus).

11. Available at: http://dic.academic.ru/dic.nsf/ruwiki/277240 (accessed 22 February 2010). (Rus).

12. Available at: http://cendomzn.ucoz.ru/index/0-30108 (accessed 21 April 2008). (Rus).

13. Baranov M.I. An anthology of the distinguished achievements in science and technique. Part 27: Portrait of the Kharkov mathematician Naum Il"ich Akhiezer. *Elektrotekhnika i elektromekhanika – Electrical engineering & electromechanics*, 2015, no.4, pp. 3-6. (Rus).

14. Available at: http://ufn.ru/ufn92/ufn92_2/Russian/r922g.pdf (accessed 18 September 2013). (Rus).

15. *Bol'shoj illjustrirovannyj slovar' inostrannyh slov* [Large illustrated dictionary of foreign words]. Moscow, Russkie slovari Publ., 2004. 957 p. (Rus).

16. Available at: http://smart.kyivstar.ua/books/10961/read/7#2 (accessed 11 May 2011). (Rus).

17. Akhiezer A.I., Pomeranchuk I.Ya. Diffraction scattering of fast neutrons and charged particles. *Uspehi fizicheskih nauk – Successes of physical sciences*, 1949, no.10, Vol.39, pp. 153-200. (Rus).

18. Akhiezer A.I., Feinberg Ya.B. Slow electromagnetic waves. *Uspehi fizicheskih nauk − Successes of physical sciences*, 1951, no.7, Vol.44, pp. 321-368. (Rus).
19. Akhiezer A.I., Polovin R.V. Elimination of divergences in quantum electrodynamics. *Uspehi fizicheskih nauk − Successes of physical sciences*, 1953, no.9, Vol.51, pp.3-40. (Rus). **doi: 10.3367/ufnr.0051.195309a.0003**.
20. Akhiezer A.I., Pomeranchuk I.Ya. Diffraction phenomena in collisions of fast particles with nucleus. *Uspehi fizicheskih nauk − Successes of physical sciences*, 1958, no.8, Vol.65, pp. 593-630. (Rus). **doi: 10.3367/ufnr.0065.195808b.0593**.
21. Akhiezer A.I., Bar'yakhtar V.G., Kaganov M.I. Spin waves in ferromagnets and antiferromagnets. *Uspehi fizicheskih nauk − Successes of physical sciences*, 1960, no.8, Vol.71, pp. 533-579. (Rus). **doi: 10.3367/ufnr.0071.196008a.0533**.
22. Akhiezer A.I., Polovin R.V. Criteria growth of the waves. *Uspehi fizicheskih nauk − Successes of physical sciences*, 1971, no.6, Vol.104, pp. 185-200. (Rus). **doi: 10.3367/ufnr.0104.197106a.0185**.
23. Akhiezer A.I., Rekalo M.P. The electric charge of elementary particles. *Uspehi fizicheskih nauk − Successes of physical sciences*, 1974, no.11, Vol.114, pp. 487-508. (Rus). **doi: 10.3367/ufnr.0114.197411d.0487**.
24. Akhiezer A.I., Shul'ga N.F. The radiation of relativistic particles in single crystals. *Uspehi fizicheskih nauk − Successes of physical sciences*, 1982, no.8, Vol.137, pp. 561-604. (Rus). **doi: 10.3367/ufnr.0137.198208a.0561**.
25. Akhiezer A.I., Shul'ga N.F. The effect of multiple scattering on the radiation of relativistic particles in amorphous and crystalline media. *Uspehi fizicheskih nauk − Successes of physical sciences*, 1987, no.3, Vol.151, pp. 385-424. (Rus). **doi: 10.3367/ufnr.0151.198703a.0385**.
26. Akhiezer A.I., Krasil'nikov V.V., Peletminskiy S.V., Yatsenko A.A. The theory of superfluid Fermi-liquid. *Uspehi fizicheskih nauk − Successes of physical sciences*, 1993, no.2, Vol.163, pp. 1-32. (Rus). **doi: 10.3367/ufnr.0163.199302a.0001**.
27. Akhiezer A.I., Shul'ga N.F., Truten' V.I., Grinenko A.A., Syshchenko V.V. Dynamics of high energy charged particles in straight and bent crystals. *Uspehi fizicheskih nauk − Successes of physical sciences*, 1995, no.10, Vol.165, pp. 1165-1192. (Rus). **doi: 10.3367/ufnr.0165.199510c.1165**.
28. Available at: http://www.kipt.kharkov.ua/itp/akhiezer/ru/about/baryakhtar-peletminskiy (accessed 15 July 2010). (Rus).
29. Khramov Yu.A. *Istoriia fiziki* [History of Physics]. Kiev, Feniks Publ., 2006. 1176 p. (Rus).
30. Ivanov V.E., Feinberg Ya.B., Sitenko A.G., Lyubarskiy G.Ya., Beresteckiy V.B., Volkov D.V., Peletminskiy S.V., Polovin R.V., Stepanov K.N. Alexander Il'ich Akhiezer (On his sixtieth birthday). *Uspehi fizicheskih nauk − Successes of physical sciences*, 1971, no.10, Vol.105, pp.371-372. (Rus). **doi: 10.3367/ufnr.0105.197110l.0371**.
31. Bar'yakhtar V.G., Volkov D.V., Zelenskiy V.F., Lazarev B.G., Peletminskiy S.V., Sitenko A.G., Stepanov K.N., Feinberg Ya.B., Fomin P.I. Alexander Il'ich Akhiezer (On his eightieth birthday). *Uspehi fizicheskih nauk − Successes of physical sciences*, 1992, no.2, Vol.162, pp.191-192. (Rus). **doi: 10.3367/ufnr.0162.199202g.0191**.
32. Available at: http://www.kipt.kharkov.ua/itp/akhiezer/ru/about/stepanov (accessed 22 May 2012). (Rus).
33. Bar'yakhtar V.G., Lazarev B.G., Lapshin V.I., Peletminskiy S.V., Sitenko A.G., Stepanov K.N., Feinberg Ya.B., Fomin P.I., Shul'ga N.F., Bolotovskiy B.M., Ioffe B.L., Feinberg E.L. In memory of Alexander Il'ich Akhiezer. *Uspehi fizicheskih nauk − Successes of physical sciences*, 2000, no.8, Vol.170, pp. 917-918. (Rus). **doi: 10.3367/ufnr.0170.200008h.0917**.

Received 17.08.2015

M.I. Baranov, Doctor of Technical Science, Chief Researcher,
Scientific-&-Research Planning-&-Design Institute «Molniya»
National Technical University «Kharkiv Polytechnic Institute»,
47, Shevchenko Str., Kharkiv, 61013, Ukraine,
phone +38 057 7076841, e-mail: eft@kpi.kharkov.ua

How to cite this article:
Baranov M.I. An antology of the distinguished achievements in science and technique. Part 31: Portrait of the Kharkiv physicist Alexander Ilyich Akhiezer. *Electrical engineering & electromechanics*, 2016, no.2, pp. 3-10. doi: 10.20998/2074-272X.2016.2.01.

UDC 621.3 **doi: 10.20998/2074-272X.2016.2.02**

G.G. Zhemerov, D.V. Tugay

COMPONENTS OF TOTAL ELECTRIC ENERGY LOSSES POWER IN PQR SPATIAL COORDINATES

Purpose. *To obtain relations determining the components of the total losses power with p-q-r power theory for three-phase four-wire energy supply systems, uniquely linking four components: the lowest possible losses power, losses power caused by the reactive power, losses power caused by the instantaneous active power pulsations, losses power caused by current flowing in the neutral wire.* ***Methodology.*** *We have applied concepts of p-q-r power theory, the theory of electrical circuits and mathematical simulation in Matlab package.* ***Results.*** *We have obtained the exact relation, which allows to calculate the total losses power in the three-phase four-wire energy supply system using three components corresponding to the projections of the generalized vectors of voltage and current along the pqr axis coordinates.* ***Originality.*** *For the first time, we have established a mathematical relationship between spatial representation of instantaneous values of the vector components and the total losses power in the three-phase four-wire energy supply systems.* ***Practical value.*** *We have elucidated an issue that using the proposed methodology would create a measuring device for determining the current value of the components of total losses power in three-phase systems. The device operates with measuring information about instantaneous values of currents and voltages.* References 15, tables 1, figures 3.

Key words: **energy supply system, p-q-r power theory, the minimum possible losses, total losses power, Matlab-model of the three-phase energy supply system**..

Цель. *Целью статьи является получение соотношений для определения составляющих суммарной мощности потерь с использованием p-q-r теории мощности для трехфазных четырехпроводных систем электроснабжения, однозначно связывающих четыре компоненты: минимально возможную мощность потерь; мощность потерь, обусловленную реактивной мощностью; мощность потерь, обусловленную пульсациями мгновенной активной мощности; мощность потерь, обусловленную протеканием тока в нулевом проводе.* ***Методика.*** *Для проведения исследований использовались положения p-q-r теории мощности, теория электрических цепей, математическое моделирование в пакете Matlab.* ***Результаты.*** *Получено точное расчетное соотношение, позволяющее рассчитать суммарную мощность потерь в трехфазной четырехпроводной системе электроснабжения через три составляющие, соответствующие проекциям обобщенных векторов тока и напряжения на оси pqr системы координат.* ***Научная новизна.*** *Впервые установлена математическая связь между пространственным векторным представлением мгновенных величин и составляющими мощности суммарных потерь в трехфазных четырехпроводных системах электроснабжения.* ***Практическое значение.*** *Использование предложенной методики позволит создать измерительный прибор для определения текущего значения составляющих мощности суммарных потерь в трехфазных системах, оперирующий измерительной информацией о мгновенных значениях токов и напряжений.* Библ. 15, табл. 1, рис. 3.

Ключевые слова: **система электроснабжения, p-q-r теория мощности, минимально возможные потери, мощность суммарных потерь, Matlab-модель трехфазной системы электроснабжения.**

Introduction. The development of the modern theories of instantaneous active and reactive power in 1983, 1984 [1, 2] has allowed experts in the area of electrical engineering to change their views on such concepts as «reactive power», «apparent power», «unbalance power», «distortion power» [1-5]. On the basis of new theories the active filter control devices methods for energy supply systems (ESS), using the conversion of spatial coordinate systems were further developed, which opened up new directions and was the development of power electronics. The developed theories, operating with spatial vectors of currents and voltages, among which are the p-q theory, improved p-q theory of power, i_d-i_q method, cross-vector theory and p-q-r theory of instantaneous power [6-9], inspired the creation of conversion system control algorithms with near to unity power factor. [10] The principal possibility of the energy efficiency increasing of the ESS with nonlinear consumers at the connection of the power active filter (PAF) is shown [6, 10, 11, 15]. Currently there is no completed general theory linking the losses of electrical energy in the ESS with the provisions of the modern theories of instantaneous active and reactive power. Improving the energy efficiency of energy supply systems by PAF measures for specific operation modes solves a number of practical problems, such as determining the need for and the installation location of the power compensator, the creation of active power filter control algorithms, ensuring the work of distributed energy supply systems with the highest possible efficiency.

The goal of the paper is to develop the principles of the modern theories of instantaneous active and reactive power and to obtain calculation relations for determining the components of the additional electrical energy losses power in three-phase ESS by using pqr spatial coordinates.

An equivalent circuit of the three-phase ESS with PAF. The complex branched power supply system circuit of low and medium voltage consumers may be represented as a simple equivalent circuit shown in Fig. 1. The three-phase sinusoidal voltage source *Source* through line *Line* with resistors R_s is connected to the load unit *Load* which can include resistors, reactors, capacitor banks, nonlinear elements, current and voltage sources. The resistance of the neutral conductor is taken into account by the resistance R_n. If we take into account that the source and the load can operate in symmetric and unbalanced modes, then at the unidirectional flow of energy in the ESS from the source to the load may be 96 different variants of combinations of parameters «source-load» system, in which there are additional losses [13].

In the equivalent circuit (see Fig. 1) line inductance L_s is moved into the load, which is generally a reasonable assumption and facilitates further analysis of the ESS. In the unit load connection point parallel to the PAF is connected, the power circuit of which is an autonomous PWM inverter on transistor-diode modules, with the capacitor bank in the DC link. To monitor the status of the ESS and generating control actions in the circuit according to Fig. 1, sensors of currents and voltages are used, by which the phase voltages at the terminals of the connection source u_{sa}, u_{sb}, u_{sc}, the phase voltages at the load connection terminals u_{La}, u_{Lb}, u_{Lc}, as well as the phase load currents i_{La}, i_{Lb}, i_{Lc} and power compensator i_{ca}, i_{cb}, i_{cc} are measured.

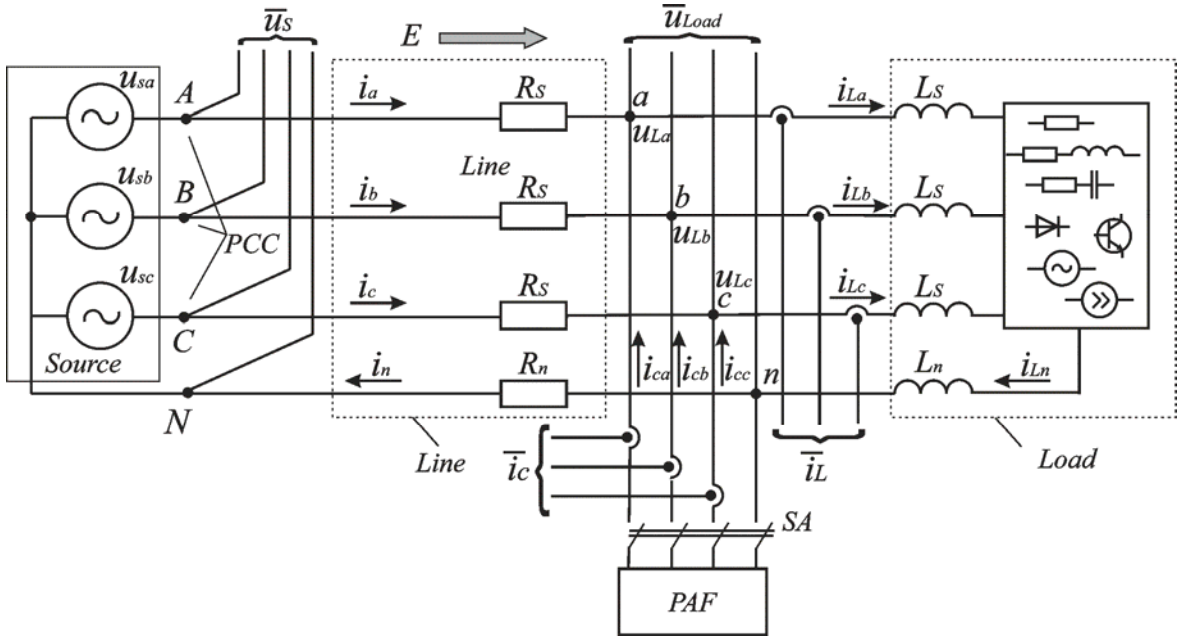

Fig. 1. An equivalent circuit of the three-phase ESS with PAF

When the switch SA is opened phase load currents are equal to the corresponding source phase currents.

The measured instantaneous values allow at any time to obtain information on the value of the instantaneous active power and the instantaneous reactive power. The first one is defined as the scalar product of two spatial vectors of voltage and current of the three-phase ESS presented, for example, in a coordinate system *a*, *b*, *c*, and the second one is the vector product of the same vectors:

$$p_S = \left|\vec{u}_S\right| \cdot \left|\vec{i}\right| \cdot \cos\varphi\,, \tag{1}$$

$$\vec{q}_S = \vec{u}_S \times \vec{i}_S = \begin{bmatrix} q_{sa} \\ q_{sb} \\ q_{sc} \end{bmatrix} = \tag{2}$$

$$= \left[\begin{vmatrix} u_{sb} & u_{sc} \\ i_b & i_c \end{vmatrix} \cdot \begin{vmatrix} u_{sc} & u_{sa} \\ i_c & i_a \end{vmatrix} \cdot \begin{vmatrix} u_{sa} & u_{sb} \\ i_a & i_b \end{vmatrix} \right]^T,$$

where

$$\vec{u}_S = \left[\vec{i}\,u_{sa} \;\; \vec{j}u_{sb} \;\; \vec{k}u_{sc}\right]^T \tag{3}$$

is the spatial vector of the network voltage in the coordinate system *a*, *b*, *c*, $\vec{i}, \vec{j}, \vec{k}$ are orts of directions by the axes *a*, *b*, *c* of the coordinate system;

$$\vec{i} = \left[\vec{i}\,i_a \;\; \vec{j}i_b \;\; \vec{k}i_c\right]^T \tag{4}$$

is the spatial vector of current in the coordinate system *a*, *b*, *c*.

Components of the additional energy losses power in three-phase ESS. In the absence of the three-phase ESS of calculated reactive power and constant in time instantaneous active power schedule the system is operating with the highest possible efficiency. The value of the highest possible efficiency is determined by the ratio of the power of three-phase resistive short circuit P_{sc} to the average calculated in the repetition time period, useful active load power P_{usf} [13]:

$$\eta_{\max} = \frac{1}{2} + \sqrt{\frac{1}{4} - \frac{1}{k_{sc}}}\,, \tag{5}$$

where

$$k_{sc} = \frac{P_{sc}}{P_{usf}}\,. \tag{6}$$

The indicated condition

$$\begin{aligned} &p_{puls} = 0 \;\Lambda\; P_{usf} = \text{const}, \\ &q = 0, \end{aligned} \tag{7}$$

is performed in the ESS with symmetrical three-phase source and symmetrical resistive load. Violation of condition (7) leads to a rise in the ESS of additional losses power

$$\Delta P_{\Sigma} = \Delta P_{\min} + \Delta P_{add}\,, \tag{8}$$

where $\Delta P_{\min}$ is the minimal possible losses power determined by the relation (5); ΔP_{add} is the additional losses power.

In [13] following the adoption of a number of assumptions an universal calculation ratio determined the power of total losses as the sum of four components, presented in parts of useful active power P_{usf} was obtained

$$\Delta P_{\Sigma *} = \Delta P_{\min *} \times$$
$$\times \left(1 + Q_{RMS*}^2 + P_{pulsRMS*}^2\right) + \Delta P_{n*} \Big|_{P_{usf} = const}, \quad (9)$$

where

$$\Delta P_{puls*} = \Delta P_{\min *} \cdot P_{pulsRMS*}^2 \quad (10)$$

is the relative component of power additional losses due to the variable component of the instantaneous power of the three-phase ESS, $P_{pulsRMS*}$ is the relative mean-square value of the variable active power component calculated in the repetition time period;

$$\Delta P_{Q*} = \Delta P_{\min *} \cdot Q_{RMS*}^2 \quad (11)$$

is the relative component of the power of additional losses due to the instantaneous reactive power of the three-phase ESS, Q_{RMS*} is the relative mean-square value of the module of the reactive power vector $|\vec{q}|$ calculated in the repetition time period;

$$\Delta P_{n*} = \frac{\Delta P_n}{P_{usf}} = \frac{R_S}{T \cdot P_{usf}} \int_t^{t+T} i_n^2 dt \quad (12)$$

is the relative losses power in the neutral conductor, calculated in the repetition time period T, due to the current i_n flow.

Check of the formula (9) on a specially created mathematical model showed the high accuracy in determining the total losses power for three-phase three-wire ESS in a symmetrical three-phase operation mode of the three-phase source. Using the formula (9) for four-wire ESS under certain combinations of parameters leads to considerable error arising from the lack of accounting (9) the mutual influence of the electromagnetic processes in the phase conductors and the neutral conductor.

In [14] it was proposed the refinement of the formula (9) by introducing an additional fifth component of the power of the additional losses power due to the mutual influence of the electromagnetic processes in the phase wires and the neutral wire of the three-phase ESS, ΔP_{mut*}

$$\Delta P_{\Sigma *} = \frac{\Delta P_{\Sigma}}{P_{usf}} = \Delta P_{\min *} + \Delta P_{puls*} + \\ + \Delta P_{q*} + \Delta P_{n*} + \Delta P_{mut*} \Big|_{P_{usf} = \text{const}}. \quad (13)$$

The indicated way could minimize the error of calculation of the total losses power for four-wire ESS, however the calculation algorithm become more complicated, and any practical difficulties in the use of the adjusted ratio arose.

Representation of power components of additional losses of the three-phase ESS in pqr spatial coordinates. The greatest opportunities to extract components of the instantaneous losses power and components, requiring compensation in three-phase four-wire systems are presented by the p-q-r theory of instantaneous active and reactive power [9]. The mathematical apparatus of p-q-r theory, described in detail in the literature, is associated with a spatial transition from the Cartesian coordinate system *abc* to the pqr system. Transformation of coordinate systems is carried out in two stages: generalized spatial vectors of voltages and currents from the *abc* coordinate system using the direct Clark Transformation matrix are transferred to a fixed spatial αβ0 system:

$$\begin{bmatrix} u_\alpha \\ u_\beta \\ u_0 \end{bmatrix} = \sqrt{\frac{2}{3}} \cdot \begin{bmatrix} 1 & -\frac{1}{2} & -\frac{1}{2} \\ 0 & \frac{\sqrt{3}}{2} & -\frac{\sqrt{3}}{2} \\ \frac{1}{\sqrt{2}} & \frac{1}{\sqrt{2}} & \frac{1}{\sqrt{2}} \end{bmatrix} \cdot \begin{bmatrix} u_{Sa} \\ u_{Sb} \\ u_{Sc} \end{bmatrix}, \quad (14)$$

$$\begin{bmatrix} i_\alpha \\ i_\beta \\ i_0 \end{bmatrix} = \sqrt{\frac{2}{3}} \cdot \begin{bmatrix} 1 & -\frac{1}{2} & -\frac{1}{2} \\ 0 & \frac{\sqrt{3}}{2} & -\frac{\sqrt{3}}{2} \\ \frac{1}{\sqrt{2}} & \frac{1}{\sqrt{2}} & \frac{1}{\sqrt{2}} \end{bmatrix} \cdot \begin{bmatrix} i_{La} \\ i_{Lb} \\ i_{Lc} \end{bmatrix}, \quad (15)$$

followed by a transition from αβ0 coordinate system into a rotating coordinate system pqr.

$$\begin{bmatrix} i_p \\ i_q \\ i_r \end{bmatrix} = \frac{1}{u_{\alpha\beta 0}} \begin{bmatrix} u_0 & u_\alpha & u_\beta \\ 0 & -\frac{u_{\alpha\beta 0} u_\beta}{u_{\alpha\beta}} & \frac{u_{\alpha\beta 0} u_\alpha}{u_{\alpha\beta}} \\ u_{\alpha\beta} & -\frac{u_0 u_\alpha}{u_{\alpha\beta}} & -\frac{u_0 u_\beta}{u_{\alpha\beta}} \end{bmatrix} \begin{bmatrix} i_0 \\ i_\alpha \\ i_\beta \end{bmatrix}, \quad (16)$$

where

$$u_{\alpha\beta 0} = \sqrt{u_\alpha^2 + u_\beta^2 + u_0^2}, \quad (17)$$

$$u_{\alpha\beta} = \sqrt{u_\alpha^2 + u_\beta^2}. \quad (18)$$

In the symmetrical mode of the three-phase source of the four-wire ESS the system pqr allows to extract four components of the instantaneous power:

$$\begin{bmatrix} P_{AV} + p_{puls} \\ q_q \\ q_r \end{bmatrix} = u_p \cdot \begin{bmatrix} i_{p-} + i_{p\sim} \\ i_r \\ i_q \end{bmatrix}, \quad (19)$$

where

$$u_p = u_{\alpha\beta 0} = u_s = \sqrt{u_\alpha^2 + u_\beta^2 + u_0^2} = \\ = \sqrt{u_a^2 + u_b^2 + u_c^2} = const \quad (20)$$

is the module of the voltage space vector, which in pqr coordinates coincides with the direction of the axis p; P_{AV} and p_{puls} are, respectively, the constant calculated in the repetition time period, and the variable components of the instantaneous active power of the ESS; i_{p-} and $i_{p\sim}$ are, respectively, the constant and variable components of the projection of the generalized space vector of the current on the p-axis of the pqr coordinate system; q_q and q_r are, respectively, the instantaneous reactive power with respect to r-axis and q-axis.

Transfer of electrical energy from the source to the load with the least possible losses causes a DC component of the instantaneous active power, the other three components generally to be compensated. Exclusion from

the system of the variable component of the instantaneous power will allow compensating amplitude asymmetry of network currents. Exclusion from the system of reactive power by the *q*-axis current will permit compensating the neutral wire. Exclusion from the system of reactive power by the *r*-axis will permit compensating the phase angle between the corresponding phase voltages and currents.

We express additional losses power components in the pqr coordinates. The total losses power in the three-phase four-wire ESS by the equivalent circuit (see Fig. 1) can be represented by two components:

$$\Delta p_{\Sigma} = \Delta p_s + \Delta p_n = i^2 \cdot R_s + i_n^2 \cdot R_n, \quad (21)$$

where Δp_s and Δp_n are respectively, the instantaneous losses power in the three-phase line and instantaneous losses power in the neutral wire;

$$i^2 = \left[i_a^2 \;\; i_b^2 \;\; i_c^2\right]^T = \left[i_p^2 \;\; i_q^2 \;\; i_r^2\right]^T \quad (22)$$

is the square of the network current module;

$$i_n = i_a + i_b + i_c \quad (23)$$

is the instantaneous value of the zero conductor current.

Let us consider the case when the resistance of the zero conductor equals to the resistance of the line wire

$$R_n = R_s. \quad (24)$$

In the symmetric mode of the source the neutral conductor current in the pqr system can be expressed from (15) through the projection of the resulting current vector on the *r*-axis in accordance with the fact that the *r*-axis of the rotating pqr coordinate system is fixed and coincides with the direction of the axis 0 of the coordinate system αβ0:

$$i_n = \sqrt{3} \cdot i_r. \quad (25)$$

Then substituting (22)-(25) into (21) we obtain

$$\Delta p_{\Sigma} = R_s \cdot \left(i_p^2 + i_q^2 + 4 \cdot i_r^2\right). \quad (26)$$

Expressing projections of currents in the prq system through the respective power (19) and passing to relative units, the ratio can be written to determine the relative total instantaneous losses power in the coordinates pqr

$$\Delta p_{\Sigma *} = \frac{1}{k_{sc}} \cdot \left(p_*^2 + q_{r*}^2 + 4 \cdot q_{q*}^2\right). \quad (27)$$

or for the average, calculated in the repetition time period, value

$$\Delta P_{\Sigma *} = \frac{1}{k_{sc}} \cdot \left(P_{RMS*}^2 + Q_{rRMS*}^2 + 4 \cdot Q_{qRMS*}^2\right). \quad (28)$$

Thus, the relative total losses power in the pqr coordinate system can be represented by the sum of three components corresponding to the losses power by each of the coordinate axes

$$\Delta P_{\Sigma *} = \Delta P_{p*} + \Delta P_{q*} + \Delta P_{r*}. \quad (29)$$

Let us compare the relation (28) with the previously obtained relation (13). The square of the RMS active power value by the *p*-axis of the pqr coordinate system can be decomposed into two components

$$P_{RMS*}^2 = P_{AV*}^2 + P_{pulsRMS*}^2 = \left(1 + \Delta P_{\Sigma *}\right)^2 + P_{puls*}^2. \quad (30)$$

The coefficient, which expresses the ratio of the power of the resistive short circuit of the three-phase ESS, can be determined by the relative power of the minimum possible losses

$$\frac{1}{k_{sc}} = \frac{\Delta P_{\min *}}{\left(1 + \Delta P_{\min *}\right)^2}. \quad (31)$$

The square of the modulus of the vector of the relative RMS reactive power

$$Q_{RMS*}^2 = Q_{qRMS*}^2 + Q_{rRMS*}^2. \quad (32)$$

Relative average losses in the neutral wire

$$\Delta P_{n*} = \frac{3 \cdot Q_{qRMS*}^2}{k_{sc}}. \quad (33)$$

Substituting (30)-(33) to (28) and calculating the roots of a quadratic equation, we can write the ratio to calculate the relative total losses power through the components adopted previously

$$\Delta P_{\Sigma *} = \frac{1 + \Delta P_{\min *}^2 - \sqrt{\left(1 - \Delta P_{\min *}^2\right)^2 - 4 \cdot \Delta P_{\min *} \times}}{2 \cdot \Delta P_{\min *}} \times \left. \frac{\times \left(\Delta P_{puls*} + \Delta P_{q*} + \Delta P_{n*} \cdot \left(1 + \Delta P_{\min *}\right)^2\right)}{2 \cdot \Delta P_{\min *}} \right|_{P_{usf} = const} \quad (34)$$

The exact calculation expression (34) with a slight error may be replaced by a simplified relationship

$$\Delta P_{\Sigma *} = \Delta P_{\min *} + \Delta P_{puls*} + \Delta P_{q*} + \left. + \Delta P_{n*} \cdot \left(1 + \Delta P_{\min *}\right)^2 \right|_{P_{usf} = \text{const}} \quad (35)$$

Comparing (35) with (13) proposed earlier allows us to express additional fifth component, due to the mutual influence of the electromagnetic processes in the lines and the neutral conductor,

$$\Delta P_{mut*} = \Delta P_{n*} \cdot \left(\Delta P_{\min *}^2 + 2 \cdot \Delta P_{\min *}\right). \quad (36)$$

We write the relations expressing the components of additional losses power of the universal equation, through the relevant components in the pqr coordinates

$$\Delta P_{Q*} = \left(1 + \Delta P_{\min *}\right)^2 \cdot \left(\Delta P_{r*} + \frac{\Delta P_{q*}}{4}\right), \quad (37)$$

$$\Delta P_{puls*} = \left(1 + \Delta P_{\min *}\right)^2 \cdot \Delta P_{p*} - \left. - \Delta P_{\min *} \cdot \left(1 + \Delta P_{p*} + \Delta P_{q*} + \Delta P_r\right)^2, \right. \quad (38)$$

$$\Delta P_{n*} = \frac{3}{4} \cdot \Delta P_{q*}, \quad (39)$$

$$\Delta P_{mut*} = \frac{3}{4} \cdot \left(\Delta P_{\min *}^2 + 2 \cdot \Delta P_{\min *}\right) \cdot \Delta P_{q*}. \quad (40)$$

Components of additional losses power by the universal relation (37)-(40) in the coordinate representation (28) depend on the lowest possible losses power, which in its turn is a function of the active resistance of the line. Due to the fact that the measurement of resistance in the line is difficult to implement real-time task, we express the lowest possible losses power through the instantaneous values of currents and voltages measured according to Fig. 1. Substituting equation (31) to (28) and performing the transformations, we obtain the formula for the calculation of the relative power of the minimum possible losses

$$\Delta P_{\min *} = \frac{P_{pqr*} - 2 \cdot \Delta P_{\Sigma *} - \sqrt{P_{pqr*}^2 - 4 \cdot \Delta P_{\Sigma *} \cdot P_{pqr*}}}{2 \cdot \Delta P_{\Sigma *}}, \quad (41)$$

where

$$P_{pqr*} = P_{RMS*}^2 + Q_{rRMS*}^2 + 4 \cdot Q_{qRMS*}^2. \quad (42)$$

The relative power of total losses can be determined by the instantaneous values of currents and voltages, measured in accordance with Fig. 1, or by projections on the *p*-axis of generalized spatial vectors of currents and voltages in the pqr coordinate system:

$$\Delta P_{\Sigma *} = \frac{1}{T} \int_{t}^{t+T} \left(\left(i_{pL} + i_{pc} \right) \cdot u_{ps} - i_{pL} \cdot u_{pL} \right) dt, \quad (43)$$

where i_{pL}, i_{pc} are respectively projections on the *p*-axis of the pqr coordinate system of generalized space vectors of the load current and compensator current; u_{ps}, u_{pL} are respectively projections on the *p*-axis of the pqr coordinate system of generalized spatial vectors of the network voltage and the voltage at the terminals of the load connection.

With the principles of the p-q-r theory of instantaneous active and reactive power, as well as the relations (37)-(43) the total losses power in the ESS can be extracted into separate components, describing the universal calculation expression (13). In order to take advantage of the proposed method it is enough to have information about the instantaneous values of currents and voltages measured in the ESS using PAF.

The increase reserve of the ESS efficiency when PAF connecting. The economic efficiency of PAF connection from the point of the reduce of losses power in the ESS will be achieved when the total losses power in the ESS after connecting of the compensator will be smaller than before its connection

$$\Delta P_{on*} < \Delta P_{\Sigma *}. \quad (44)$$

If after connecting PAF the active load power remains unchanged, then the inequality (44) can be represented as

$$\Delta P_{c*} + \Delta P_{saf*} < \Delta P_{add*}, \quad (45)$$

where ΔP_{c*} is the power of losses, required to maintain the voltage on the capacitor of the DC link of the PAF above peak value of the network voltage; ΔP_{saf*} is the losses power of the power compensator.

Define the maximum possible effect of increasing efficiency by adopting the ideal compensator and useful power unchanged before and after the connection of the PAF. Fig. 2 shows a Matlab-model of the equivalent circuit of a three-phase ESS with PAF, with characteristics corresponding to the circuit of Fig. 1. The model consists of a power circuit, voltage and current sensors, measurement subsystem, subsystem of the ESS mode setting, the subsystem of total losses power components calculation, and virtual instrumentation. The Matlab-model permits investigating the operation of the three-phase ESS in 96 indicated variants in which additional losses can arise. For the modelling a three-phase four-wire ESS with symmetrical three-phase voltage source at $R_n = R_s$ was selected. The parameters of the model's elements: $k_{sc} = 5 \div 30$; $U_m = 311.13$ V; $f_s = 50$ Hz; $P_{usf} = \text{const} = 400.1$ kW.

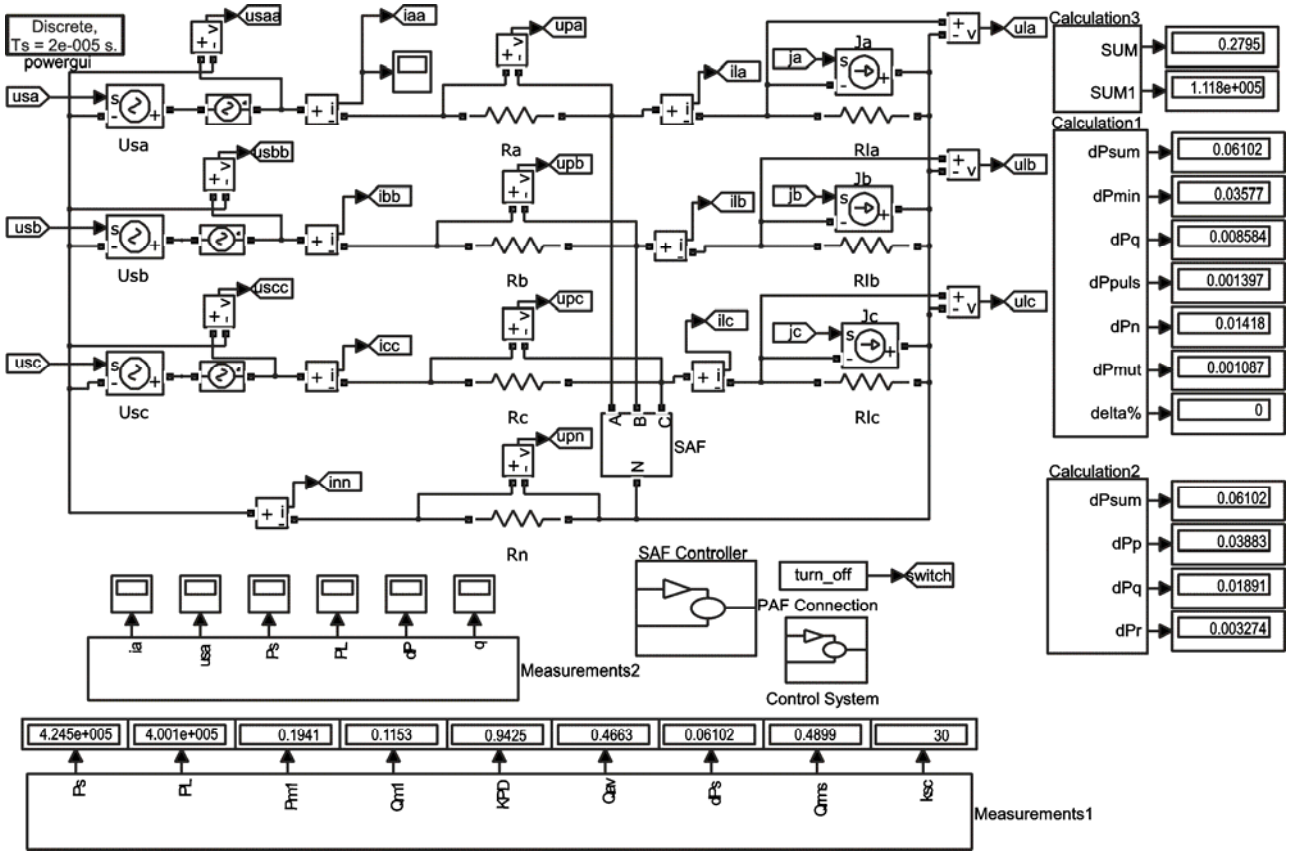

Fig. 2. A Matlab-model of the equivalent circuit f the three-phase ESS with PAF

As an example we consider three separate factors of the arising additional losses in the ESS:

1. Symmetrical active-reactive load. We accept $\varphi = 20°$.

2. Asymmetrical resistive load. We accept the active resistances of three phases of the load

$$\begin{aligned} R_{La} &= k_{la} \cdot R_L, \\ R_{Lb} &= k_{lb} \cdot R_L, \\ R_{Lc} &= k_{lc} \cdot R_L, \\ k_{La}^2 + k_{Lb}^2 + k_{Lc}^2 &= 3, \end{aligned} \tag{46}$$

$k_{la} = 1$, $k_{lb} = 1.3$, $k_{lc} = 0.5568$.

3. Symmetrical nonlinear load. We accept the current of the phase A

$$i_a = \sum_{n=2k\mp1} i_k = \sum_{n=2k\mp1} \frac{U_m}{n \cdot (R_s + R_L)} \cdot \sin(n \cdot \vartheta), \tag{47}$$

$k = 1, 2, 3...18$.

Six modes of the ESS were taken to summarize the simulation results corresponding to the combination of three of indicated factors:

Mode 1 – symmetrical active-reactive load.

Mode 2 – asymmetrical resistive load.

Mode 3 – symmetrical nonlinear load.

Mode 4 – asymmetrical active-reactive load.

Mode 5 – symmetrical mixed (active-inductive and nonlinear) load.

Mode 6 – asymmetrical nonlinear load.

Using this model, the total losses power components by the universal formula (13) and in the pqr coordinates (29) were calculated. And the results of the calculation for the six modes adopted, in percentage terms, are summarized in Table 1.

The Table 1 shows that in these modes the greatest contribution to the total losses power two components make: component of the additional losses power due to the instantaneous reactive power, and the components of additional losses power due to current flow in the neutral wire.

Fig. 3 shows a reserve for increasing the efficiency for the considered six modes of operation of the ESS: a large area of the zone of the increase of efficiency, bathed in a dark color in the Figure, corresponds to more favorable technical and economic conditions when using the PAF. The economic feasibility of the PAF use increases for the ESS, where several factors leading to additional electric power losses can simultaneously take place. As an example of such ESS municipal networks at the level of individual consumers or consumer groups can serve.

Conclusions.

1. A technique of representation of components of total losses power in three-phase ESS based on the use of the pqr theory of instantaneous active and reactive power is substantiated. According to the proposed technique the total losses power can be represented as the sum of three components ΔP_{p*}, ΔP_{q*}, ΔP_{r*} defined by the projections of generalized spatial vectors of current and voltage on the axis of the pqr coordinate system.

2. Using spatial coordinate transformations of p-q-r coordinates of the theory of instantaneous active and reactive power, an exact relation (34) is obtained, taking into account the four components of the total losses power: power of the lowest possible losses; additional losses power due to the instantaneous reactive power; additional losses power due to fluctuations of the instantaneous active power; additional losses power due to the current flowing in the neutral wire.

3. Comparison of the exact calculation relation (34) with the previously proposed universal formula (15) made it possible to determine the fifth component of the additional losses power due to the mutual influence of electromagnetic processes in the lines of the three-phase ESS and the neutral wire.

4. The method of calculating the additional components of the total losses power is determined. The method based on the use of measuring information about the values of instantaneous current and voltage in the ESS with PAF. Using this method will allow developing a measuring device that registers the components of the losses power at the current time, the scope of which may be associated with the development of mode control algorithms of the ESS with minimal losses of electric energy.

5. The method of determining the reserve of the increasing the efficiency of the ESS at using PAF to substantiate the economic efficiency of its installation is proposed.

REFERENCES

1. Akagi H., Kanazawa Y., Nabae A. Generalized theory of the instantaneous power in three phase circuits. *Int. Power Electronics Conf.*, Tokyo, Japan, 1983, pp. 1375-1386.

2. Akagi H., Kanazawa Y., Nabae A. Instantaneous reactive power compensators comprising switching devices without energy storage components. *IEEE Transactions on Industry Applications*, 1984, vol.IA-20, no.3, pp. 625-630. **doi: 10.1109/TIA.1984.4504460**.

3. Nabae A., Tanaka T. A new definition of instantaneous active-reactive current and power based on instantaneous space vectors on polar coordinates in three-phase circuits. *IEEE Transactions on Power Delivery*, 1996, vol.11, no.3, pp. 1238-1243. **doi: 10.1109/61.517477**.

4. Czarnecki L.S. What is wrong with the Budeanu concept of reactive and distortion power and why it should be abandoned. *IEEE Transactions on Instrumentation and Measurement*, 1987, vol.IM-36, no.3, pp. 834-837. **doi: 10.1109/TIM.1987.6312797**.

5. Czarnecki L.S. Misinterpretations of some power properties of electric circuits. *IEEE Transactions on Power Delivery*, 1994, vol.9, no.4, pp. 1760-1769. **doi: 10.1109/61.329509**.

6. Ghassemi F. Should the theory of power be reviewed? *L'energia electrica*, 2004, vol.81, pp. 85-90.

7. Peng F.Z., Ott G.W., Adams D.J. Harmonic and reactive power compensation based on the generalized instantaneous reactive power theory for three-phase four-wire systems. *IEEE Transactions on Power Electronics*, 1998, vol.13, no.6, pp. 1174-1181. **doi: 10.1109/63.728344**.

8. Afonso J., Couto C., Martins J. Active filters with control based on p-q theory. *IEEE Industrial Electronics Society Newsletter*, 2000, vol.47, no.3, pp. 5-10.

9. Soares V., Verdelho P., Marques G.D. An instantaneous active and reactive current component method for active filters. *IEEE Transactions on Power Electronics*, 2000, vol.15, no.4, pp. 660-669. **doi: 10.1109/63.849036**.

Table 1

Results of determination of components of the total losses power

k_{sc}	$\Delta P_{\Sigma*}$	Components of the total losses power by the universal formula (13), %					In the coordinates pqr, %		
		$\Delta P_{\min*}/\ \Delta P_{\Sigma*}$	$\Delta P_{q*}/\ \Delta P_{\Sigma*}$	$\Delta P_{\text{puls}*}/\ \Delta P_{\Sigma*}$	$\Delta P_{n*}/\ \Delta P_{\Sigma*}$	$\Delta P_{mut*}/\ \Delta P_{\Sigma*}$	$\Delta P_{p*}/\ \Delta P_{\Sigma*}$	$\Delta P_{q*}/\ \Delta P_{\Sigma*}$	$\Delta P_{r*}/\ \Delta P_{\Sigma*}$
Mode 1									
5	0.4792	79.71	16.60	0	0	3.72	91.32	0	8.69
10	0.1514	83.89	15.79	0	0	0.00	87.58	0	12.43
15	0.09199	84.12	15.75	0	0	0.00	86.43	0	13.57
20	0.0662	84.18	15.74	0	0	0.00	85.89	0	14.12
25	0.05172	84.22	15.72	0	0	0.00	85.56	0	14.44
30	0.04245	84.24	15.71	0	0	0.00	85.35	0	14.65
Mode 2									
5	0.4465	85.55	4.32	2.64	2.64	4.87	95.10	3.52	1.38
10	0.1559	81.47	5.89	2.67	7.58	2.41	87.81	10.10	2.10
15	0.09752	79.35	6.44	2.65	9.81	1.73	84.64	13.07	2.28
20	0.07126	78.20	6.74	2.63	11.06	1.35	82.89	14.75	2.36
25	0.05621	77.50	6.92	2.62	11.85	1.11	81.64	15.79	2.40
30	0.04644	77.00	7.04	2.61	12.39	0.94	81.05	16.52	2.43
Mode 3									
5	0.5046	75.70	10.29	0.15	4.81	9.06	89.79	6.41	3.79
10	0.1801	70.53	12.12	0.14	13.04	4.19	77.40	17.39	5.19
15	0.1141	67.82	12.62	0.13	16.52	2.94	72.65	22.02	5.37
20	0.084	66.34	12.86	0.12	18.39	2.27	70.07	24.51	5.40
25	0.06655	65.46	12.99	0.12	19.58	1.84	68.50	26.07	5.41
30	0.05514	64.85	13.10	0.12	20.37	1.55	67.43	27.20	5.41
Mode 4									
5	0.6077	62.85	23.33	1.87	1.74	10.21	86.05	2.32	11.64
10	0.1902	66.78	22.13	2.05	6.47	2.55	76.08	8.63	15.27
15	0.1185	65.30	22.26	2.00	8.67	1.71	72.11	11.55	16.30
20	0.08644	64.47	22.32	1.97	9.92	1.31	70.06	13.22	16.72
25	0.06816	63.91	22.36	1.95	10.72	1.07	68.76	14.29	16.96
30	0.0563	63.52	22.38	1.93	11.27	0.89	67.87	15.03	17.10
Mode 5									
5	0.5046	75.70	9.45	1.05	4.81	9.00	90.25	6.41	3.35
10	0.1801	70.53	11.35	0.96	13.04	4.14	78.01	17.39	4.59
15	0.1141	67.82	11.89	0.91	16.52	2.89	73.27	22.02	4.74
20	0.084	66.34	12.15	0.88	18.39	2.22	70.70	24.51	4.77
25	0.06655	65.46	12.31	0.86	19.58	1.79	69.12	26.09	4.78
30	0.05514	64.85	12.42	0.84	20.37	1.50	68.04	27.20	4.78
Mode 6									
5	0.5663	67.45	11.07	3.53	5.72	12.24	88.49	7.62	3.89
10	0.2	63.51	13.10	2.87	15.42	5.09	74.25	20.56	5.17
15	0.1266	61.12	13.61	2.58	19.23	3.47	69.07	25.63	5.32
20	0.0931	59.86	13.85	2.44	21.21	2.64	66.36	28.27	5.35
25	0.0737	59.11	13.98	2.35	22.43	2.13	64.74	29.88	5.36
30	0.06102	58.60	14.07	2.29	23.24	1.78	63.63	30.99	5.37

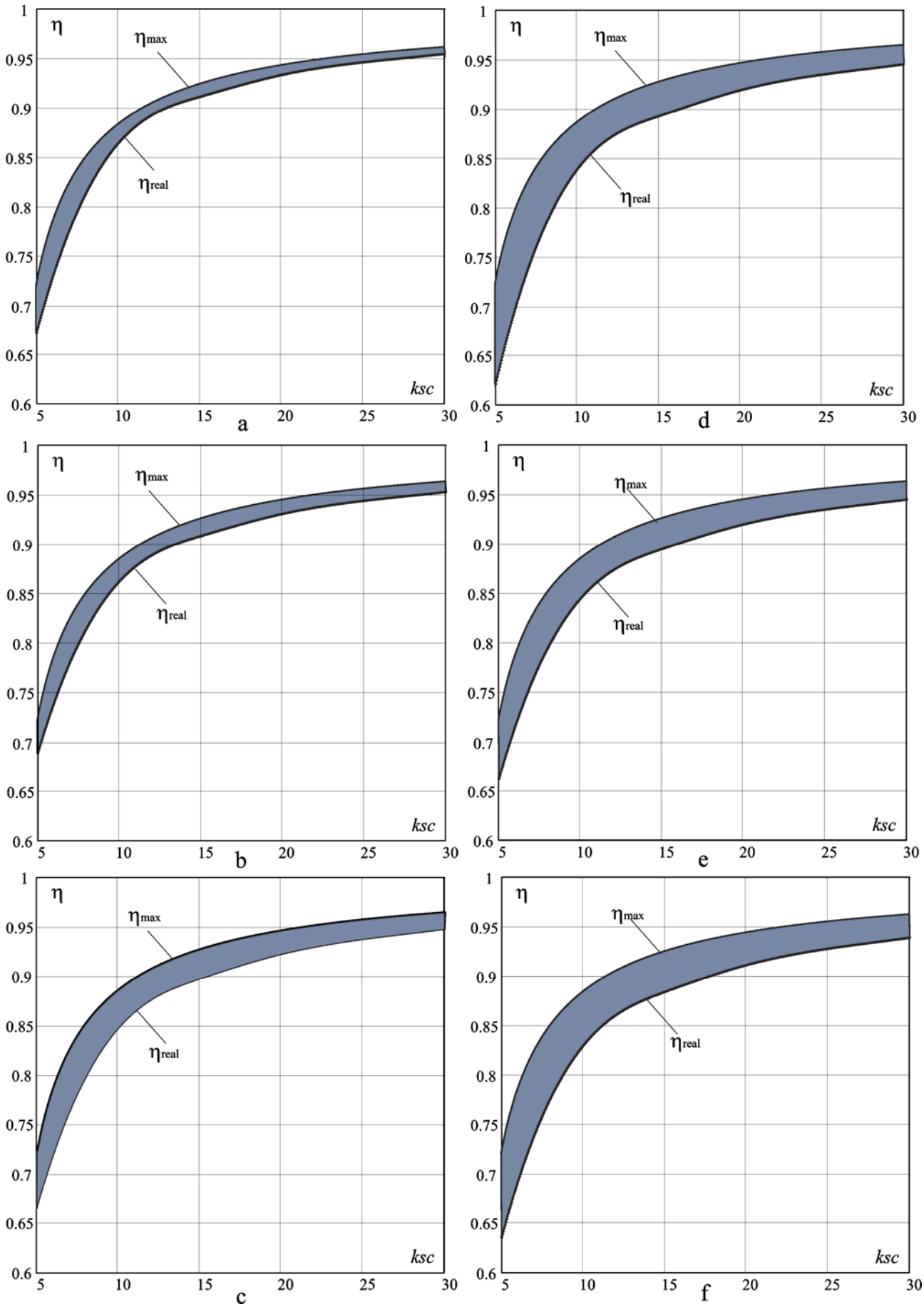

Fig. 3. Reserve of the increase of the efficiency of the three-phase four-ware ESS:
a – in the mode 1; *b* – in the mode 2; *c* – in the mode 3; *d* – in the mode 4; *e* – in the mode 5; *f* – in the mode 6

10. Kim H.S., Akagi H. The instantaneous power theory on the rotating p-q-r reference frames. *Proceedings of the IEEE 1999 International Conference on Power Electronics and Drive Systems. PEDS'99 (Cat. No.99TH8475)*, 1999, pp. 422-427. **doi: 10.1109/PEDS.1999.794600**.

11. Shidlovskii A.K. *Tranzistornye preobrazovateli s uluchshennoi elektromagnitnoi sovmestimost'iu* [Transistor converters with improved electromagnetic compatibility]. Kiev, Naukova Dumka Publ., 1993. 272 p. (Rus).

12. Mykhal's'kyy V.M. *Zasoby pidvyshchennya yakosti elektroenerhiyi na vkhodi i vykhodi peretvoryuvachiv chastot iz shyrotno-impul'snoyu modulyatsiyeyu* [Means improve power quality input to output frequency converters with pulse-width modulation]. Kiev, Instytut elektrodynamiky NAN Ukrayiny Publ., 2013. 340 p. (Ukr).

13. Zhemerov G.G., Tugay D.V. Physical meaning of the «reactive power» concept applied to three-phase energy supply systems with non-linear load. *Elektrotekhnika i elektromekhanika – Electrical engineering & electromechanics*, 2015, no.6, pp. 36-42. (Rus). **doi: 10.20998/2074-272X.2015.6.06.**

14. Zhemerov G.G., Tugay D.V. An universal formula clarification to determine the power losses in the three-phase energy supply systems. *Visnyk NTU «KhPI» – Bulletin of NTU «KhPI»*, 2015, no.12, pp. 339-343. (Rus).

15. Artemenko M.Yu., Batrak L.M., Mykhalskyi V.M., Polishchuk S.Y. Analysis of possibility to increase the efficiency of three-phase four-wire power system by means of shunt active filter. *Tekhnichna elektrodynamika – Technical electrodynamics*, 2015, no.6, pp. 12-18. (Ukr).

Received 02.02.2016

G.G. Zhemerov[1]*, Doctor of Technical Science, Professor,*
D.V. Tugay[2]*, Candidate of Technical Science, Associate Professor,*
[1] National Technical University «Kharkiv Polytechnic Institute», 21, Frunze Str., Kharkiv, 61002, Ukraine.
[2] O.M. Beketov National University of Urban Economy in Kharkiv,
12, Revolution Str., Kharkiv, 61002, Ukraine.
phones +380 57 7076312, +380 57 7073111
e-mail: zhemerov@gmail.com, tugaydv@yandex.ua

How to cite this article:
Zhemerov G.G., Tugay D.V. Components of total electric energy losses power in pqr spatial coordinates. *Electrical engineering & electromechanics*, 2016, no.2, pp. 11-19. doi: 10.20998/2074-272X.2016.2.02.

UDC 621.3.013 **10.20998/2074-272X.2016.2.03**

V.S. Grinchenko, K.V. Chunikhin, N.V. Grinchenko

LOW-FREQUENCY MAGNETIC FIELD SHIELDING BY A CIRCULAR PASSIVE LOOP AND CLOSED SHELLS

Purpose. To analyze the shielding factors for a circular passive loop and conductive closed shells placed in a homogeneous low-frequency magnetic field. Methodology. We have obtained simplified expressions for the shielding factors for a circular passive loop and a thin spherical shell. In addition, we have developed the numerical model of a thin cubical shell in a magnetic field, which allows exploring its shielding characteristics. Results. We have obtained dependences of the shielding factors for passive loops and shells on the frequency of the external field. Analytically determined frequency of the external magnetic field, below which field shielding of a passive loop is expedient to use, above which it is advisable to use a shielding shell. References 10, figures 4.
Key words: **shielding factor, magnetic field, circular passive loop, thin shell**.

Проведен сравнительный анализ эффективности экранирования однородного низкочастотного магнитного поля электропроводящим кольцом и замкнутыми оболочками. Получены упрощенные выражения для эффективности экранирования магнитного поля электропроводящим кольцом и тонкостенной сферической оболочкой. Разработана численная модель тонкостенной кубической оболочки в магнитном поле, позволяющая исследовать её экранирующие характеристики. Приведены зависимости эффективности экранирования кольцом и замкнутыми оболочками от частоты внешнего поля. Аналитически определена частота внешнего магнитного поля, ниже которой для экранирования поля целесообразно использовать электропроводящее кольцо, выше которой целесообразно использовать замкнутую оболочку. Библ. 10, рис. 4.
Ключевые слова: **эффективность экранирования, магнитное поле, электропроводящее кольцо, тонкостенная оболочка.**

Introduction. Negative effect of the magnetic field (MF), in particular the low-frequency magnetic field, on the human health [1] as well as limitations on levels of MF in which the stable operation of modern equipment is guaranteed [2] require reducing values of magnetic flux density to accepted ones.

Let's consider a problem of the homogeneous low-frequency MF mitigation in a local domain. Shielding systems are divided into passive and active by the way of power supply. In some works [3, 4] there is proposed to use systems of active shielding for the MF mitigation in the local domain. However, in this work the consideration will be limited by passive electromagnetic shielding. To reduce the external MF in the local domain the electromagnetic shields are manufactured as thin closed shells and usually they have shape of a box or a cylinder with equipment located inside them [5-9]. In [9] there was proposed to use a circular passive loop for the low-frequency MF shielding. In [10] an expression for the shielding factor was written more exactly, and radius of the domain within the circular passive loop in which it is recommended to place equipment was determined.

The goal of this work is to compare shielding properties of the circular passive loop (see Fig. 1,*a*) and thin closed shells (see Fig. 1,*b*,*c*) at various frequencies of the external MF as well as to determine a criterion of utilization of one or another shielding element.

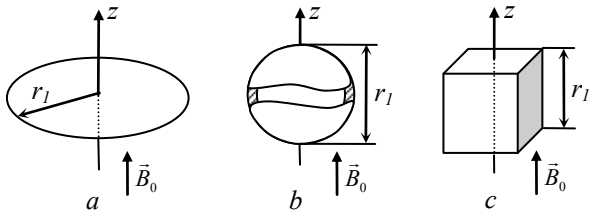

Fig. 1

At the analysis shells of cubic and spherical shapes are considered. A shielding shell has the spherical shape seldom but frequently closed shields of various shape can be approximately substituted by a spherical shield of the equivalent volume in such a way that three coordinate dimensions of the substituted shield approach to the diameter of spherical one [5].

The MF shielding by a circular passive loop. Shielding factor *SF* is the ratio of the RMS value of the external magnetic flux density to the RMS value of the magnetic flux density at the utilization of the shield. Let's assume that a circular passive loop of the radius r_1 with a round cross-section of the radius r_2 is placed in the homogeneous low-frequency MF (see Fig. 1,*a*). The loop's plane is oriented perpendicular to the external MF, and the magnetic flux density complex amplitude is $\dot{\vec{B}}_0 = \vec{e}_z \cdot B_0$, where B_0 is the external MF amplitude, $\vec{e}_z$ is the ort. The frequency of the external MF is *f*, Hz. Then, the shielding factor for the circular passive loop [10] in the sighting point (r, z) equals to

$$SF = \frac{B_0}{\sqrt{\left| B_0 + \dot{B}_z^{coil} \right|^2 + \left| \dot{B}_r^{coil} \right|^2}}, \qquad (1)$$

where

$$\dot{B}_z^{coil} = \frac{\mu_0 \dot{I}}{2\pi\sqrt{(r_1 + r)^2 + z^2}} \cdot \left[\frac{r_1^2 - r^2 - z^2}{(r_1 - r)^2 + z^2} \cdot E(k) + K(k) \right],$$

$$\dot{B}_r^{coil} = \frac{\mu_0 \dot{I}\, z}{2\pi r\sqrt{(r_1 + r)^2 + z^2}} \cdot \left[\frac{r_1^2 + r^2 + z^2}{(r_1 - r)^2 + z^2} \cdot E(k) - K(k) \right],$$

are components of MF created by the inducted in the passive loop current; the complex amplitude of the current is

$$\dot{I} = \frac{\pi}{\mu_0} \cdot \frac{r_1 B_0}{\frac{7}{4} - \ln\frac{8r_1}{r_2} + j \cdot \frac{1}{\mu_0 \pi f \sigma r_2^2}};$$

$K(k)=\int_0^{\pi/2}\frac{d\varphi}{\sqrt{1-k^2\sin^2\varphi}}$, $E(k)=\int_0^{\pi/2}\sqrt{1-k^2\sin^2\varphi}\,d\varphi$,

are complete elliptic integrals of the 1st and the 2nd kind, respectively; $k=\sqrt{\frac{4r_1 r}{(r_1+r)^2+z^2}}$ is the numerical coefficient; σ is the loop's conductivity, S/m; $\mu_0 = 4\pi\cdot10^{-7}$ H/m is the magnetic constant; j is the imaginary unit.

As it was shown in [10], if r_1 is the passive loop radius then it is useful to limit the shielding domain located in its central part by a sphere of radius $r_1/2$. The shielding factor SF is a function of the sighting point coordinates. Minimal SF takes places on the shielding domain's bound on the circular loop's axis: $SF_{coil}=SF\left(r=0, z=\frac{r_1}{2}\right)$. Using (1) we obtain the final expression for the circular passive loop's shielding factor:

$$SF_{coil}=\left[1+\frac{\frac{16\pi^2}{125}+\frac{8\pi}{5\sqrt{5}}\left(\frac{7}{4}-\ln\frac{8r_1}{r_2}\right)}{\left(\frac{7}{4}-\ln\frac{8r_1}{r_2}\right)^2+\left(\frac{1}{\mu_0\pi f\sigma r_2^2}\right)^2}\right]^{-1/2}. \quad (2)$$

The MF shielding by a conductive spherical shell. A problem of the MF determination within a thin conductive spherical shell placed in the homogeneous low-frequency MF (see Fig. 1,*b*) is considered in [5]. In this work the calculation of the shielded MF is carried out at the following assumptions. Firstly, the shell thickness d_s is supposed to be much less than the MF penetration depth to the conductor δ. Secondly, the thickness d_s is supposed to be much less than the shell radius R. At these assumptions the MF within the shell is homogeneous, and the shielding factor equals to

$$SF_{sphere}^{(Kaden)}=\left|\operatorname{ch} kd_s+\frac{1}{3}\cdot\left(K+\frac{2}{K}\right)\cdot\operatorname{sh} kd_s\right|, \quad (3)$$

where $K = kR$ and $k=\sqrt{j\mu_0 2\pi f\sigma+\frac{2}{R^2}}$ are the nondimensional coefficient and the coefficient with dimensionality m^{-1}, respectively; σ is the spherical shell conductivity, S/m. In (3) the spherical shell relative permeability is assumed to be equal 1.

For the considered in the present work dimensions and frequencies the following relation takes place: $\delta<<R$. Considering the expansion of the second member of (3) by the small parameter δ/R, we obtain the expression for the shielding factor for the conductive spherical shell placed in the homogeneous low-frequency MF:

$$SF_{sphere}=\sqrt{1+\left(\frac{\mu_0 2\pi f\sigma R d_s}{3}\right)^2}. \quad (4)$$

The MF shielding by a conductive cubic shell. Analytical calculation of the MF within a conductive cubic shell placed in the external MF (see Fig. 1,*c*) is very difficult. Therefore, it is useful to use the numerical modeling. Because of the exciting field is low-frequency, the MF is described by the equation obtained from the Ampere's circuital law in quasi-static approach:

$$\begin{cases}\Delta\dot{\vec{A}}^{(i)}=-j\mu_0 2\pi f\sigma\dot{\vec{A}}^{(i)},\\ \Delta\dot{\vec{A}}^{(e)}=0,\end{cases} \quad (5)$$

where $\dot{\vec{A}}^{(i)}, \dot{\vec{A}}^{(e)}$ are complex amplitudes of the vector potential of the electromagnetic field inside and outside the cubic shell's walls, respectively; σ is its conductivity, S/m. In (5) the cubic shell relative permeability is assumed to be equal 1.

To «link» solutions of the system (5) it is necessary to set conditions on the interface of the air region and conductive shell's walls:

$$\begin{cases}\dot{A}_\tau^{(i)}=\dot{A}_\tau^{(e)},\\ \operatorname{rot}\left(\dot{\vec{A}}^{(i)}\right)_\tau=\operatorname{rot}\left(\dot{\vec{A}}^{(e)}\right)_\tau,\end{cases} \quad (6)$$

where the index τ indicates that tangential for the interface vectors components are taken.

On the calculation region's bound the MF is supposed to be undisturbed, and the magnetic potential is set to equal to

$$\begin{cases}\dot{A}_x=-y\cdot B_0/2,\\ \dot{A}_y=x\cdot B_0/2,\\ \dot{A}_z=0,\end{cases} \quad (7)$$

where x, y are coordinates of the point on the calculation region's bound. For the correct utilization of (7), the calculation region's dimension is selected much more that the cubic shell edge.

The described problem is solved by the Finite Element Method using the software package *COMSOL Multiphysics*. To solve the problem, the interface «*Magnetic Fields*» which is a part of the «*AC/DC Module*» was used. This interface permits to model processes described by the equations (5). Building the 3D model for the option «*Space Dimension*», the variant «*3D*» was set. In all domains the mesh «*Free Tetrahedral*» was used, and within the cubic shell walls the mesh was finest.

Input parameters of the model are the amplitude B_0 and the frequency f of the external MF, the conductivity σ, the edge length a, and the walls thickness d_c of the cubic shell. The calculation result is the distribution of the RMS value of the magnetic flux density $B_{rms}(x,y,z)$.

The cubic shell placed in the homogeneous MF $\dot{\vec{B}}_0=\vec{e}_z\cdot B_0$ is shown in Fig. 2. The MF frequency is equal to 150 Hz. The borders of the cubic shell are shown by a dashed line. The shell is made of copper, the edge length is equal to 0.3 m, and the wall thickness is equal to 0.27 mm. The isolines in the Fig. 2 correspond to values of $SF^{-1}(x,y,z)=\frac{B_{rms}(x,y,z)}{B_0/\sqrt{2}}$ from 0.8 to 1.05. The distribution is built in the plane $y = 0$. In the center of the shell under consideration $SF^{-1} = 0.81$. Hence, the variation of SF^{-1} within the shell is less than 1 %. Therefore, the shielding factor for the cubic shell is determined as

$$SF_{cube}=\min\left\{\frac{B_0/\sqrt{2}}{B_{rms}(x,y,z)}\,\middle|\,\sqrt{x^2+y^2+z^2}<\frac{a}{3}\right\}.$$

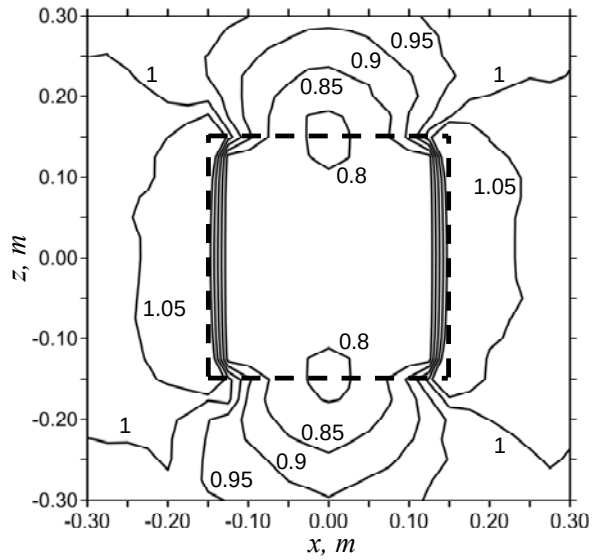

Fig. 2

The comparison of shielding factors for a passive loop and shells. Let's determine the dependence of the shielding factors on the external field frequency for a circular passive loop and conductive shells (spherical and cubic) placed in the homogeneous low-frequency MF. We assume that a passive loop and shells are made from copper with conductivity $\sigma = 5.41 \cdot 10^7$ S/m. The passive loop radius is assumed to be r_1=0.3 m. We consider two cases when the loop's cross-section radius r_2 equals to 2.5 mm and 5 mm. Because of the domain of the shielding by the circular passive loop is a sphere of the radius of $r_1/2$ [10], for the comparison of the passive loop's and shells' shielding characteristics let's assume the spherical shell radius $R = r_1/2$ and the cube edge length $a = r_1$. Besides, for the correctness of the shielding characteristics comparison, the passive loop's and shells' metal intensities should be the same. Therefore, the spherical shell thickness d_s and cubic shell one d_c are determined as follows:

$$d_s = 2\pi r_2^2 / r_1,$$

$$d_c = (\pi r_2)^2 / (3 r_1).$$

In Fig. 3 the shielding factor dependence on the external MF frequency in the case r_2 = 2.5 mm is represented. The full line corresponds to SF_{coil}, the dashed line corresponds to SF_{sphere}, and dots correspond to SF_{cube}. The dependences $SF_{coil}(f)$ and $SF_{sphere}(f)$ are obtained by using analytical expressions (2) and (4), respectively. The dependence $SF_{cube}(f)$ is obtained by interpolation of numerical modeling results depicted by dots in Fig. 3.

From the presented dependences it can be seen that at frequencies less than f_0 = 217 Hz the effectiveness of the shielding by the circular passive loop is higher that the effectiveness of the shielding by the spherical shell. From physical point of view, it can be explained by the change of the mechanism of the MF mitigation in the shielded domain. At $f < f_0$ the MF mitigation is determined by the inducted conduction current only, but at $f > f_0$ it is necessary to take into account the contribution of the MF attenuation in the shell's walls. As it is shown from Fig. 3 at frequencies 200-250 Hz the shielding factor equals to 1.15-1.20.

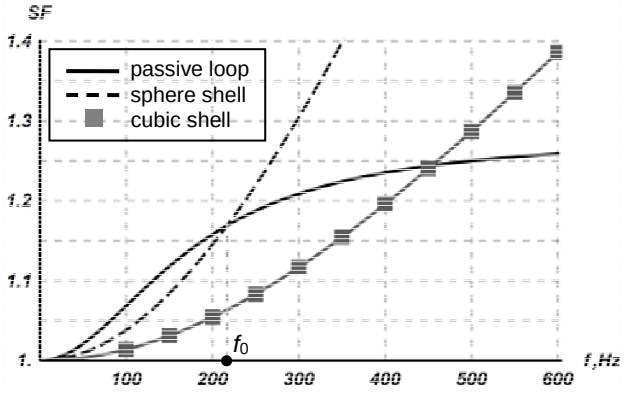

Fig. 3

As it was supposed the cubic shell's shielding characteristics are lower in the comparison with spherical one's at all frequency spectrum. In its turn, the cubic shell's shielding characteristics are lower than passive loop's ones at frequencies less than 454 Hz that is two times greater than f_0 (see Fig. 3).

In Fig. 4 the shielding factor dependence on the external MF frequency in the case r_2 = 5 mm is represented. In this case, f_0 equals to 56 Hz.

The shielding factor is higher than in the previous case that is explained by the metal intensity increase in four times. However, the curves' character is the same. As it can be seen from Fig. 4 the shielding factor of 1.15-1.20 is reached at frequencies 50-60 Hz.

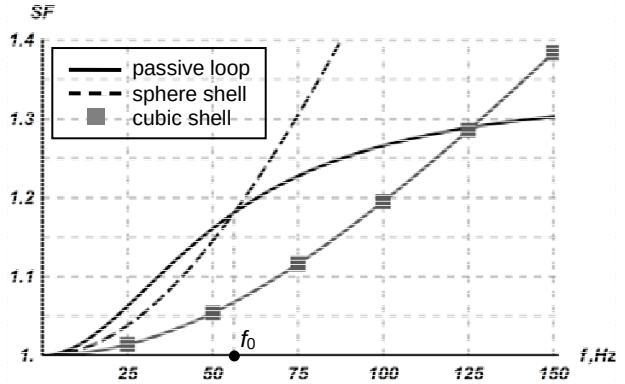

Fig. 4

As the shells' metal intensity increases, their walls' thickness increases too. As a result, the penetration depth δ at which the absorption mechanism becomes prevailing in the MF shielding increases, too. Therefore, as the metal intensity increases the value of the frequency f_0 decreases. The value of the frequency f_0 can be obtained analytically from the equation

$$SF_{coil}\big|_{f=f_0} = SF_{sphere}\big|_{f=f_0}.$$

Using (2) and (4) we obtain:

$$f_0 = \frac{6}{\mu_0 \sigma} \cdot \frac{R}{V} \times$$

$$\times \frac{\sqrt{-\left(\frac{4}{9}+\frac{16}{125}\right)\cdot\pi^2 + \frac{8\pi}{5\sqrt{5}}\cdot\left(-\frac{7}{4}+\ln(32\pi)+\frac{1}{2}\ln\frac{R^3}{V}\right)}}{-\frac{4\pi}{5\sqrt{5}}-\frac{7}{4}+\ln(32\pi)+\frac{1}{2}\ln\frac{R^3}{V}},$$

where $V = 2\pi r_1 \cdot \pi r_2^2 = 4\pi R^2 \cdot d_s$ is the metal intensity of the circular passive loop and shell; R is the radius of the shielded domain.

Calculating the numerical coefficients with precision till three significant digits, we obtain the final expression for f_0:

$$f_0 = \frac{12,7}{\mu_0 \sigma} \cdot \frac{R}{V} \cdot \frac{\sqrt{0,694 + \ln \frac{R^3}{V}}}{3,47 + \ln \frac{R^3}{V}}.$$

So, in the region $f > f_0$ in order to mitigate the MF in the region of the radius R at given metal intensity V it is useful to use the closed conductive shell. If the external MF frequency $f < f_0$, it is useful to use the circular passive loop with radius $2R$.

Conclusions.

1. Analytical expressions for shielding factors for the circular passive loop and conductive spherical shell are obtained which together with developed numerical model of the cubic shell permit to compare their effectiveness of the external MF shielding at various frequencies.

2. The external MF frequency f_0 is determined which can serve as a criterion of the expediency of the circular passive loop utilization. At the MF frequency less than f_0, the passive loop shielding factor is higher than the shielding factor for the equivalent volume spherical shell. At the MF frequency less than $2f_0$, passive loop shielding factor is higher than the shielding factor for the equivalent volume cubic shell.

REFERENCES

1. International Commission on Non-Ionizing Radiation Protection. ICNIRP Guidelines for limiting exposure to time-varying electric and magnetic fields (1 Hz-100 kHz). *Health Physics*, 2010, vol.99, no.6, pp. 818-836. **doi: 10.1097/HP.0b013e3181f06c86.**

2. Korol' E.G., Pantelyat M.G. EMC requirements of technical devices at electric power facilities and industrial. *Visnyk NTU «KhPI» – Bulletin of NTU «KhPI»*, 2013, no.15, pp. 35-60. (Rus).

3. Rozov V.Yu. Assuirov D.A. Method of the active shielding of technical objects external magnetic field. *Tekhnichna elektrodynamika – Technical electrodynamics*, 2006, no.3, pp. 13-16. (Rus).

4. Kuznetsov B.I., Nikitina T.B., Bovdui I.V., Voloshko A.V., Vinichenko E.V., Kotliarov D.A. Active screening of magnetic field near power station generator buses. *Elektrotekhnika i elektromekhanika – Electrical engineering & electromechanics*, 2013, no.6, pp. 66-71. (Rus).

5. Kaden H. Wirbelströme und Schirmung in der Nachrichtentechnik. – Springer Berlin Heidelberg, 1959. **doi: 10.1007/978-3-540-32570-3**.

6. Buccella C., Feliziani M., Maradei F., Manzi G. Magnetic field computation in a physically large domain with thin metallic shields. *IEEE Transactions on Magnetics*, 2005, vol.41, no.5, pp. 1708-1711. **doi: 10.1109/TMAG.2005.846059**.

7. Kistenmacher P., Schwab A. Low-frequency shielding effectiveness of inhomogeneous enclosures. *Proceedings of IEEE International Symposium on Electromagnetic Compatibility*, 1996, pp. 347-352. **doi: 10.1109/ISEMC.1996.561256**.

8. Clairmont B.A., Lordan R.J. 3-D modeling of thin conductive sheets for magnetic field shielding: calculations and measurements. *IEEE Transactions on Power Delivery*, 1999, vol.14, no.4, pp. 1382-1393. **doi: 10.1109/PESW.1999.747382**.

9. Roginskiy V.Yu. *Ekranirovanie v radioustroystvah* [Shielding in radio devices]. Leningrad, Energiya Publ., 1969. 112 p. (Rus).

10. Grinchenko V.S., Chunikhin K.V. Shielding of a uniform alternating magnetic field using a circular passive loop. *Elektrotekhnika i elektromekhanika – Electrical engineering & electromechanics*, 2015, no.2, pp. 31-34. (Rus).

Received 11.01.2016

V.S. Grinchenko[1], *Candidate of Technical Science,*
K.V. Chunikhin[1],
N.V. Grinchenko[2], *Candidate of Technical Science,*
[1] State Institution «Institute of Technical Problems of Magnetism of the NAS of Ukraine»,
19, Industrialna Str., Kharkiv, 61106, Ukraine,
e-mail: vsgrinchenko@gmail.com, kvchunikhin@gmail.com
[2] Ukrainian State University of Railway Transport,
7, Feuerbach Sq., Kharkiv, 61050, Ukraine.

How to cite this article:
Grinchenko V.S., Chunikhin K.V., Grinchenko N.V. Low-frequency magnetic field shielding by a circular passive loop and closed shells. *Electrical engineering & electromechanics*, 2016, no.2, pp. 20-23. doi: 10.20998/2074-272X.2016.2.03.

UDC 621.3.013 **doi: 10.20998/2074-272X.2016.2.04**

A.V. Yerisov, K.D. Pielievina, D.Ye. Pelevin

CALCULATION METHOD OF ELECTRIC POWER LINES MAGNETIC FIELD STRENGTH BASED ON CYLINDRICAL SPATIAL HARMONICS

Purpose. Simplification of accounting ratio to determine the magnetic field strength of electric power lines, and assessment of their environmental safety. Methodology. Description of the transmission lines of the magnetic field by using techniques of spatial harmonic analysis in the cylindrical coordinate system is carried out. Results. For engineering calculations of electric power lines magnetic field with sufficient accuracy describes their first spatial harmonic magnetic field. Originality. Substantial simplification of the definition of the impact of the construction of transmission line poles on the value of its magnetic field and the bands of land alienation sizes. Practical value. The environmentally friendly projection electric power lines on the level of the magnetic field. References 6, tables 1, figures 4.

Key words: **electric power line, magnetic field, environmental safety, cylindrical spatial harmonics.**

На основе пространственного гармонического анализа магнитного поля в цилиндрической системе координат предложен метод расчета индукции магнитного поля линий электропередачи. Показано, что магнитное поле линий электропередачи с достаточной для инженерных расчетов точностью описывается первой цилиндрической пространственной гармоникой. Использование предложенного метода позволяет существенно упростить определение влияния конструкции опор линий электропередачи на величину их магнитного поля и на ширину полос отчуждения земельных участков. Библ. 6, табл. 1, рис. 4.

Ключевые слова: **линия электропередачи, магнитное поле, цилиндрические пространственные гармоники.**

Introduction. One of the problems solved by the designers of overhead transmission lines (TL) in assessing their environmental safety is determination of dimensions $\pm X_s$ of the trackside width, as shown in Fig. 1. Among the factors which determine the width of the strips are installed on their border $\pm X_s$ limits [1, 2] of the value of the module of the magnetic field (MF) strength vector B_l produced by TL at the height h_0 of the earth's surface. Under these restrictions, the value of the module B_l away $-X_s \ge x \ge X_s$ from the TL should be less than the specified value B_s of the magnetic field strength. Borders $(-X_s; +X_s)$ of the strip of alienation by the parameter B_s are determined by the calculated dependence (magnetograms) of the TL magnetic field strength module B_l (Fig. 1).

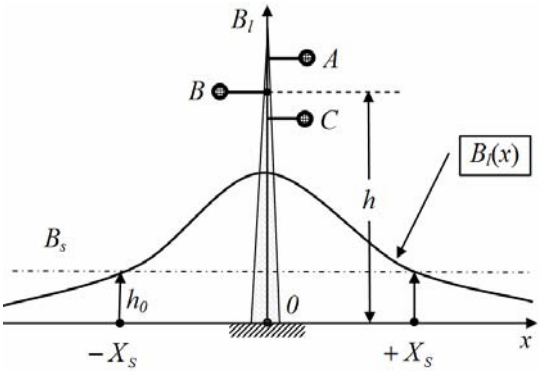

Fig. 1. Magnetograms of the TL

Problem definition. To simplify the calculation of the MF of the TL in the far field (at the border of the exclusion zone of the TL) multidipole transmission line models [3], based on the use of spherical spatial harmonics are utilized. At the same calculation relations are quite complex, and final calculation results are, as a rule, in numerical format, which complicates the practical need to establish cause – effect relationships between design parameters of transmission lines and distribution of their MF strength.

The goal of the work is to simplify the settlement of relations to determine the MF strength of the TL and evaluate their environmental safety.

The goal of the work proposed to be carried through the use of cylindrical space harmonics to calculate the magnetic field strength of the TL.

Presentation of research materials. At the description of the TL magnetic field we assume that:

- Phase conductor lines are parallel current filaments of infinite length and infinitely small diameter.
- Line currents $\dot{I}_A$, $\dot{I}_B$ $\dot{I}_C$ form a symmetrical system:

$$\dot{I}_A = I\ ,\ \dot{I}_B = \alpha^2 I\ ,\ \dot{I}_C = \alpha I\ , \qquad (1)$$

where $a = e^{j4\pi/3}$.

Under what assumptions spatial harmonic analysis of the magnetic field of the TL can be made in a cylindrical coordinate system (r, φ, Y) which Y-axis passes through the center of a circle of minimum radius $r_{\min}$ where all current filaments fit (Fig. 2).

Relation (1) allows to represent module of the magnetic field strength $B_l(x)$ of three-phase line at an arbitrary point in space P as the modulus of the sum of the magnetic field strengths $\vec{B}_{A-0}(P)$, $\vec{B}_{B-0}(P)$, $\vec{B}_{C-0}(P)$ respectively of three independent closed broaching circuits $A-0$, $B-0$ и $C-0$ (see Fig. 2).

$$B_s(P) = \left|\vec{B}_{A-0}(P) + \vec{B}_{B-0}(P) + \vec{B}_{C-0}(P)\right|. \qquad (2)$$

When the selected track (along the Y-axis) of passing of inverse wires with currents, $-\dot{I}_A$, $-\dot{I}_B$ and $-\dot{I}_C$ the position of each of three circuits define respectively filaments coordinates of phases A, B, C.

Spatial harmonic analysis of the MF of a closed current circuit. There is a closed current circuit, for example, $A-0$ (Fig. 2).

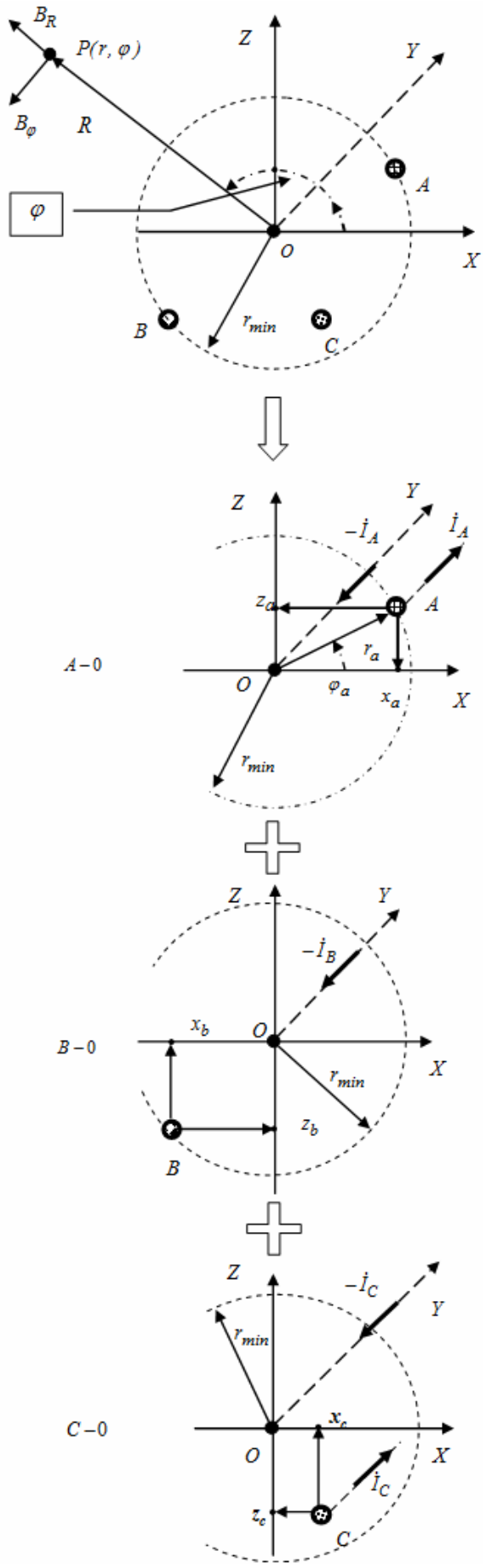

Fig. 2. Representation of a three-phase line as three independent circuits

Vector potential $A_{(A-0)Y}$ of the magnetic field of such a circuit in the arbitrary point of the space $P(r,\varphi,Y)$ is determined as a sum of the corresponding vector potentials A_{ay}, A_{oy} of the current of the phase A and the opposite current and taking into account [4] it can be determined by the relation

$$A_{(A-0)y} = A_{oy} + A_{ay} = \mu_0 \frac{I}{2\pi} \ln r - \\ - \mu_0 \frac{I}{2\pi} \ln \sqrt{\left(r^2 + (r_a)^2 - 2rr_a \cos(\varphi - \varphi_a)\right)}. \quad (3)$$

Relation (3) can be represented as Fourier series after that for the external region ($r \geq r_{\min}$) it will have the known form [5]

$$A_{(A-0)Y} = \mu_0 \frac{I}{2\pi} \sum_{n=1}^{N} \left(\frac{1}{r}\right)^n \left(\frac{(a_{an} \cos n\varphi + b_{an} \sin n\varphi)}{n}\right), \quad (4)$$

where a_{an}, b_{an} are the amplitudes of the n-th order of the magnetic field's vector potential of the current circuit A–0

$$a_{an} = (r_a)^n \cos n\varphi_a, \; b_{an} = (r_a)^n \sin n\varphi_a . \quad (5)$$

Magnetic vector potential's harmonics (4) determine also the corresponding harmonics of its magnetic field strength B_{ar} and $B_{a\varphi}$:

$$B_{ar} = \frac{\mu_0}{r} \frac{dA_{(A-0)Y}}{d\varphi} = \frac{\mu_0 I}{2\pi} \sum_{n=1}^{\infty} \frac{[a_{an} \sin n\varphi + b_{an} \cos n\varphi]}{r^{n+1}}, \quad (6)$$

$$B_{a\varphi} = \frac{\mu_0}{2\pi} \frac{dA_{(A-0)y}}{dr} = -\frac{\mu_0 I}{2\pi} \sum_{n=1}^{\infty} \frac{(a_{an} \cos n\varphi + b_{an} \sin n\varphi)}{r^{n+1}}. \quad (7)$$

Magnetic field strength module B_{an} of the n harmonic in the point $P(r,\varphi,Y)$ will be dependent on the r-coordinate

$$B_{an} = \mu_0 \frac{I}{2\pi \cdot r^{n+1}} \sqrt{(a_{an})^2 + (b_{an})^2} . \quad (8)$$

Table 1 represents values of amplitudes a_{an}, b_{an} of two first harmonics for the circuit A–0 in the coordinate system X, Y, Z (Fig. 2).

Table 1

Amplitudes of the magnetic field strength harmonics for the current circuit A – 0

Amplitude of harmonics	Relations for the circuit with coordinates x_a, z_a
a_{a1}	x_a
b_{a1}	z_a
a_{a2}	$(x_a)^2 - (z_a)^2$
b_{a2}	$2x_a \cdot z_a$

This format of the amplitudes a_{an}, b_{an} representation harmonizes well with the design document for TL pylons which regulates coordinates of points of suspension of its wires with respect to earth surface.

By analogy with (5) amplitudes of harmonics a_{bn}, b_{bn} and a_{cn}, b_{cn} of circuits B – 0 and C – 0 are respectively determined:

$$a_{bn} = \alpha^2 \cdot (r_b)^n \cos n\varphi_b, \; b_{bn} = \alpha^2 \cdot (r_b)^n \sin n\varphi_b, \\ a_{cn} = \alpha^2 \cdot (r_c)^n \sin n\varphi_c, \; b_{cn} = \alpha^2 \cdot (r_c)^n \sin n\varphi_c. \quad (9)$$

The structure of series (6), (7) is such that as r increases the contribution of high-order harmonic components in the magnetic field strength B_r and B_φ reduces.

So, the magnetic field strength at a distance of two-wire line $x \geq r_{min}$ is described mainly by its first (n = 1) harmonic constructed as illustrated by equation (8) magnetogram in Fig. 3. It also presents the results of calculations by the Biot-Savart-Laplace low in accordance with [6].

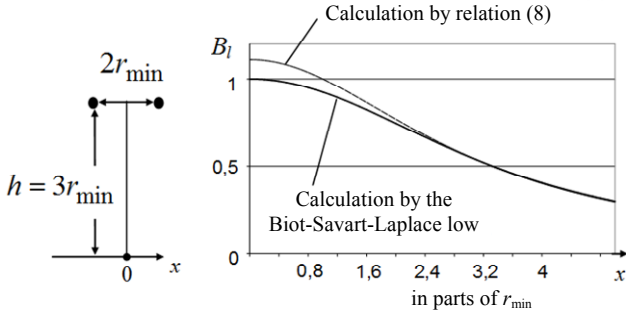

Fig. 3. Magnetograms of B_l of a two-wire line at unit current I

Comparison of the calculation results (Fig. 3) shows that the distance from the transmission line axis at a distance of more than r_{min} the error of the proposed method in comparison with the exact method [6] does not exceed 10 %, which confirms the possibility of using the first cylindrical space harmonics to calculate the MF of the TL at the boundary of their protected areas.

The magnetic field of single-circuit TL. Single circuit lines have one set of phase conductors. Their relative positions to each other and the Earth's surface determines the design of the (profile) of a TL pylon.

According to that shown in Fig. 2 «magnetic» interpretation of the transmission line, amplitudes a_{ln} and b_{ln} of harmonics of its magnetic field taking into account (1) and (2) are presented in the form of a sum corresponding to the amplitude of its independent circuits A–0, B–0, C–0:

$$a_{ln} = a_{an} + \alpha^2 a_{bn} + \alpha a_{cn}, b_{ln} = b_{an} + \alpha^2 b_{bn} + \alpha b_{cn}. \quad (10)$$

The first significant harmonic of single-circuit TL is the harmonic of the order (n = 1). Its amplitudes a_{ln} and b_{ln} taking into account (5), (10) equal:

$$a_{l1} = x_a + \alpha^2 \cdot x_b + \alpha \cdot x_c, b_{l1} = z_a + \alpha^2 \cdot z_b + \alpha \cdot z_c. \quad (11)$$

It should be note that values of the amplitude a_{l1} and $b_{l1\ of\ the}$ first harmonic (n = 1) do not depend on the beginning of the selected coordinate system X, Y, Z.

Knowledge of amplitudes of the first harmonic a_{l1} and b_{l1} of the magnetic field of the TL allows by using the relation (7) to build its magnetogram

$$B_l(x) \approx B_{l1}(x) = \mu_0 I \frac{\left|\sqrt{(a_{l1})^2 + (b_{l1})^2}\right|}{2\pi \cdot \left((h - h_0)^2 + x^2\right)}, \quad (12)$$

where h is the distance from the ground level (Fig. 1) to the center of the circle r_{min} which fit all current lines of the TL.

For ease of calculation the distance h can be set equal to the average height h_a, h_b, h_c of the respectively suspension of phase conductors A, B and C

$$h \approx 1/3\left(h_a + h_b + h_c\right). \quad (13)$$

After simple but cumbersome transformations the relation (12) can be reduced to the form:

$$B_l(x) \approx \mu_0 I \frac{d_{rms}}{2\sqrt{2}\pi \cdot \left((h - h_0)^2 + x^2\right)}, \quad (14)$$

where d_{rms} is the mean square distance between the wires of the TL

$$d_{rms} = \sqrt{(d_{AB})^2 + (d_{BC})^2 + (d_{CA})^2},$$

where d_{AB}, d_{BC}, d_{CA} is the distance between the suspension points on a support phase wires A and B, B and C, C and A, respectively.

Analytical representation of magnetograms (14) permits to determine the size of the band $\pm X_s$ of the exclusion for a given parameter B_l

$$\pm X_s = \sqrt{\frac{\mu_0 \cdot I \cdot d_{rms}}{2\sqrt{2} \cdot \pi \cdot B_l} - (h - h_0)^2}. \quad (15)$$

This relationship establishes a mutual relationship between the size $\pm X_s$ of the strip of alienation and TL characteristics – its current (I) loading and designs (profile) of its pillars, namely the average height h of wires suspension points and mean square distance d_{rms} between them.

Underground cable TL. Magnetograms of underground cable lines, similar to the single-circuit air TL are determined by the first (n = 1) harmonic of their magnetic field strength.

Below relations for magnetograms for two most commonly used cable laying (Fig. 4) obtained by taking into account (8) and (14) are presented.

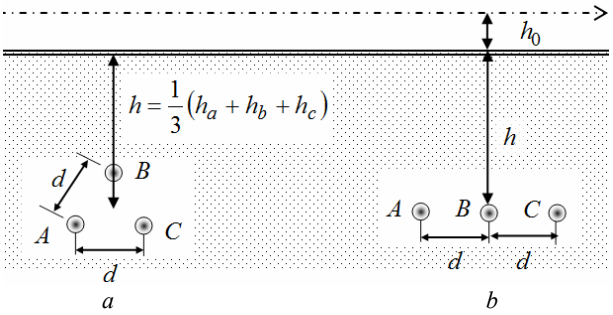

Fig. 4. «Triangle» (a) and «flat» (b) cable line laying

For the cable «flat laying»

$$B_l(x) \approx \mu_0 I \frac{\sqrt{3} \cdot d}{2\ \pi \cdot \left((h + h_o)^2 + x^2\right)}. \quad (16)$$

For the cable laying by «triangle»

$$B_l(x) \approx \mu_0 I \frac{\sqrt{3} \cdot d}{2\sqrt{2} \cdot \pi \cdot \left((h + h_o)^2 + x^2\right)}. \quad (17)$$

Conclusions.

1. It is shown that for the calculation of the magnetic field strength of transmission lines on the border of protected zones with limited accuracy (less than 10%), the first cylindrical space harmonic of its magnetic field can be used.

2. The simplified calculation relations of the magnetic field strength of the TL based on cylindrical spatial harmonics, allowing to simplify the calculation of the TL magnetic field distribution and assess the impact of the TL design peculiarities on the width of the land rights of way to ensure environmental safety are proposed.

REFERENCES

1. *Pravyla ulashtuvannja elektroustanovok 5-te vyd., pererobl. j dopovn. (stanom na 22.08.2014)* [Electrical Installation Regulations. 5 edition, Revised and enlarged (as of 22/08/2014)]. Kharkiv, Fort Publ., 2014. 800 p. (Ukr).

2. Stepanov I.M. Constructive modification reducing the intensity of the magnetic field on the tracks of overhead and cable power lines. *ELEKTRO. Elektrotekhnika, elektroenergetika, elektrotekhnicheskaia promyshlennost' – ELEKTRO. Electrical engineering, power industry, electrical industry*, 2009, no.3. pp. 36-41. (Rus).

3. Rozov V.Yu., Reutskyi S.Yu., Pelevin D.Ye., Pyliugina O.Yu. The magnetic field of power transmission lines and the methods of its mitigation to a safe level. *Tekhnichna elektrodynamika – Technical Electrodynamics*, 2013, no.2, pp. 3-9. (Rus).

4. Shtafl M. *Elektrodinamicheskie zadachi v elektricheskikh mashinakh i transformatorakh* [Electrodynamic problems in electrical machines and transformers]. Moscow, Leningrad, Energiia Publ., 1966. 200 p. (Rus).

5. Jabłoński P. Cylindrical conductor in an arbitrary time-harmonic transverse magnetic field. *Przegląd Elektrotechniczny – Electrotechnical Review*, 2011, no.5, pp. 49-53.

6. Rozov V.Yu., Reutskyi S.Yu., Pyliugina O.Yu. Method of calculating the magnetic field of three-phase power lines. *Tekhnichna elektrodynamika – Technical Electrodynamics*, 2014, no.5, pp. 11-13. (Rus).

Received 04.12.2015

A.V. Yerisov[1],
K.D. Pielievina[1],
D.Ye. Pelevin[1], *Candidate of Technical Science,*
[1] State Institution «Institute of Technical Problems of Magnetism of the NAS of Ukraine»,
19, Industrialna Str., Kharkiv, 61106, Ukraine.
phone +380 572 992162,
e-mail: erisov@yandex.ua, pelevindmitro@ukr.net

How to cite this article:
Yerisov A.V., Pielievina K.D., Pelevin D.Ye. Calculation method of electric power lines magnetic field strength based on cylindrical spatial harmonics. *Electrical engineering & electromechanics*, 2016, no.2, pp. 24-27. doi: 10.20998/2074-272X.2016.2.04.

UDC 621.3.015.52 **doi: 10.20998/2074-272X.2016.2.05**

M.I. Baranov

A NEW HYPOTHESIS AND PHYSICAL BASES OF ORIGIN OF ROSARY LIGHTING IN THE ATMOSPHERE OF EARTH

Purpose. Development and scientific ground of new hypothesis of origin of rosary lightning (RL) is in the air atmosphere of Earth. Methodology. Electrophysics bases of technique of high (ever-higher) impulsive voltage and large (weak) impulsive currents, and also theoretical bases of quantum physics. Results. The substantive provisions of new hypothesis of origin are formulated RL. Taking into account these positions bases of close electrophysics theory of origin are developed in an air atmosphere RL. Basic electrophysics terms, resulting in the transition of linear lightning (LL) in RL, are indicated. Originality. First on the basis of conformities to the law of quantum physics the new electrophysics mechanism of education is offered RL from LL. It is set that this mechanism the wave longitudinal distributing of drifting lone electrons is underlaid in the plasma cylindrical channel of a long spark storm digit in an air atmosphere, resulting in forming in him of «light» («hot») and «dark» («cold») longitudinal areas of periodic electronic wavepackages (EWP). It is shown that for LL information the areas of EWP periodically up-diffused along the channel of lightning are characterized the small and unnoticeable for observers lengths, and for RL − by large lengths and by sight noticeable for observers from earth. Practical value. Deepening of scientific knowledges about physics of such global atmospheric phenomenon as lightning. Expansion of scientific presentations of humanity about circumferential tellurians nature and difficult natural physical processes, flowings in it. References 15, figures 4.

Key words: **linear lightning, rosary lightning, physical bases, plasma channel of a storm discharge, drifting lone electrons, electronic wavepackages, «hot» («light») and «cold» («dark») longitudinal areas of electronic wavepackages of channel of a storm discharge.**

Приведены новая гипотеза и базирующиеся на ней физические основы возникновения в воздушной атмосфере Земли чёточной молнии (ЧМ). Показано, что в основе электрофизического механизма формирования этого вида молнии находится волновое продольное распределение свободных электронов, движущихся в плазменном канале линейной молнии (ЛМ) на стадии протекания в нем длительной компоненты тока грозового разряда. Из-за малой плотности тока в плазменном канале ЛМ на данной стадии разряда в нем происходит образование таких относительно длительно существующих волновых электронных пакетов, которые характеризуются сравнительно большими и поэтому визуально видимыми наблюдателями вначале ЛМ и затем ЧМ размерами своих периодически распределенных вдоль канала молнии «горячих» («светлых») и «холодных» («темных») продольных участков. Библ. 15, рис. 4.

Ключевые слова: **линейная молния, чёточная молния, физические основы, плазменный канал грозового разряда, дрейфующие свободные электроны, волновые электронные пакеты, «горячие» («светлые») и «холодные» («темные») продольные участки волновых электронных пакетов канала грозового разряда**.

Introduction. Well-known and most studied kind of powerful natural electrical short-time spark discharge in the air atmosphere of the Earth is the linear lightning (LL) [1-4], the appearance of which is shown in Fig. 1.

Fig. 1. General view of the brightly glowing plasma channel in the atmosphere of the long spark discharge of the LL between the positive charged cloud and ground [5]

As a rule, the length of the plasma channel between LL storm cloud with a negative (positive) U_L potential to ± (30-50) MV and the ground is measured in hundreds of meters, and the limit can be up to several kilometers [1-5]. The diameter of the plasma channel of LL in air in accordance with the [1-5] can range from tens of centimeters to several meters. Currently, LL physics thanks to the results of theoretical and experimental work by domestic [2-4] and foreign scientists and experts [1], presented in the review of the monograph [5] is presented at a high scientific and technical level. However, so far in the engineering and electrophysics of high voltages, the technique of large (small) pulse currents, as well as low- and high-current technique of long (short) sparks in the gas (air) medium lacking scientific and technical data, or strictly even approximately explain the transformation (though not as often and not always) in an air atmosphere LL later in rosary lighting (RL). The emergence of the RL, or «*bead lightning*» [1] in the electrically active air

atmosphere is a well-established scientific fact, documented by numerous visual observers of this relatively rare and interesting natural atmospheric phenomena [1, 5, 6]. Existing RL theories today are based on the fact that this kind of lightning in extrahigh voltage two-electrode system «charged cloud - earth» [1, 6]:

1) is the result of periodic interruption of the plasma channel lightning cloud or rain;

2) due to the instability of the plasma lightning discharge channel with a longitudinal shock because it arises in the pinch effect, leading to its transverse «waist» and education channel of sausage type;

3) is a series of sphere-like arc discharge, appearing on the site of an earlier «waste» a large pulse current of a lightning discharge plasma channel LL in the final stage of a long course of it a small continuous current;

4) caused by the relatively long emission of longitudinal sections of a cylindrical plasma channel LL having an unusually large radius. The past decade with the advent of the scientific world in these RL theories have shown that these theoretical approaches have been poorly reasoned, and in the end not scientifically consistent.

In this context, the development of a new approach to scientific explanation of the origin and the short time of existence in an air atmosphere of such natural phenomena as the RL is an **actual** scientific and technical problem, research expands our knowledge of the surrounding nature and the physical processes occurring in it.

1. Problem definition. We consider from the electrophysical position the formation and flow of LL in an air atmosphere at altitudes up to 1000 m, containing in its composition many entrained upward (downward) by air currents atoms of various chemical elements, including nitrogen *N*, oxygen *O*, carbon *C*, silicon *Si*, sulfur *S*, iron *Fe*, lead *Pb* and others. Some of these atoms produced are molecules of various oxides substances are in an air atmosphere, especially by-products of combustion and the organic fuel oxidation in thermal power stations and large industrial enterprises, rising from the tall chimneys of the earth's atmosphere with the hot flue waste of their continued operation. Note that the current of LL at these altitudes the air in the atmosphere is characterized by two main components [7, 8]: pulse *A*-component (with normalized amplitude I_{mL} of up to 200 kA and a duration τ_p till 0.5 ms) and long-term *C*-component (with averaged I_{mL} value over 200 A and duration τ_p till 1000 ms). We suppose that in the event of an air atmosphere plasma channel LL these atoms (molecules) of matter and their oxides are involved in the complex physical processes occurring in the «thin» the atomic level in the core of the channel having a local cylindrical configuration. Without going at this stage in these processes, we note only that these substances will microformations due to the high temperature in the plasma channel LL (order $(20\text{-}30)\cdot10^3$ K [9]) undergo ultrafast processes of impact and thermal ionization. These atoms (molecules) of a substance will be the main «suppliers» of additional free electrons in the LL channel, the electron temperature T_e of which will support and determine its aforementioned heat flow as it pulsed stage *A*-component of the current and the flow step it prolonged the *C*-component of the current of the lightning discharge. We assume that the motion of free electrons in the plasma channel LL determines the transfer of electrical charge from both the negatively charged part of the storm cloud to ground *(«lightning of negative polarity»)*, and by the negatively charged surface of the earth to the positively charged part of the storm cloud («*lightning positive polarity*»). Required to consider on the basis of known scientific principles possibility of RL by a certain transformation in her stage LL flow in its long plasma channel *C*-components of the lightning current as well as establish the main electrical conditions in the plasma channel LL and air atmosphere, providing a transformation of one type of lightning in another.

2. The formulation of the proposed hypothesis of the RL forming in an air atmosphere. According to [10] the term «*hypothesis*» comes from the Greek word meaning «*assumption*» Applied to our case this term will mean a scientific hypothesis put forward to explain the nature of physical phenomena in the RL, sometimes flowing in electrically active air atmosphere. By definition, this assumption requires experimental verification and theoretical justification in order to be credible scientific theory. Experimental verification of the phenomenon of the RL was made earlier by his numerous foreign observers [1, 6]. According to the experimental data given in [5, 6], RL leakage occurs at the end of the LL. The RL compared to the LL is characterized by relatively large time of its existence [1, 6]. Fig. 2,*a*,*b* show the main phase flow of LL and RL, filmed by observers of natural electrophysical phenomena and presented in [5, 6]. In Fig. 3 an enlarged form on the former site of the plasma channel LL presented some «light» rosaries of RL separated in the area of the channel of lightning from each other «dark» rosary of RL. Based on the currently available conclusive experimental data obtained in direct RL observations in air [1, 6], and the set of fundamental theoretical and experimental laws wave longitudinal distribution of drifting electrons in the metal conductors with a pulsed current [11], proposed here the hypothesis of occurrence and development in the air atmosphere of the RL includes the following main provisions:

- RL is a specific kind of electrical short-long spark discharge in air arising at the final stage of the flow in the air atmosphere of LL;
- RL appears on the stage of the flow in the plasma channel LL cylindrical shape relatively large diameter long-term *C*-component of the current lightning, which is characterized by continuous currents in the hundreds and tens of Amperes at the length of their flow channel is not less than 1 s;

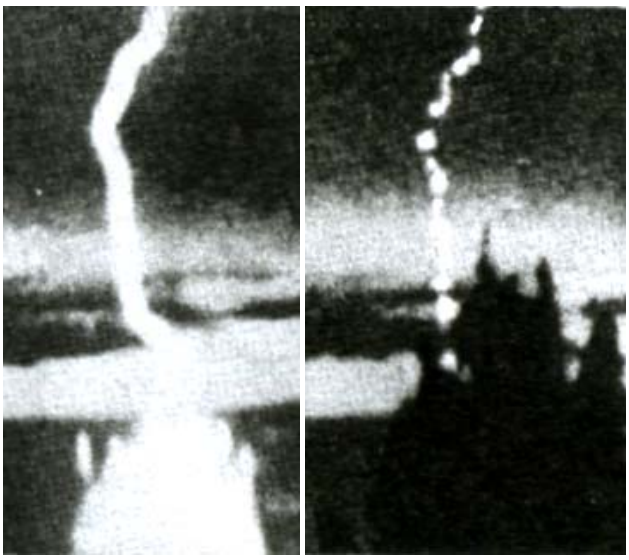

a *b*

Fig. 2. Main phases of flow in the area of the plasma channel curved lightning initially the LL (a), and then the RL (b) in an air atmosphere of the Earth [5, 6]

Fig. 3. General view of the individual «light» and «dark» rosaries of the RL observed from the ground in an air atmosphere [5, 6]

- zone of the RL appearance is the main plasma channel LL, and the duration of the RL of existence in an air atmosphere of the Earth is determined by the duration of the flow of small continuous current at a stage long-term *C*-component of the lightning current components;
- electronic current conduction in a plasma cylindrical channel LL and subsequently arising on its basis a modified plasma channel RL obeys the laws of quantum physics, and is characterized by the data channels corresponding wave periodic longitudinal and radial distribution of their drifting free electrons initially in the high channel LL, and then in low-current RL channel;
- RL is a result of electrophysical transformation occurring in the plasma channel LL with a large pulse current *A*- component of the wave electron packets (WEP) with small and not visible to observers LL their lengths periodically distributed along the channel of the lightning discharge on the «hot» («light») and «cold» («dark») longitudinal sections in the WEP with large and therefore visually visible from the ground observers RL lengths of its relatively «hot» («light»), and «cold» («dark») longitudinal sections periodically along a modified plasma RL channel.

3. Scientific substantiation of the proposed hypothesis of the RL origin in an air atmosphere. To begin with, the WEP in the plasma channel of the lightning discharge on its initial and final stages flow similar to the WEP, introduced and used in the study [11] the periodic wave longitudinal and radial distributions drift of free electrons in the crystal structure of metal wires with DC, AC and pulsed electric current, a relatively «hot» with length Δz_{hn} and «cold» with length Δz_{hn} quantized longitudinal portions. The sum of the lengths of these sections ($\Delta z_{hn}+\Delta z_{cn}$) forms a quantized step of WEP longitudinal periodic structures in the plasma channel of lightning. Moreover, the value of the step ($\Delta z_{hn}+\Delta z_{cn}$) is always equal to the length of the half-wave quantized $\lambda_{en}/2$ de Broglie for drifting in the channel of free electrons lightning. In turn, the value of $\lambda_{en}/2$ in the plasma lightning channel is performed as follows quantum mechanical ratio:

$$\lambda_{en}/2 = l_k/n, \qquad (1)$$

where l_k is the length of the cylindrical plasma channel of lightning; n = 1,2,3,..., n_m is the integer quantum number; $n_m=2n_k^2$ is the maximum value of the quantum number n [11]; n_k is the principal quantum number of atoms ionized matter [12] presenting in the plasma channel of the lightning discharge in the air atmosphere of the Earth in the course of the stage it pulsed *A*- and long-term *C*-components of the lightning current.

From (1) we see that the minimum value of the half-wave length of the electron de Broglie $\lambda_{en}/2$ in the plasma lightning channel will correspond to the maximum value of the quantum number $n = n_m$. Following classical quantum mechanical ratio can be used in the estimations of minimum average $\lambda_{en}/2$ de Broglie half-wave length for drift of free electrons in the plasma channel of a lightning discharge [12]:

$$\lambda_e/2 = h/2(m_e v_D), \qquad (2)$$

where $h = 6.626\cdot10^{-34}$ J·s is the Plank constant; $m_e=9.108\cdot10^{-31}$ kg is the electron rest mass; $v_D=\delta_m/(e_0 n_{e0})$ is the maximum value of the mean free electron drift velocity in the plasma channel of lightning, are formed when electric breakdown of long air gap in the discharge system «charged cloud - ground»; $\delta_m\approx4I_{mL}/(\pi d_k^2)$ is the maximum value of the current density in the plasma channel lightning of diameter d_k; $e_0=1.602\cdot10^{-19}$ C is the module of the electron's electrical charge; n_{e0} is the average value of the density of free electrons drifting in the plasma channel of lightning.

3.1. Assessment of the minimum lengths of the «hot» Δz_{hL} and «cold» Δz_{cL} longitudinal sections of WEP for LL. According to the calculated and experimental data presented in [11, 13], the «hot» WEP longitudinal sections in a round metallic conductor with a pulse current of high density in comparison with its «cold» longitudinal portions substantially different levels of electron temperature T_e (about 3.5 times). Caused by this feature is enhanced, compared with the average initial (up to the current flow) in a cylindrical volume conductor drifting concentration of free electrons in the «hot» longitudinal sections of WEP, the middle of which correspond to the amplitudes of propagating along the conductor of electronic half-waves of de Broglie. At the same time in the «cold» longitudinal sections of the conductor due to the wave nature of the distribution of its cylindrical volume drift of free electrons occurs reduced bulk density of considered microcarriers of the charge. As a result of the longitudinal wave drifting periodic distribution of free electrons in a conductor is formed by a non-uniform longitudinal periodic temperature field. In addition, according to [14], the experimental study the phenomenon of the electric explosion (EE) in the air thin round copper wires (length is 60 mm, diameter is 100 mm) by passing-of them from the high-voltage generator of impulse currents (GIC) sine decaying exponentially discharge current of high density ($\delta_m \approx 6.4 \cdot 10^{12}$ A/m^2) in the explosive destruction of the products dispersed solid copper (in fact, in «metal» plasma) by the high-speed photorecording method periodic strata were recorded, consisting of layered longitudinal periodic disk-like structures of varying luminosity containing alternating between a «light» width Δz_h and «dark» width Δz_c longitudinal sections. These areas formed in pairs in the low-current discharge air gap GIS with «metallic» plasma step periodic structure WEP length about $(\Delta z_h + \Delta z_c) \approx 1.76$ mm. Obviously, in the case of the specified EV thin copper wires «light» longitudinal sections of his «metal» of the plasma in the discharge air gap correspond to «hot» areas of WEP and its «dark» longitudinal sections - «cold» WEP areas. In this regard, quite reasonable to say that the «hot» longitudinal sections of a minimum length Δz_{hL} in the plasma channel of lightning arising in extra high discharge air gap system «charged cloud - earth», will meet his «light» longitudinal sections, and «cold «longitudinal sections Δz_{cL} minimum length of the plasma channel of lightning – its «dark» longitudinal sections. Fig. 4 schematically shows the quality «hot» («light»), and «cold» («dark») periodic longitudinal sections WEP plasma channel of lightning, which occurs in an air atmosphere of the Earth.

Minimum length Δz_{hL} of «hot» («light»), a longitudinal section of WEP in the plasma channel LL formed in the extra high discharge air gap system «charged cloud – land», on the basis of quantum mechanical uncertainty Heisenberg relations [12] with regard to drifting it (this channel) free electrons can be approximately determined from the following analytical expression [13]:

$$\Delta z_{hL} \approx e_0 n_{e0} h (m_e \delta_m)^{-1} / [8 + (\pi - 2)^2]. \qquad (3)$$

For the numerical evaluation by (3) of Δz_{hL} values we assume that the plasma channel high current flow in the LL stage it pulse *A*-components of the lightning current has the following initial geometrical and electrical parameters [1, 8, 12]: $d_k \approx 1$ m; $n_{e0} \approx 10^{25}$ m^{-3}; $I_{mL} \approx 100$ kA; $\delta_m \approx 1.27 \cdot 10^5$ A/m^2. Then from (3) follows that $\Delta z_{hL} \approx 1$ mm. With regard to (2) the minimum average length $\lambda_e/2$ of half-wave of de Broglie for the case we would be roughly equal $\lambda_e/2 \approx 0{,}5 e_0 n_{e0} h (m_e \delta_m)^{-1} \approx 4.6$ mm. As a result, the minimum length Δz_{cL} of «cold» («dark») of a longitudinal section of WEP in the plasma channel LL at this stage of development of its plasma channel will take the numerical value of about $\Delta z_{cL} \approx \lambda_e/2 - \Delta z_{hL} \approx 3.6$ mm. It is seen that values of Δz_{hL} and Δz_{cL} for «hot» («light») and «cold» («dark») periodic longitudinal sections of WEP almost three orders of magnitude smaller than the diameter of the plasma channel d_k lightning at the stage of formation and flow in it LL. Visually capture the viewer from the ground such sites WEP for LL is almost impossible.

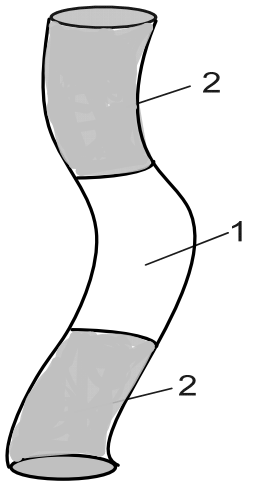

Fig. 4. Schematic scaleless image of the «hot» («light») and «cold» («dark») longitudinal sections of the periodic structure of WEP in the plasma of the curvilinear channel of lightning, developing in an air atmosphere of the Earth (1 - «light» («hot») segment of the cylindrical channel of lightning; 2 - «dark» («cold») segment of the cylindrical channel of lightning)

3.2. Assessment of the minimum lengths of the «hot» Δz_{hL} and «cold» Δz_{cL} longitudinal sections of WEP for the RL. To do this, we assume that at the stage of the flow in the plasma channel of the lightning discharge of long-term *C*-component of the lightning current adopted diameter of $d_k \approx 1$ m of the channel due to the inertia of the thermal processes in it and in the meantime the order of 0.5 ms has not had time to change and remained so same as in the previous step occurrence

on it a pulse *A*-component of the lightning current component. In addition, we believe that the average concentration (bulk density) n_{e0} free electrons in the case of flow along the plasma channel lightning long-term *C*-component of the lightning current also remained the same and approximately equal $n_{e0}\approx10^{25}$ m^{-3}. Suppose that in this case, a continuous long lightning current is characterized by the following parameters [7, 8]: $I_{mL}\approx100$ A; $\delta_m\approx1.27\cdot10^2$ A/m^2. Substituting these initial data in (3) we see that in this case the minimum length Δz_{hL} of «hot» («light»), a longitudinal section of WEP in the lightning channel will be numerically for about $\Delta z_{hL}\approx1$ m. From the calculated ratio $\lambda_e/2\approx0{,}5e_0n_{e0}h(m_e\delta_m)^{-1}$ we find that at the stage of the flow in the received plasma channel lightning long-term *C*-components of lightning current the minimum average length $\lambda_e/2$ half wave of de Broglie numerically will be approximately 4.6 m. Then, the minimum length Δz_{cL} of «cold» («dark») longitudinal section of WEP in the plasma channel of lightning at the final stage of its course will take the numerical value of about $\Delta z_{cL}\approx\lambda_e/2-\Delta z_{hL}\approx3.6$ m. The quantitative results for longitudinal WEP a plasma channel in step lightning thereon prolonged percolation of lightning current components conclusively indicate that lightning analyzed cylindrical channel may be partitioned into a relatively large and so the «bright» and «dark» detectable visually by observers from the ground surface, longitudinal portions (single rosaries, periodically along the flow path in an air atmosphere described by powerful long spark discharge. Therefore, according to forth herein approximate reporting the results of the RL «born» from the LL flowing in the extra high bit long air gap two-electrode system «charged cloud - land» in the final stages of its existence.

3.3. Evaluation of the possible number of «hot» Δz_{hL} and «cold» Δz_{cL} longitudinal sections of WEP for the RL. Number n_L of individual rosaries, each containing one «hot» («light») and one «cold» («dark») longitudinal section periodically distributed WEP in the plasma channel of the lightning discharge in the RL, taking into account (1) can be formally assessed by the following approximate formula:

$$n_L \approx 2l_k / \lambda_e . \qquad (4)$$

When $l_k\approx460$ m and $\lambda_e/2\approx4.6$ m from (4) we obtain that $n_L\approx100$. Obtained in the first approximation quantitative result for the number n_L of rosaries in the RL is in conflict with a numerical indicator of the maximum value of the quantum number n_m of (1) defined by the principal quantum number n_k of ionized atoms of matter, caught up in the flow area of the cylindrical channel of LL and then RL. Apparently, according to the data given in the above section 1 and staging in the periodic system of chemical elements by D.I. Mendeleev [12], the quantum number $n_m\geq n_L$ applied to the plasma channel of the lightning discharge in the air at $n_k\approx6$ should not exceed $2n_k^2\approx72$. This implies certain restrictions on the numerical values of the possible length l_k of the cylindrical plasma channel of the lightning discharge in the case of occurrence in it's the RL, the minimum length $\lambda_e/2$ of half-waves of de Broglie electron traveling in the channel, and the number of n_L of individual rosaries in the plasma channel of RL.

3.4. Evaluation of the temperature of «hot» Δz_{hL} longitudinal sections of WEP in the plasma channel of RL. We suppose that this temperature due to the initial non-isothermal electron and ion gas in a long high-current discharge channel LL will be determined by the electron temperature T_e of the plasma channel of the lightning discharge flow at the stage it pulse *A*-component of the lightning current. Taking into account the short duration of this stage of development of lightning (about 0.5 ms), the virtual absence of her radial heat transfer from the channel lightning into the surrounding airspace and LL relatively large inertia of thermal processes, to assess the electron temperature T_e of «hot» («light») longitudinal sections of WEP Δz_{hL} length in the plasma channel RL in the light of the approximate calculation of the thermal state of quasi-neutral ionized gas in the air gaps of high-voltage spark gaps, given in [11], we can use the following relation:

$$T_e \approx 5{,}83[I_{mL}^{1/3}/(\sigma_c t_m)]^{1/4}, \qquad (5)$$

where $\sigma_c=5.67\cdot10^{-8}$ W·(m^2·K^4)$^{-1}$ is the Stefan-Boltzmann constant [12]; t_m is the time (in seconds) corresponding amplitude I_{mL} (in Amperes) of lightning current on the electrical percolation stage in its long air spark gap pulse *A*-component of powerful lightning current.

Assuming that at the initial stage of the development of LL $I_{mL}\approx100$ kA and $t_m\approx10$ μs [4], (5) for the electron temperature T_e of «hot» («light») rosaries of RL in the first approximation, we find that it is in the present case It is about $31\cdot10^3$ K. This calculated level of the thermodynamic temperature of the plasma channels of LL and RL corresponds to a known temperature in the spark channels of high-current electrical discharges in gases [8, 9, 11].

3.5. Assessment of the duration of the existence of the RL in air atmosphere. The duration t_L of existence of RL after final stage of LL flow can be estimated from the following relationship:

$$t_L \approx q_L / I_{mL}, \qquad (6)$$

where q_L is the electric charge flowing on the stage of continuous long-term *C*-component of the lightning current with its average value I_{mL} modified due transformed longitudinal sections of WEP plasma channel of LL.

At $q_L\approx200$ C [7, 8] and adopted continuous current value $I_{mL}\approx100$ A at this current stage of formation of the RL the numerical value of the duration t_L of occurrence of this type of lightning will be by (6) of about 2 s. This value t_L is significantly longer than the flow of the LL, including the duration of its initial stage with a large pulse

current *A*-component of the current of lightning and its final stage at the beginning of the course of a long-term *C*-component of the lightning current.

3.6. Assessment of geometrical form of «hot» and «cold» longitudinal sections of WEB for the RL. The geometric shape of individual rosaries of the RL (its «light» and «dark» longitudinal sections) must follow the original configuration of the local cylindrical curved overall length of the plasma channel LL. Boundary zone of «light» and «dark» longitudinal sections of WEP in the RL channel should probably contain the ellipsoidal surface (see Fig. 3) caused no abrupt change in these areas of bulk density n_{e0} of drifting free electrons, and its smooth change of one of the main universal physical laws of our nature – exponential law [15]. Because of the possible longitudinal non-uniformity of distribution of the majority carriers of electricity (free electrons) in a plasma channel RL geometric dimensions (length and diameter) of the individual rosaries («light» and «dark» longitudinal sections periodically changing WEP) may differ from each other, and themselves rosaries acquire a deformed and non-canonical appearance.

4. The formulation of the electrophysical conditions of the emergence of the RL in air atmosphere. We give below the main electrophysical conditions under which, in the author's opinion, the transformation of LL to RL is possible flowing in air atmosphere:

- diameter d_k of the cylindrical channel of the lightning discharge in the air a long discharge gap of extrahigh voltage two-electrode system «charged cloud - land», the value of the large current to flow in this stage of the channel impulse *A*-component of the current of lightning and continuous weak current to flow through it step long-term *C*-components of the lightning current and the average bulk density n_{e0} drift of free electrons in the channel of the lightning discharge should foster it (the lightning channel) such periodic WEP, longitudinal «hot» («light»), and «cold» («dark») sites which vary respectively, in the range of thousandths parts of a meter for the LL to a few tens of meters, and for the RL;
- length l_k of the cylindrical plasma channel of the lightning discharge in the air a long discharge gap extrahigh voltage two-electrode system «charged cloud - ground» and the minimum average length of de Broglie electron half-waves $\lambda_e/2$ in the plasma channel of lightning must satisfy quantum mechanical equation (1);
- in the long air discharge gap extrahigh voltage two-electrode system «charged cloud – ground» and, respectively, in a cylindrical plasma channel lightning should mainly be present are ionized atoms of matter formed with their electronic subshells and free electrons entering the plasma channel of lightning will contribute to the implementation of (1) and $n_L \le n_m$.

In the author's view, failure to comply with the above conditions, in many cases, the flow of air in the atmosphere of the most studied species of lightning as the LL and does not cause the appearance of the RL after LL.

Conclusions.

1. A new hypothesis of such a little-studied natural atmospheric phenomena like the RL and is given in a first approximation, its scientific basis, built on the fundamental laws of quantum physics.

2. It is shown that what may occur in the plasma channel Lee on stage flow through it for at least 1000 ms of continuous long-term *C*-component of the current of lightning with its values in its decline («tail») in the hundreds and tens of Amperes.

3. On the base of the RL electrophysical formation mechanism from LL may lie the transformation of the plasma channel lightning periodic WEP and short (up to a few millimeters in length) «hot» («light») and «cold» («dark») longitudinal sections on phase flow in the «hot» («light») it a pulse *A*-component of the current of lightning discharge in the WEP with their long-term (up to tens of meters in length) and «cold» («dark») longitudinal sections in the final stages of the occurrence of a lightning discharge in its plasma channel continuous long-term *C*-component of the lightning current.

4. The basic electrophysical conditions under which the possible formation of electrically active air atmosphere of the Earth RL, appearing in a modified by this transformation of longitudinal periodic WEP plasma channel of LL at its final stage of development after the leakage of the pulse *A*-component of the lightning discharge current are formulated.

REFERENCES

1. Yuman M.A. *Molniya* [Lightning]. Moscow, Mir Publ., 1972. 327 p. (Rus).

2. Bazelyan E.M., Horin B.N., Levitov V.I. *Fizicheskye i inzhenernye osnovy molniezashchity* [Physical and engineering bases lightning protection]. Leningrad, Gidrometeoizdat Publ., 1978. 223 p. (Rus).

3. Bazelyan E.M, Raiser Yu.P. *Fizyka molnii i molnyezashchita* [The physics of lightning and lightning protection]. Moscow, Fizmatlit Publ., 2001. 319 p. (Rus).

4. Kuzhekin I.P., Larionov V.P., Prokhorov E.N. *Molniya i molnyezashchita* [Lightning and lightning protection]. Moscow, Znak Publ., 2003. 330 p. (Rus).

5. Kravchenko V.I. *Molniya. Elektromahnitny faktory i porazhayushchie vozdeystviya na tekhnycheskie sredstva* [Lightning. Electromagnetic factors and their impact on the striking technical objects]. Kharkov, NTMT Publ., 2010. 292 p. (Rus).

6. Barry J. *Sharovaya molniya y chetochnaya molniya* [Ball lightning and rosary lightning]. Moscow, Mir Publ., 1983, 288 p. (Rus).

7. Baranov M.I., Koliushko G.M., Kravchenko V.I., Nedzel'skii O.S., Dnyshchenko V.N. A Current Generator of the Artificial Lightning for Full-Scale Tests of Engineering Objects. *Pribory i tehnika eksperimenta − Instruments and Experimental Technique*, 2008, no.3, pp. 401-405. **doi: 10.1134/s0020441208030123**.

8. Baranov M.I. *Izbrannye voprosy elektrofiziki. Tom 2, Kn. 2: Teoriia elektrofizicheskikh effektov i zadach* [Selected topics of Electrophysics. Vol.2, Book 2. A theory of electrophysical effects and tasks]. Kharkiv, NTU «KhPI» Publ., 2010. 407 p. (Rus).
9. Raiser Yu.P. *Fizika gazovogo razryada* [Physics of gas discharge]. Moscow, Nauka Publ., 1987. 592 p. (Rus).
10. *Bol'shoj illjustrirovannyj slovar' inostrannyh slov* [Large illustrated dictionary of foreign words]. Moscow, Russkie slovari Publ., 2004. 957 p. (Rus).
11. Baranov M.I. *Izbrannye voprosy elektrofiziki: Monografija v 2-h tomah. Tom 2, Kn. 1: Teorija elektrofizicheskih effektov i zadach* [Selected topics of Electrophysics: Monograph in 2 vols. Vol. 2, book. 1: Theory of electrophysics effects and tasks]. Kharkov, NTU «KhPI» Publ., 2009. 384 p. (Rus).
12. Kuz'michev V.E. *Zakony i formuly fiziki* [Laws and formulas of physics]. Kiev, Naukova Dumka Publ., 1989. 864 p. (Rus).
13. Baranov M.I. Features heating thin bimetallic conductor large pulse current. *Elektrichestvo – Electricity*, 2014, no.4, pp. 34-42. (Rus).
14. Sobolev N.N. The study of electrical explosion of thin wires. *Zhurnal eksperimental'noy i teoreticheskoy fiziki – Journal of experimental and theoretical physics*, 1947, Vol.17, no.11, pp. 986-997. (Rus).
15. Baranov M.I. Phenomenon of physical fields distributing on the exponential law in nature and educa-tional process. *Elektrotekhnika i elektromekhanika − Electrical engineering & electromechanics*, 2004, no.3, pp. 111-115. (Rus).

Поступила (received) 05.10.2015

M.I. Baranov, Doctor of Technical Science, Chief Researcher,
Scientific-&-Research Planning-&-Design Institute «Molniya»
National Technical University «Kharkiv Polytechnic Institute»,
47, Shevchenko Str., Kharkiv, 61013, Ukraine,
phone +38 057 7076841, e-mail: eft@kpi.kharkov.ua

How to cite this article:
Baranov M.I. A new hypothesis and physical bases of origin of rosary lighting in the atmosphere of Earth. *Electrical engineering & electromechanics*, 2016, no.2, pp. 28-34. doi: 10.20998/2074-272X.2016.2.05.

UDC 621.311.62 **doi: 10.20998/2074-272X.2016.2.06**

Yu.V. Batygin, E.A. Chaplygin, O.S. Sabokar

ESTIMATING THE LIMIT POSSIBILITIES OF THE STEP CHARGING SYSTEM FOR CAPACITIVE ENERGY STORAGE

The aim of the article is to estimate the limit possibilities of step-by-step charging the capacitive energy storage which are caused by the achievement of a balance among the processes of the receiving and losing of electromagnetic energy. Originality. For the first time a step the charging system as a high power converter for pulsed load was considered, that allow to simplify similar charging systems and make its chipper while saving output characteristics and common quality. Methodology of the analysis applied is based on the classic electric circuits theory. All of the resulted carried out, were obtained as the differential equation solutions and its behavior was analyses analytically. Results. The basic diagram of the step-by-step charging system what is an alternative to the traditional variant with the step-up transformer was described. This system realizes the serial charge voltage increasing by the separate portions of energy, which has been, accumulated preliminary in the inductive energy storage. The formulas for estimating the limit possibilities of the step-by-step charging were got. These limits are caused by achieving a balance of the entering and losing electromagnetic energy. The applicability of the formulas was illustrated by numerical examples. Practical value. According to the results that were obtained, it is possible to note, that the step charging system is acceptable to be used as a high power converter for capacitive storage charging. References 5, figures 1.

Key words: **capacitive energy storage, step-charged system, analytical analysis, electrical circuits, inductive energy storage.**

Описана принципиальная схема ступенчатого заряда емкости, альтернативной традиционному варианту с повышающим трансформатором и предполагающей последовательное повышение зарядного напряжения за счёт подачи отдельных порций энергии, предварительно запасённой в обмотке специального индуктивного накопителя. Получены формулы для оценки предельных возможностей ступенчатого заряда, обусловленных достижением баланса в процессах поступления и потерь электромагнитной энергии. Применимость формул проиллюстрирована численными примерами. Библ. 5, рис. 1.

Ключевые слова: **емкостной накопитель энергии, система ступенчатого заряда, аналитический анализ, электрические цепи, индуктивный накопитель энергии.**

Introduction, analysis of publications. The traditional scheme of the capacitor storage charge comprises two main components: a voltage step-up transformer and rectifier (Fig. 1,*a*). Not stopping on description of the efficiency and highly successful examples of the long exploitation of the different electrical engineering devices, it should note this scheme is not without shortcomings. Among the most significant shortcomings, the real performance cumbersome is the main (including weight and overall dimensions, electronic components, etc.) and its relatively high cost [1, 2].

So-called step-by-step charging systems for capacitor banks are devoid of these shortcomings. The effectiveness of this charge is based on the «portioned» pumping of the capacitive electromagnetic energy by the voltage pulses the amplitude of which increases in time [3, 4].

However, how it follows from a priori phenomenological considerations the practical possibilities of scheme with the immediate implementation of the step-by-step charging are quite limited.

According to the physical point of view the above mentioned limitations are caused by the fact when the next charging voltage pulse comes to the capacitance input a discharge is occurring simultaneously. Upon the reaching of a balance between the incoming electromagnetic energy level and the level of its loss the charging process must stop, and the amplitude of the voltage on the capacitance (as well as the stored energy!) should be remained unchanged.

The aim of the article is estimating the limit possibilities of step-by-step charging the capacitive energy storage which are caused by the achievement of a balance among the processes of the receiving and losing of electromagnetic energy.

The calculated relationships, the numerical estimates. At the beginning a brief description of the step-by-step charging scheme for the capacitor energy storage which was adopted as a calculation model and was shown at the Fig. 1,*b* will be given.

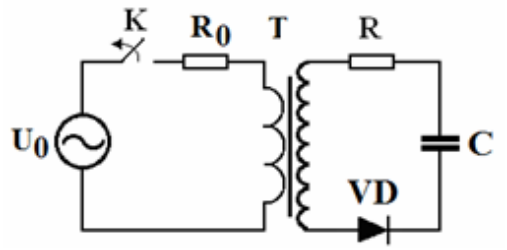

a

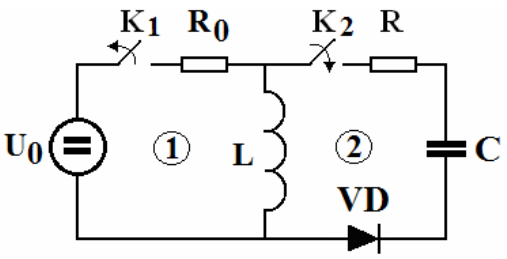

b

Fig. 1. The schematics charging of the capacitive energy storage: *a* – it is the traditional variant with the step-up charging transformer *T*; *b* – it is a variant without a step-up charging transformer

This scheme consists of 2 major blocks: 1 – inductance L (a block of energy charging) which could be presented by DC or rectified voltage source with an amplitude U_0 and 2 – a block which transforms a pre-stored magnetic energy into electrical energy capacitor storage C (R_0 and R – are current-limiting resistors).

Initially, the switch K_1 is closed, K_2 – open. Through the resistor R_0 the signal from the voltage source U_0 enters in the loop circuit 1 and charges the inductive storage L.

Upon reaching the maximum accumulated magnetic energy the key K_1 is being opened and the key K_2 is being closed. The transformation of inductance energy L into capacitive energy C is occurring. The capacitor is being charged up to some voltage level that is equal to the sum of the initial value and of some increment.

At the end of the charge switch K_2 is opened and the switch K_1 is closed. The circuit takes up the initial state and the above described process is being repeated.

In solving the problem according to the formulated aim the mathematical apparatus of the electrical circuit theory was used [5].

Leaving out the details of integrating the differential equation which describes the transition process in the circuit blocks 1 and the necessary mathematical transformations the final expression for the current in the inductor can be wrote.

$$J(t) = \frac{U_0}{R_0} \cdot \left(1 - e^{-\frac{t}{\tau_0}} \right), \qquad (1)$$

where $\tau_0 = L/R_0$ – is the time constant of the «$R_0 - L$» circuit.

After time to $t \geq 3 \cdot \tau_0$ in accordance with (1) $J(t) \to J_m = U_0 / R_0$. It means the current and the electromagnetic energy are achieving their maximum.

Further, in accordance with the description of the processes in the step-by-step charging scheme in Fig. 1 the charge of the capacitor storage C is occurring.

Similarly to the above the details integrating of the equation of the transition process in the circuit 2 (for open K_1 and closed K_2) were omitted, and the final expression for the voltage on the capacitance $U_C(t)$ was written.

$$U_C(t) = e^{-\delta t} \left[\left(\left(\frac{J_m}{\omega C} \right) + \frac{\delta}{\omega} \cdot U_{C0} \right) \cdot \sin(\omega t) + U_{C0} \cdot \cos(\omega t) \right], \qquad (2)$$

where $\delta = R / 2L$ – is the damping rate; $\omega = \sqrt{\omega_0^2 - \delta^2}$ – is the oscillation frequency; $\omega_0 = \frac{1}{\sqrt{LC}}$ – is the own circuit frequency; U_{C0} – is the initial capacitance voltage; $J_m = U_0 / R_0$ – is the inductor current at the moment of commutation.

The maximum increment of voltage in the arbitrary cycle relatively to the initial value takes place after time equaled to a quarter of the oscillation period – $\omega \cdot t = \pi/2$

$$\Delta U_C(t) = U_C\left(t = \frac{\pi}{2\omega} \right) - U_{C0} = e^{-\delta_0 \cdot \frac{\pi}{2}} \left[\left(\left(\frac{J_m}{\omega C} \right) + \delta_0 \cdot U_{C0} \right) - U_{C0} \right], \qquad (3)$$

where $\delta_0 = \delta / \omega$ – is the relative damping rate.

Charging time what is equaled to the quarter of the period is conditioned by the diode presence in the circuit 2.

Accepting the idealization when $\delta_0 \to 0$ which relates to the maximum possible values of the output parameters of the charge with the lowest possible energy dissipation in the active resistance of the circuit according to the dependence (3) we get

$$\lim_{\delta_0 \to 0} \Delta U_C\left(t = \frac{\pi}{2\omega} \right) \approx U_0 \cdot \left(\frac{Z}{R_0} \right) - U_{C_0}, \qquad (4)$$

where $N = \frac{U_{C0}}{U_0} \approx \frac{Z}{R_0} = \frac{1}{R_0} \cdot \sqrt{\frac{L}{C}}$ is the circuit wave resistance.

It is clear the condition of the balance in the process of income and loss of electromagnetic energy is equaled to zero growth in the next charging cycle, that is $\lim_{\delta_0 \to 0} \Delta U_C\left(t = \frac{\pi}{2\omega} \right) \to 0$. If to take into account that the initial value of the voltage on the capacitance in the same charging cycle is the result of accumulation process starting with the voltage of the external source U_0 during the previous cycles it is possible to write $U_{C0} = NU_0$.

According to the remarks above, with help of the relation (4), we find that

$$N = \frac{U_{C0}}{U_0} \approx \frac{Z}{R_0} = \frac{1}{R_0} \cdot \sqrt{\frac{L}{C}}. \qquad (5)$$

The dependence (5) is the solution of the formulated aim. It fixes the limiting number of the possible cycles of the capacitor storage charge to achieve the maximum voltage value, which is the highest for the given parameters of the system.

Numerical estimates.

Let us, it is necessary to charge the capacitive energy storage C =1200 μF of the magnetic pulse plant up to U_{C0} = 2.2 kV by the AC source U_0 = 220 V. An active circuit resistance of the branch with the magnetic energy inductive storage is R_0 = 0.1 Ohm. [1].

It is necessary to find the next data:

- the required quantity of charging cycles N;
- the value of inductance that ensures the implementation of the step-by-step charging process L;
- the maximum charge current of the inductive storage J_m;
- time of achievement of the maximum inductor current t_L.

From (5) we find the required number of charge cycles:

$$N = \frac{U_{C0}}{U_0} = \frac{2200}{220} = 10. \qquad (6)$$

The value of inductance that ensures the implementation of the step-by-step charging process is also determined by (5)

$$L = (N \cdot R_0)^2 \cdot C = (10 \cdot 0.1)^2 \cdot 1200 \cdot 10^{-6} = 0.0012 \text{ H}. \qquad (7)$$

The maximum charging current of the inductive storage is based on (1),

$$J_m = \frac{U_0}{R_0} = \frac{220}{0.1} = 2.2 \text{ kA}. \quad (8)$$

The necessary time term to reach the maximum current at the inductive storage could be find as (formula (1))

$$t \geq 3 \cdot \frac{L}{R_0} = 3 \cdot \frac{0.0012}{0.1} = 0.036 \text{ s}. \quad (9)$$

Thus, the charge up of capacity C = 1200 μF up to 2.2 kV with mains voltage equaled to ~ 220 V can be carried out during 10 cycles of the step-by-step charge, with a maximum charging current in the inductance circuit ~ 2.2 kA. The necessary voltage level could be achieved in ~ 0.036 s.

Conclusions.

1. The work and benefits of the capacitance step-by-step charging system which is a successful alternative to the traditional scheme with step-up transformer and based on the portioned energy charge was described.

2. The estimation of limit possibilities of the step-by-step charging for the capacitive energy storage which are caused by achievement of balance among the processes of receiving and losing the electromagnetic energy was fulfilled.

3. The simple calculated ratios were received. Their applicability was illustrated by some numerical examples.

REFERENCES

1. Batygin Yu.V., Lavinskiy V.I., Khimenko L.T. *Impul'snyye magnitnyye polya dlya progressivnykh tekhnologiy. Tom 1. Izdaniye vtoroye, pererabotannoye i dopolnennoye*. [Pulsed magnetic fields for advanced technologies. Vol.1. 2nd edition, revised and enlarged.] Kharkov, MOST-Tornado Publ., 2003. 284 p. (Rus).

2. Orlov B.D., Dmitriyev Yu.V., Chakalev A.A., Sidyakin V.A., Marchenko A.L. *Tekhnologiya i oborudovaniye kontaktnoy svarki* [Technology and equipment for the contact welding]. Moscow, Mechanical Engineering Publ., 1975. 536 p. (Rus).

3. John D. Lenk. *Simplified Design of Switching Power Supplies*. Elsevier Publishing House, 1996. 235 p. Electronic ISBN: 9780080517209.

4. Marasco K. How to Apply DC-to-DC Step-Up (Boost) Regulators. *Analog Devices. AN-1132 Application Note: 2011*. Available at: http://www.analog.com/media/ru/technical-documentation/application-notes/AN-1132.pdf (accessed 22 May 2012).

5. Atabekov G.I. *Osnovy teorii tsepei* [The base of the circuits theory]. Moscow. Energy Publ., 1969. 427 p. (Rus).

Yu.V. Batygin[1]*, Doctor of Technical Science, Professor,*
E.A. Chaplygin[1]*, Candidate of Technical Science, Associate Professor,*
O.S. Sabokar[1]*,*
[1] Kharkov National Automobile and Highway University,
25, Petrovskogo Str., Kharkov, 61002, Ukraine.
phone +38 057 7073727, e-mail: batygin48@mail.ru, chaplygin.e.a@gmail.com, o.s.sabokar@gmail.com

How to cite this article:
Batygin Yu.V., Chaplygin E.A., Sabokar O.S. Estimating the limit possibilities of the step charging system for capacitive energy storage. *Electrical engineering & electromechanics*, 2016, no.2, pp. 35-37. doi: 10.20998/2074-272X.2016.2.06.

UDC 621.319 **doi: 10.20998/2074-272X.2016.2.07**

G.V. Bezprozvannych, A.G. Kyessayev

RELAXATIONS LOSSES IN POLYETHYLENE INSULATION OF COAXIAL CABLE STRUCTURE DURING AGING IN HIGH HUMIDITY CONDITIONS

Introduction. The presence of free moisture in power cables leading to the formation of tree structures - water treeing, which originate in the amorphous phase polyethylene and are a major cause of degradation of the polymer insulation. They represent the damage of the polymer size from several microns to 1 mm, developing technology for insulation defects under the combined action of the electric field and the moisture diffusing from the environment. Water treeing destroys the polymer chain, resulting in the formation of microcavities filled with moisture. The dynamics of water treeing and subtle properties largely depend on the composition, morphology of the polymer insulation, chemical nature of the defect, in which they originate. Due to the force of gravity in the water formed typical only for her region with locally ordered structure - clusters, which cause loss of relaxation. Purpose. Features presence of relaxation losses in high-frequency range in polyethylene insulation during aging in high humidity conditions of samples power and RF cables. Methodology. Samples of the power cable for the voltage of 35 kV with a cross-linked polyethylene insulation radial water-blocking protection from moisture and radio-frequency coaxial cable with thermoplastic insulation for 1440 hours in a humidity of 100%. The dielectric loss tangent measured resonance method before and after aging. Originality. Experimentally found evidence of the existence in the polymer cable insulation free water in the form of areas with locally ordered structure - clusters. It is found that the solid polyethylene insulation in the frequency dependence of dielectric loss tangent maximum relaxation shown one at 10 MHz in the initial state, and there are two additional frequency range 500 kHz - 5 MHz after moistening. For cross-linked polyethylene insulation characteristic of large width Δf of the frequency spectrum in which the observed relaxation losses. It is obvious that the width of each of the relaxation maxima is associated with characteristic fractal cluster size. It is important that the hydrated solid and foamed polyethylene insulation to show individuality, typical only for water clusters which are detected by high-frequency dipole relaxation peaks dielectric loss tangent. There is a positive correlation between the bandwidth Δf of relaxation maxima and the rate of decrease of insulation resistance by applying a high DC voltage. Practical value. Establishing a correlation between the bandwidth of relaxation maxima and the rate of decrease in the insulation resistance test objects in the laboratory makes it possible to diagnose the presence of free moisture in the power and RF cables by measuring the insulation resistance in exploitation. References 10, figures 7.

Key words: **water treeing, moisturizing cables, solid and foamed polyethylene insulation, dielectric loss tangent, water clusters, relaxation peaks.**

Выполнены измерения в диапазоне частот 50 кГц – 20 МГц тангенса угла диэлектрических потерь образцов силового и радиочастотного коаксиального кабелей в исходном состоянии и после увлажнения в условиях 100% влажности. После старения установлено появление дополнительных релаксационных максимумов для сплошной термореактивной и термопластичной полиэтиленовой изоляции, что обусловлено группированием свободной воды в кластеры соответствующей формы и фрактальной размерности. Для кабелей со вспененной термопластичной полиэтиленовой изоляцией в не состаренном состоянии присуще проявление релаксационных потерь за счет наличия воды в газообразных включениях. Установлена положительная корреляция между шириною полосы релаксационных максимумов и скоростью уменьшения сопротивления изоляции от приложенного высокого постоянного напряжения. Библ. 10, рис. 7.

Ключевые слова: **водные триинги, увлажнение кабелей, сплошная и вспененная полиэтиленовая изоляция, тангенс угла диэлектрических потерь, кластеры воды, релаксационные максимумы.**

Introduction. The presence of free moisture in the power cable leading to the formation of tree structures, – water treeing (Fig. 1) [1-7], *which are generated in the amorphous phase of the polyethylene, i.e. on the boundaries of the grains-crystallites* (Fig. 2), and are a major cause of degradation of the polymer insulation. Water treeings are damages of polymer sized from a few microns (Fig. 1, 2) to 1 mm, developing on technological defects of insulation under the combined action of the electric field and the moisture diffusing from environment. Together with moisture aggressive substances penetrate to the insulation. They destroy the polymer chains, resulting in the formation of microcavities filled with moisture.

Dielectric strength in treeing is significantly reduced, which increases the strength on the undamaged part of the insulation and accelerates the process of treeing growth [5]. Aging at the conditions of operation or tests at increased temperature (90 °C) is significantly lower than at lower temperatures (20 – 40 °C): water

Fig. 1. Photo of emerging water treeing in cross-linked polyethylene insulation of power cable, obtained by power electron microscope [4]

treeing grows less rapidly. The dynamics of water treeing and their subtle properties largely depend on the composition, morphology of the polymeric insulation, the chemical nature of the defect, on which they originate.

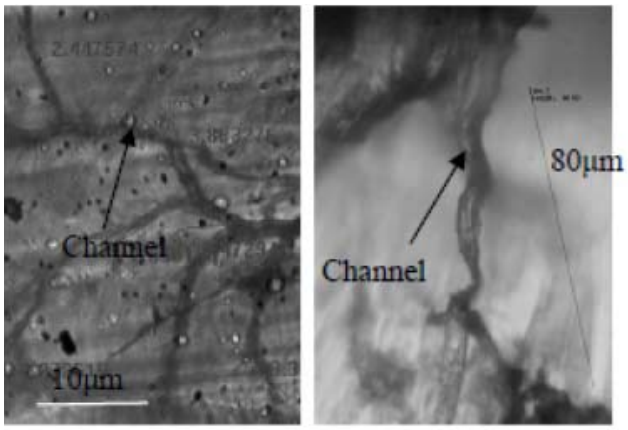

Fig. 2 [6]

Problem definition. Water treeing can be quantitatively described in terms of the fractal dimension, i.e. the concept of the quantity characterizing the geometric structure of stochastic objects [8, 9]. Current concepts in this area connected with the fact that most of the natural stochastic structures have so-called scaling symmetry (scale invariance): they are viewed equally at different magnifications (Fig. 3). With the help of the algorithm for constructing the stochastic fractals using iterated function it is possible to model the complex fractal structure of water treeing in polymer cable insulation.

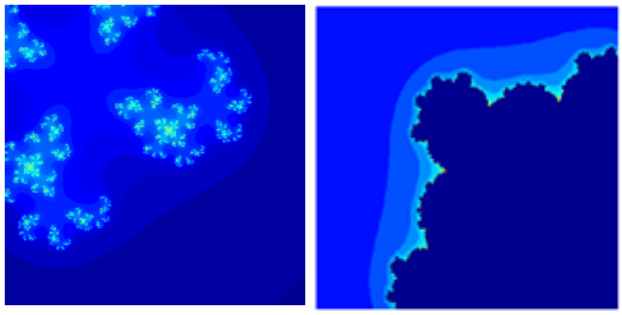

a *b*

Fig. 3. The results of the construction of the classic Julia fractals (*a*) and Mandelbrot fractals (*b*) in the Matlab environment

In accordance with relaxation theory by Dissado – Hill [10] due to the attractive forces in liquids (water) *are formed area with a locally ordered structure – clusters*, structure, composition and the energy value of the chemical bonds between molecules which depend on the type of liquid and solid medium, in which it is situated. *In each of the liquid there are the basic, typical for it, clusters that define its structure.*

In a two-level model, the relaxation of a group of atoms or molecules (cluster) associated with transitions from one minimum to the other two variants of the orientation corresponding to the minima in the potential curve (Fig. 4).

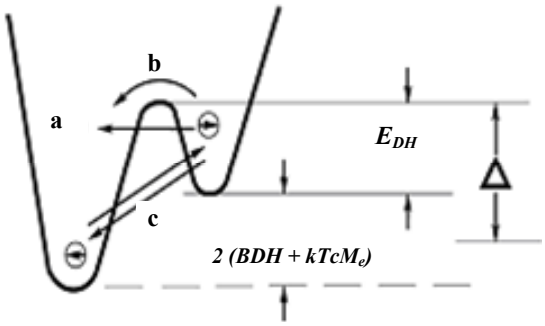

Fig. 4. Energy diagram of a two-layer system: *a* – process related with rotational and vibrational intramolecular oscillations, *b* – intra-cluster activation relaxation process, *c* – inter-cluster process of simultaneous exchange of molecules

The difference in energy values between these two minima, i.e. height of the barrier, which is overcome by the synchronous exchange of molecules between adjacent clusters is written explicitly as

$$\Delta\varphi = 2\,(B_{DH} + k\,T_c\,M_e)\,,$$

where k is the Boltzmann constant, T_c critical characteristic temperature (the phase transition temperature, for example, the glass transition temperature), M_e is the unit vector of the longitudinal component of the dipole moment of the cluster

$$M_e = \tanh\left(\frac{B_{DH} + kT_cM_e}{kT}\right).$$

The degree of structural ordering of the minimum size of the average cluster is characterized by the parameter $0 \le n_{DH} \le 1$. At $n = 0$ the clusters are not formed, and the correlation between the processes of reorientation of molecules absents. When $n = 1$ the clusters have a crystal structure in which the processes of molecules reorientation are fully correlated. Clusters, in their turn, are part of the inter-cluster formations, the degree of structural order in which is determined by the parameter $1 - m_{DH}$, and $0 \le m_{DH} \le 1$. Boundary values $m_{DH} = 0$ and $m_{DH} = 1$ correspond to a perfect crystal lattice and the liquid with an ideal hydrodynamic flow.

For the cluster model by Dissado – Hill the dispersion relative electrical permittivity ε*(ω) is described by the equation

$$\frac{\varepsilon^*(\omega) - \varepsilon_{\infty DH}}{\varepsilon_s - \varepsilon_{\infty DH}} = \left(1 + \frac{i\omega}{\omega_p}\right)^{n-1} \frac{{}_2F_1\left[1-n, 1-m; 2-n; \left(1+\frac{i\omega}{\omega_p}\right)^{-1}\right]}{{}_2F_1(1-n, 1-m; 2-n; 1)},$$

where $\varepsilon_{\infty DH}$ is the high-frequency limit of the area of dispersion, polarization due to the contribution of the fast polarization species (ion and electron bias) and a high-frequency relaxation process, ${}_2F_1[\ldots]$ are the Gaussian hypergeometric functions.

The above equation corresponds to the Debye equation for $n = 0$, $m = 1$, $\omega_p = \tau_D^{-1}$. Maximum of dielectric losses ε'' takes place at $\omega = \omega_p$ only in the case $n = m$.

At each temperature there is a distribution of clusters in shape and size, which correspond to the mean-square square of the dipole moment of the cluster $\left\langle \bar{\mu}_c^2 \right\rangle$.

The goal of the paper is investigation of features of manifestation of the relaxation losses in high-frequency range in polyethylene insulation at aging of samples of power and RF cables in high humidity conditions.

Test objects. As test objects samples of the coaxial cables are used.

1. A new power cable of voltage of 35 kV in single-phase design with cross-section of aluminum conductors of 95 mm^2 with the cross-linked (thermosetting) polyethylene insulation, semiconducting shields for conductor and insulation, copper screen. Design feature is the presence of semi-conductive hydrophilic water swelling tapes, providing radial cable protection from moisture.

2. A RF cable PK-50 with a two-layer thermoplastic polyethylene insulation without additional radial moisture protection. Cable for 5 years was in the room, and the cable ends were not sealed with heat-shrinkable protective caps.

3. A new RF cable EH4 (PK-75) with a thermoplastic foam polyethylene insulation without additional radial moisture protection.

4. A RF cable RG-6 (PK-75) with a thermoplastic foam polyethylene insulation and protection against moisture in the original (before operating) state as hydrophobic jelly after exploitation for 10 years.

Dynamics of changes in the relaxation losses during hydration. Test samples of the new power cable and cable PK-50 were subjected to aging in high humidity at room temperature for 1440 hours (2 months). In the initial state and after aging the dielectric loss tangent in the frequency range 50 kHz - 20 MHz by Q-meter VM 560 using resonance method were measured (Fig. 5).

For samples of RF cables EH-4 and RG-6 with foam insulation measured frequency dependence on the dielectric loss tangent are shown in Fig. 6.

Analysis of the frequency dependences shows that there is a manifestation of the general laws of the relaxation losses in the cables. So, for the power cable with thermosetting and RF cable PK-50 with thermoplastic polyethylene insulation (Fig. 5) in the initial state and after the aging the nature of the frequency dependences of dielectric loss tangent is identical.

In the initial state we can see the relaxation maximum **I**, whose width Δf is indirectly related to the amount of moisture in the insulation: in a new power cable residual free moisture is considerably less than in the cable PC-50, which was a long time at natural conditions. After aging on the frequency dependence of the relaxation there are additional peaks **II** and **III**, related to the reorientation of polar water molecules in formed new clusters of different shapes and sizes.

In the new cable EH-4 (see Fig. 6,*a*) there are three characteristic relaxation peaks associated with the manifestation of the dipole polarization of water in clusters of different shapes and sizes. In the structure of the foamed thermoplastic polyethylene insulation there are gaseous inclusions, which are filled with water, as in the initial state and during operation (see Fig. 6,*b*).

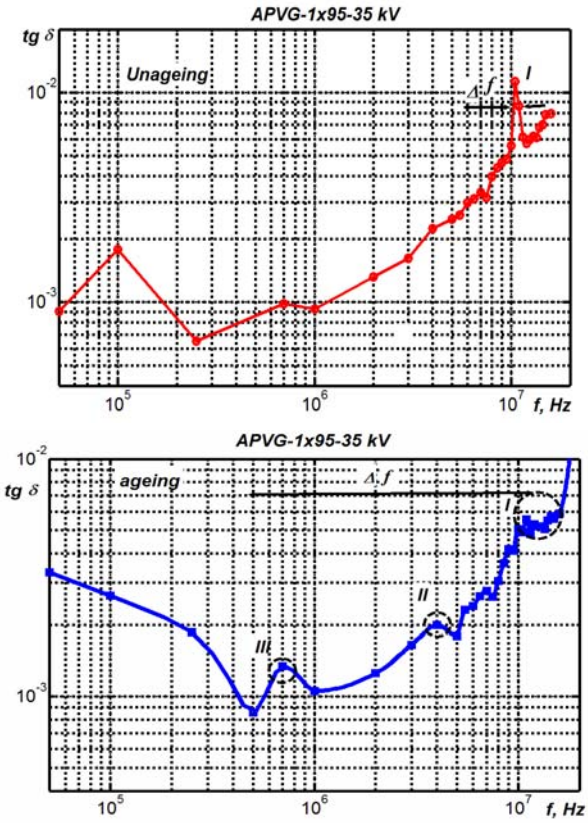

a – a power cable with a thermosetting polyethylene insulation (top picture – the original state, bottom picture – after moistening)

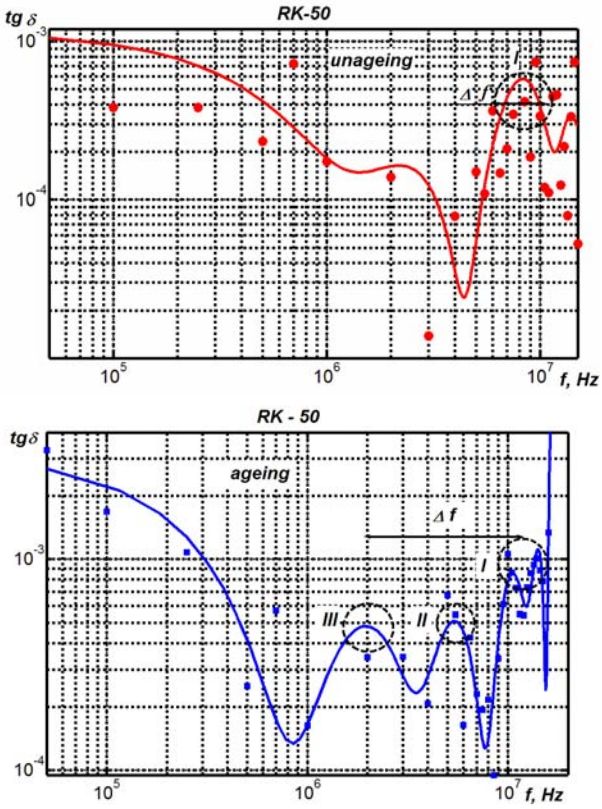

b – a RF cable with a thermosetting polyethylene insulation (top picture – the original state, bottom picture – after moistening)

Fig. 5. Dynamics of changes in the tangent of the angle of dielectric losses in cables samples in the process of moistening

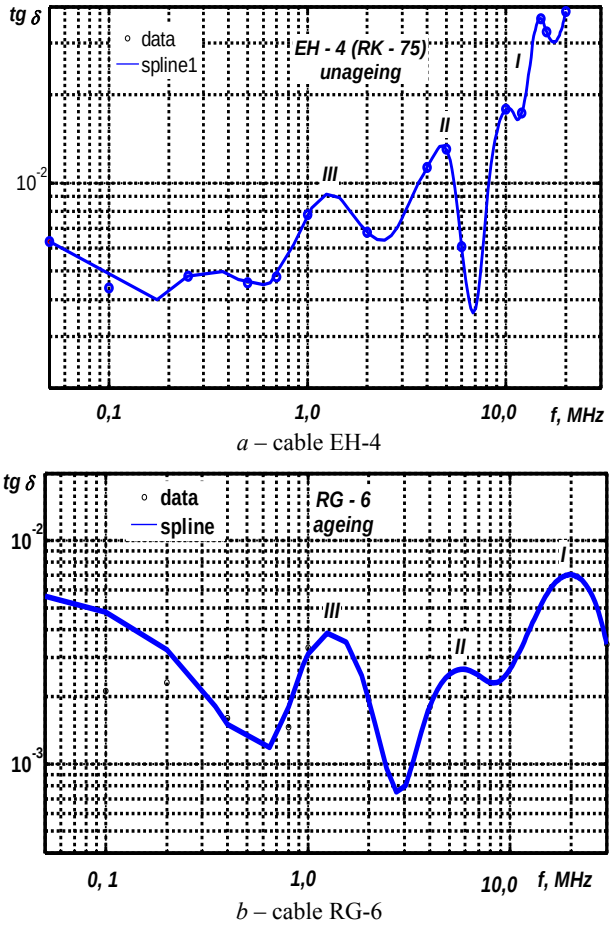

a – cable EH-4

b – cable RG-6

Fig. 6. The frequency dependence of the dielectric loss tangent of RF cables with foam thermoplastic polyethylene insulation

The correlation between the width of the spectrum of the dipole peaks and insulation resistance. Fig. 7 shows the results of the insulation resistance measurement of the power cable samples (curves 1 and 1') and radio frequency cable PK-50 (curves 2 and 2') depending on the applied DC voltage: curves 1 and 2 - the initial state, curves 1' and 2' - after moistening.

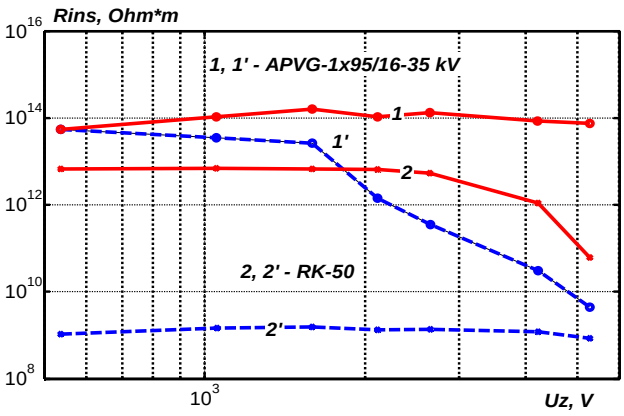

Fig. 7

In the initial state, the insulation resistance of the power cable is weakly dependent on the applied voltage (Fig. 7, curve 1). The spectral width Δf of the relaxation maximum **I** (Fig. 5,*a*, the upper picture) is small. For RF cable PK-50 in the initial state the width spectrum Δf of the relaxation maximum **I** (Fig. 5,*b*, the upper picture) is significant (about 6 MHz), which causes a decrease in the insulation resistance in 10 times when the voltage increases 10 times (from 500 to 5000 V) (Fig. 7, curve 2).

After aging for the power cable (Fig. 7, curve 1') we observe the strongly expressed dependence of insulation resistance on the applied voltage: when the voltage is increased by 10 times the insulation resistance decreased to 10,000 times. The bandwidth of the spectrum Δf of the relaxation maxima **I** - **III** (Fig. 5, the lower picture) increased almost 20 times.

For cable PK-50 spectral width Δf of the relaxation maxima **I** - **III** (see Fig. 5,*b*, the lower picture) increased only 6 times, and as a result, the insulation resistance after moisture is practically independent on the voltage. For voltage of 5 kV after aging the insulation resistance decreased to 100 times relative to the initial state. Obviously, in a thermoplastic polyethylene insulation water clusters with similar fractal dimensions are formed.

Conclusions.

So, the evidence of the existence in the polymeric insulation of the cables of free water in the form of areas with a locally ordered structure – clusters is experimentally found.

In the range of measurements of 50 kHz - 20 MHz it is found that for solid plastic insulation at frequency dependences of dielectric loss tangent one maximum of relaxation takes place at 10 MHz in the initial state and additional peaks appear in the frequency range 500 kHz - 5 MHz after moistening. For thermosetting (crosslinked) polyethylene insulation large width Δf of the frequency spectrum in which relaxation losses take place is characterized. Obviously, the width of each of the relaxation peaks is related to the characteristic fractal cluster size.

It is important that in the hydrated solid and foamed polyethylene insulation individual, typical only for water clusters detected by high-frequency relaxation dipole maxima of the dielectric loss tangent take place.

There is a positive correlation between the bandwidth Δf of the relaxation maxima and insulation resistance decrease rate on the applied high DC voltage.

REFERENCES

1. De Bellet J., Matey G., Rose L., Rose V., Filippini J., Poggi Y., Raharimalala V. Some aspects of the relationship between water treeing, morphology, and microstructure of polymers. *IEEE Trans. Elect. Insul.*, 1987, vol.EI-22, no.2, pp. 211-217. **doi: 10.1109/tei.1987.298884**.

2. Ciuprina F., Teissèdre G., Filippini J.C. Polyethylene crosslinking and water treeing. *Polymer*, 2001, vol.42, no.18, pp. 7841-7846. **doi: 10.1016/s0032-3861(01)00264-6**.

3. Dissado L.A. Understanding electrical trees in solids: from experiment to theory. *IEEE Trans. Dielect. Electr. Insul.*, 2002, vol.9, no.4, pp. 483-497. **doi: 10.1109/tdei.2002.1024425**.

4. Kato T., Yamaguchi T., Komori F., Kawahara T., Hidaka T., Suzuoki Y. Influence of structural change by AC voltage prestressing on electrical-tree inception voltage of LDPE with water-tree degradation. *2012 Annual Report Conference on Electrical Insulation and Dielectric Phenomena*, Montreal, Canada: IEEE, 2012, pp. 847-850. **doi: 10.1109/ceidp.2012.6378913**.

5. Shcherba A.A., Podoltsev A.D., Kucheriavaia I.N., Zolotarev V.M. Electric transport of polar water molecules in an

inhomogeneous electric field of polymer insulation high-voltage cables. *Tekhnichna elektrodynamika – Technical Electrodynamics*, 2010, no.5, pp. 3-9. (Rus).
6. Priya S., Mubashira Anjum A. Analysis of water trees and characterization techniques in XLPE cables. *Indian Journal of Science and Technology*, 2014, vol.7(S7), pp. 127-135.
7. Shuvalov M.Y., Mavrin M.A. Theoretical and experimental research water treeing type of «bow». *Kabeli i provoda – Cables and wires*, 2002, no.1, pp. 44-50. (Rus)
8. Mandelbrot B.B. Fractals: form, chance and dimension. – San Francisco: Freeman, 1977.
9. Dissado L.A., Hill, R.M. The fractal nature of the cluster model dielectric response functions. *Journal of Applied Physics*, 1989, vol.66, no.6, pp. 2511-2524. **doi: 10.1063/1.344264**.
10. Dissado L.A., Hill R.M. A cluster approach to the structure of imperfect materials and their relaxation spectroscopy. *Proceedings of the Royal Society A: Mathematical, Physical and Engineering Sciences*, 1983, vol.390, no.1798, pp. 131-180. **doi: 10.1098/rspa.1983.0125**.

Received 28.12.2015

G.V. Bezprozvannych[1], *Doctor of Technical Science, Professor,*
A.G. Kyessayev[1], *Postgraduate Student,*
[1] National Technical University «Kharkiv Polytechnic Institute», 21, Frunze Str., Kharkiv, 61002, Ukraine.
phone +380 57 7076010,
e-mail: bezprozvannych@kpi.kharkov.ua

How to cite this article:
Bezprozvannych G.V., Kyessayev A.G. Relaxations losses in polyethylene insulation of coaxial cable structure during aging in high humidity conditions. *Electrical engineering & electromechanics*, 2016, no.2, pp. 38-42. doi: 10.20998/2074-272X.2016.2.07.

UDC 621.317 **doi: 10.20998/2074-272X.2016.2.08**

P. Olszowiec

MODIFICATIONS OF DIODE RECTIFIER CIRCUITS FOR CONTINUOUS INSULATION MEASUREMENT IN LIVE AC IT NETWORKS

Purpose. ***In the paper there are described few systems of insulation resistance continuous measurement using an imposed DC test signal delivered by diode rectifiers. Drawbacks of this technique are pointed out and ways of these shortcomings removal are proposed.*** ***Methodology.*** ***An improved version of measuring circuit based on a single-phase diode rectifier is presented. Application of logometric measuring devices is suggested.*** ***Results.*** ***A new insulation resistance continuous measuring system is insensitive to network voltages variation and asymmetry. Modified circuit enables also implementation of a simple device for alarming the monitored network's insulation deterioration and/or earth-fault protection.*** ***Originality.*** ***Formulas describing performance of diode rectifiers under asymmetrical supply have not been available so far. Both innovations (i.e. single-phase diode rectifier and logometric meter) have not been applied widely for implementation of continuous insulation monitoring in live AC IT networks.*** ***Practical value.*** ***Use of both innovations will allow to eliminate unrequired dependence of measurement results on variable network voltages as well as their possible asymmetry. Exploitation of diode rectifier circuits for earth fault location is also possible.*** References 6, figures 9.

Key words: **low voltage AC IT networks, insulation resistance, diode rectifier, insulation resistance decline alarming, earth fault location.**

Представлена работа разных вентильных схем измерения сопротивления изоляции сетей низкого напряжения с изолированной нейтралью. Приведены формулы для вычисления эквивалентного сопротивления изоляции при асимметрии линейных напряжений сети. Предложены способы устранения недостатков этих схем с использованием однофазных выпрямителей. Показаны возможности реализации системы сигнализации о понижении сопротивления изоляции и поиска места замыкания на землю. Библ. 6, рис. 9.

Ключевые слова: **сети низкого напряжения с изолированной нейтралью, сопротивление изоляции, диодный выпрямитель, сигнализация о понижении сопротивления изоляции, поиск места замыкания на землю.**

Introduction. Insulation monitoring is indispensable for safe and reliable operation of electric systems. In low voltage unearthed networks wide application has been found by insulation monitors based on diode rectifiers. However in recent years, in spite of numerous qualities of this technology, leading position was taken by isometers exploiting superimposed test signal delivered by an auxiliary source. Most technical literature is devoted to these new methods [1]. Nevertheless it seems useful to remind traditional insulation monitors with rectifier circuits and review possible ways of their improvement.

Problem definition. Main qualities of isometers with diode rectifiers are simple construction, lack of an auxiliary test signal source, fast response, high accuracy and insensitivity to ground capacitances [2]. However these devices have got also few shortcomings limiting their application.

This paper is aimed at analysis of existing measuring systems and schemes improved by author, based on single phase rectifiers.

Existing schemes. Scheme A. The most popular insulation monitoring scheme without an auxiliary test signal source is a system with full-wave bridge rectifier fed by the monitored network (Fig. 1).

A separating transformer is fed by a line-to-line voltage whereas its secondary winding is connected by rectifier and current limiting resistor R_0 between one of conductors and ground. Rectified current is a test signal for determination of insulation-to-ground equivalent resistance R_i. Mean value $U_{0\text{-}mean}$ of voltage across R_0 resistor

$$U_{0-mean} = \sqrt{2} \cdot E_{bc} \cdot \frac{R_0}{R_0 + R_i}, \qquad (1)$$

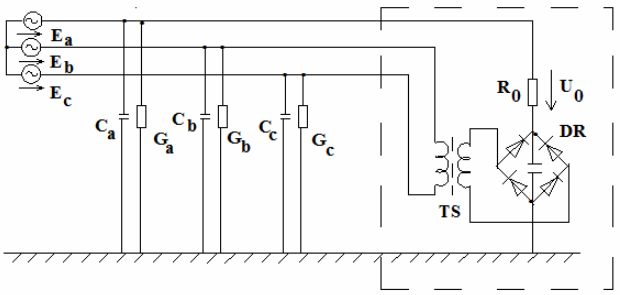

Fig. 1. Scheme A of insulation resistance measurement in a 3-phase network: TS – separating transformer, DR – full-wave bridge rectifier, R_0 – current limiting resistor, E_a, E_b, E_c – phase voltages of the source, C_a, C_b, C_c – phase-to-ground capacitances, G_a, G_b, G_c – phase insulation leakage conductances

provides information on the sought parameter R_i. Its value is given by formula

$$R_i = R_0 \cdot \frac{\sqrt{2} \cdot E_{bc} - U_{0-mean}}{U_{0-mean}}. \qquad (2)$$

The measurement result does not depend on insulation capacitances as mean values of charging and discharging currents are zero. However R_i value depends on two voltages at a time (E_{bc}, and U_0) which is the main shortcoming of this method. It is worth noting that formula (1) is true at any possible distortion of U_0 voltage waveform (Fig. 2).

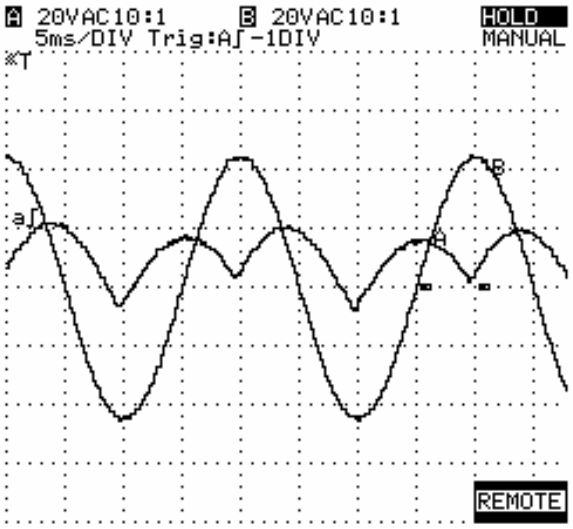

Fig. 2. Waveforms of voltages in scheme A of insulation resistance measurement in a 3-phase network (example): A – voltage U_0, B – phase-to-phase voltage

Scheme B. Measurement scheme B (Fig. 3) ensures continuous insulation monitoring too. Capacitor C is periodically charged by phases B and C through diode D. When the diode is blocked, the capacitor discharges through elements connected in series: current limiting resistor R_0 and network insulation leakage resistances.

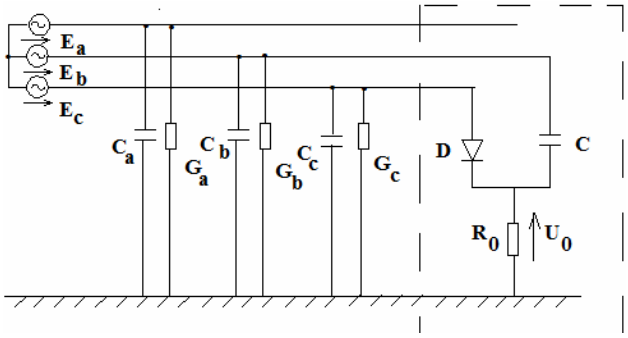

Fig.3. Scheme B of insulation resistance measurement in a 3-phase network: D – diode, C – capacitor, R_0 – current limiting resistor

Just as in scheme A mean value $U_{0\text{-}mean}$ of voltage across R_0 resistor is

$$U_{0-mean} = U_{C-mean} \cdot \frac{R_0}{R_0 + R_i}, \quad (3)$$

from where sought parameter R_i is obtained

$$R_i = R_0 \cdot \frac{U_{C-mean} - U_{0-mean}}{U_{0-mean}}, \quad (4)$$

where $U_{C\text{-}mean}$ – mean value of voltage across the capacitor.

Examples of voltages waveforms in this scheme are shown in Fig.4. There is presented periodical process of charging and discharging of the capacitor.

For C and R_0 meeting condition $C \cdot R_0 >> T$ (T – period of the network voltage), voltage across the capacitor is practically constant. In this case formula (4) is as follows

$$R_i = R_0 \cdot \frac{\sqrt{2} \cdot E_{bc} - U_{0-mean}}{U_{0-mean}}. \quad (5)$$

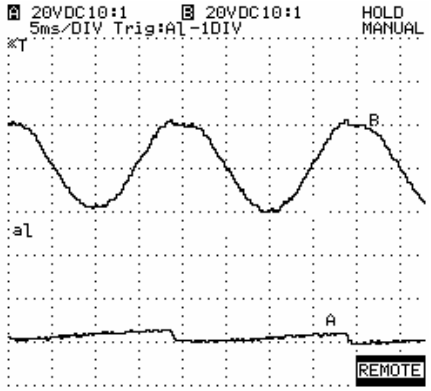

Fig. 4. Waveforms of voltages in scheme B of insulation resistance measurement in a 3-phase network (example): A – voltage U_0, B – phase-to-phase voltage

Scheme C. Three-phase rectifier with star connected diodes belongs to the most popular insulation monitoring systems (Fig. 5) [3].

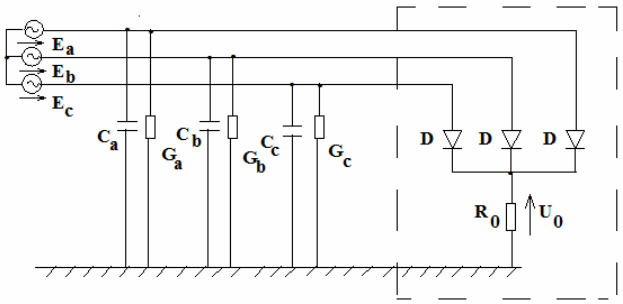

Fig. 5. Scheme C of insulation resistance measurement in a 3-phase network: D – diodes, R_0 - current limiting resistor

In this scheme there conducts diode with the highest potential of anode. Transition from one diode to another one takes place immediately when their phase voltages become equal.

For derivation of formula determining mean value of U_0 voltage across R_0 resistor in a network with asymmetrical source voltages E_a, E_b, E_c it is convenient to use expression for output voltage of a full-wave bridge rectifier (Fig. 6) [4]:

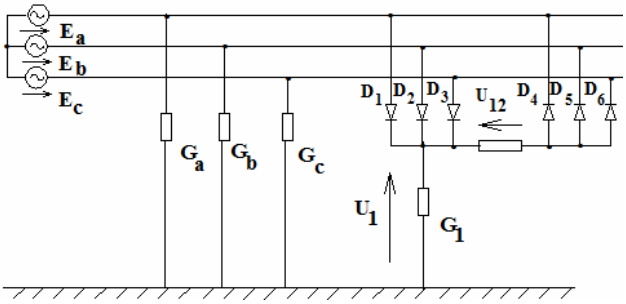

Fig. 6. Three-phase diode bridge rectifier: D_1 ... D_6 – diodes, G_1 – insulation leakage conductance of the positive pole

$$U_{12-mean} = \frac{\sqrt{2} \cdot (E_{ab} + E_{bc} + E_{ca})}{\pi}. \quad (6)$$

In this system mean value of positive pole-to-ground voltage [5] is

$$U_{1-mean} = \frac{G_i}{G_i + G_1} \cdot \frac{U_{12-mean}}{2}. \quad (7)$$

From (6) and (7) formula for mean value $U_{0\text{-}mean}$ of voltage across R_0 resistor in scheme C is obtained

$$U_{0-mean} = \frac{\sqrt{2}\cdot(E_{ab}+E_{bc}+E_{ca})}{2\pi}\cdot\frac{R_0}{R_0+R_i}. \quad (8)$$

From (8) sought value is derived

$$R_i = \left(\frac{\sqrt{2}\cdot(E_{ab}+E_{bc}+E_{ca})}{2\pi\cdot U_{0-mean}}-1\right)\cdot R_0. \quad (9)$$

Elimination of shortcomings of schemes A, B, C. Main shortcoming of methods A, B, C (except of lack of self- monitoring) is dependence of calculated parameter R_i simultaneously on the network phase-to-phase voltages and on U_0 voltage. These voltages are of course proportional but when using formulas (2) and (4) their current values must be known. If source voltages vary with time, simultaneous readings of two voltmeters must be made.

Scale of U_0 voltmeter can be graduated in kOhms only if network voltages are known and do not change.

In scheme C an additional difficulty can be caused by possible asymmetry of the source voltages. In order to accurately determine R_i parameter from formula (9), all three phase-to-phase voltages must be simultaneously measured. The latter obstacle can be overcome by a simple modification proposed by the author.

In a three-phase rectifier with star connected diodes only two diodes fed by any phase-to-phase voltage can be exploited [6] (Fig.7.).

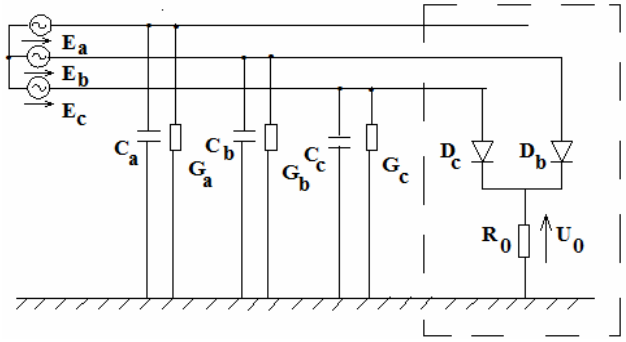

Fig. 7. Modified scheme of insulation resistance measurement with two diodes in a 3-phase network

Let the rectifier be fed by phase *b* -to-phase *c* voltage,

$$e_{bc}(t) = e_b(t) - e_c(t) = \sqrt{2}\cdot E_{bc}\cdot\sin\omega t,$$

and phase *a* voltage be determined by function $e_a(t) = \sqrt{2}\cdot E_a\cdot\sin(\omega t-\alpha)$, where parameters E_a, E_{bc}, α can assume any possible value.

Current switchover from one diode to the other one takes place when $e_{bc}(t)$ voltage is zero. Within interval $0<t<T/2$ diode D_b is open. According to the I Kirchhoff law leakage currents (to ground) balance is

$$(G_b+G_0)\cdot u_0 + G_c\cdot(-e_{bc}+u_0)+G_a\cdot(u_0-e_b+e_a)+ \\ +C_b\cdot\frac{du_0}{dt}+C_c\cdot\frac{d(-e_{bc}+u_0)}{dt}+C_a\cdot\frac{d(e_a-e_b+u_0)}{dt}=0. \quad (10)$$

Within interval $T/2<t<T$ diode D_c is open

$$(G_c+G_0)\cdot u_0 + G_b\cdot(e_{bc}+u_0)+G_a\cdot(u_0-e_c+e_a)+ \\ +C_c\cdot\frac{du_0}{dt}+C_b\cdot\frac{d(e_{bc}+u_0)}{dt}+C_a\cdot\frac{d(e_a-e_c+u_0)}{dt}=0. \quad (11)$$

Using insulation equivalent parameters of AC side $G_i = G_a + G_b + G_c$ and $C_i = C_a + C_b + C_c$, both equations assume the following form

$$(G_i+G_0)\cdot u_0 + C_i\cdot\frac{du_0}{dt}+G_a\cdot(e_a-e_b)+ \\ +C_a\cdot\frac{d(e_a-e_b)}{dt}+G_c\cdot(-e_{bc})+C_c\cdot\frac{d(-e_{bc})}{dt}=0; \quad (12)$$

$$(G_i+G_0)\cdot u_0 + C_i\cdot\frac{du_0}{dt}+G_a\cdot(e_a-e_c)+ \\ +C_a\cdot\frac{d(e_a-e_c)}{dt}+G_b\cdot e_{bc}+C_b\cdot\frac{de_{bc}}{dt}=0. \quad (13)$$

After integrating equation (12) within limits $0<t<T/2$ and equation (13) within limits $T/2<t<T$ both equations should be added. As integrals of all capacitive currents over period *T* are zero and mean value of any sinusoidal function is also zero, the following equation is obtained

$$(G_i+G_0)\cdot\frac{1}{T}\int_0^T u_0 dt = (G_i+G_0)\cdot U_{0-mean} = \frac{\sqrt{2}\cdot E_{bc}}{\pi}\cdot G_i, \quad (14)$$

from which the final formula follows

$$R_i = \frac{1}{G_i} = R_0\cdot\frac{\frac{\sqrt{2}\cdot E_{bc}}{\pi}-U_{0-mean}}{U_{0-mean}}. \quad (15)$$

In this method the result depends on voltage E_{bc} of two selected phases. Therefore neither any possible asymmetry of source voltages vectors $\underline{E_a}$, $\underline{E_b}$, $\underline{E_c}$ nor number of network's phases play any role.

The main shortcoming of all presented schemes i.e. necessity of simultaneous readings of network voltages and U_0 voltage can be eliminated with help of a system fulfilling division of two voltages values. Thus for scheme C there can be used a logometer performing division of voltages $\frac{\sqrt{2}\cdot E_{bc}}{\pi}-U_{0-mean}$ and U_{0-mean} supplied to its inputs 1 and 2 (Fig. 8). Therefore its indication corresponds to the value given by formula (15). The other way to avoid the problem is application of stabilized voltage source.

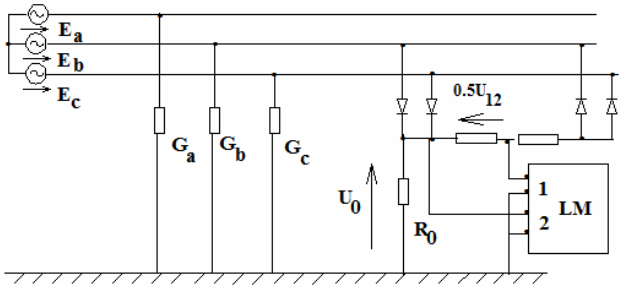

Fig. 8. Application of a logometer (*LM*) for insulation resistance continuous measurement in a 3-phase network

Additional advantages of A,B,C schemes. All presented schemes of continuous insulation monitoring with diode rectifiers have got few valuable advantages which have not been utilized fully in practice so far.

The first one is implementation of insulation level deterioration alarming. For this purpose a DC overvoltage relay should be connected in parallel with R_0 resistor. For the relay setting $U_{0\text{-}set}$ it would detect insulation resistance drop below the threshold equal to

$$R_{i-set} = R_0 \cdot \frac{E - U_{0-set}}{U_{0-set}}, \quad (16)$$

where E – voltage of the rectified test current source. For example in the scheme in Fig. 8 this is

$$E = \frac{\sqrt{2} \cdot E_{bc}}{\pi} = 0.5 \cdot U_{12-mean}. \quad (17)$$

However a significant shortcoming of this simplest solution is dependence of the alarm threshold on network voltage (E) variation for a fixed relay setting $U_{0\text{-}cp}$. Of course this disadvantage can be eliminated with help of a system fulfilling division of voltages or using stabilization of voltage source. Another solution is application of voltage relay supervising sign of the voltages difference

$$U_{0-mean} - E \cdot \frac{R_0}{R_0 + R_{i-set}},$$

which follows from (16).

The second advantage is possibility for implementation of ground faults location in AC IT networks. Ground faults can be located by measuring rectified test current with help of DC current clamp meter (e.g. Kyoritsu or Fluke). This procedure is illustrated in Fig. 9.

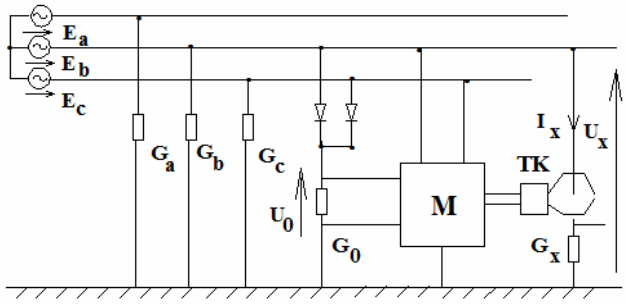

Fig. 9. Application of a scheme of insulation resistance continuous measurement in a 3-phase network for ground fault location: *M* – ground fault locator, *TK* – DC current clamp meter

As mean value of voltage of all conductors against ground is the same, mean values of leakage currents from these conductors to ground are proportional to their insulation-to-ground conductances. When searching for ground fault one can close the clamps around single conductors or multi-wire cables. Microprocessor device *M* determines equivalent insulation resistance of the entire network from (15) and insulation resistance of a single conductor «*x*» from the following formula

$$R_x = \frac{1}{G_x} = \frac{U_{x-mean}}{I_{x-mean}} \quad (18)$$

Conclusions.

1. Traditional systems of insulation continuous monitoring based on multiphase diode rectifiers are sensitive to variation of network voltages and their possible asymmetry.

2. Application of a single phase star diode rectifier enables to eliminate the above mentioned difficulties.

3. Attention should also be turned to other qualities of the presented schemes i.e. insulation level deterioration alarming and ground fault location.

REFERENCES

1. Hofheinz W. *Protective Measures with Insulation Monitoring*. VDE Verlag, 1998.

2. Tsapenko E.F. *Kontrol' izoliatsii v setiakh do 1000 V* [Insulation monitoring in networks up to 1000 V]. Moscow, Energiya Publ., 1972. (Rus).

3. Tsapenko E.F. *Zamykaniia na zemliu v setiakh 6-35 kV* [Earth faults in networks 6-35 kV]. Moscow, Energoatomizdat Publ., 1986. (Rus).

4. Olszowiec P. Unconventional Methods of Analyzing Diode Rectifiers with Asymmetrical Supply. *Computational Problems of Electrical Engineering*, 2014, no.2, pp. 33-36.

5. Olszowiec P. O wyznaczaniu napięć trójfazowych prostowników diodowych. *Wiadomości Elektrotechniczne*, 2015, vol.1, no.10, pp. 33-34. **doi: 10.15199/74.2015.10.8**.

6. Olszowiec P. *Insulation Measurement and Supervision in Live AC and DC Unearthed Systems*. Lecture Notes in Electrical Engineering, 2nd edition. Springer, 2014. **doi: 10.1007/978-3-642-29755-7**.

Piotr Olszowiec, MSc., Electrical Engineer,
Elporem i Elpoautomatyka Spółka z o.o.,
28-200 Staszow, ul. Wschodnia 10/51, Poland,
phone +48 606 613976,
e-mail: olpio@o2.pl

How to cite this article:
Olszowiec P. Modifications of diode rectifier circuits for continuous insulation measurement in live AC IT networks. *Electrical engineering & electromechanics*, 2016, no.2, pp. 43-46. doi: 10.20998/2074-272X.2016.2.08.

UDC 621.31 **doi: 10.20998/2074-272X.2016.2.09**

Yu.L. Sayenko, D.N. Kalyuzhniy

NUMERICAL ANALYSIS OF MATHEMATICAL MODELS OF THE FACTUAL CONTRIBUTION DISTRIBUTION IN ASYMMETRY AND DEVIATION OF VOLTAGE AT THE COMMON COUPLING POINTS OF ENERGY SUPPLY SYSTEMS

Purpose. *Perform numerical analysis of the distribution of the factual contributions of line sources of distortion in the voltage distortion at the point of common coupling, based on the principles of superposition and exclusions.* ***Methodology.*** *Numerical analysis was performed on the results of the simulation steady state operation of power supply system of seven electricity consumers.* ***Results.*** *Mathematical model for determining the factual contribution of line sources of distortion in the voltage distortion at the point of common coupling, based on the principles of superposition and exclusions, are equivalent. To assess the degree of participation of each source of distortion in the voltage distortion at the point of common coupling and distribution of financial compensation to the injured party by all sources of distortion developed a one-dimensional criteria based on the scalar product of vectors. Not accounting group sources of distortion, which belong to the subject of the energy market, to determine their total factual contribution as the residual of the factual contribution between all sources of distortion.* ***Originality.*** *Simulation mode power supply system was carried out in the phase components space, taking into account the distributed characteristics of distortion sources.* ***Practical value.*** *The results of research can be used to develop methods and tools for distributed measurement and analytical systems assessment of the power quality.* References 8, tables 6, figures 3.

Key words: **power quality, factual contribution, point of common coupling, voltage asymmetry, voltage deviation.**

На основе имитационного моделирования проведен сравнительный анализ математических моделей распределения фактических вкладов линейных источников искажений в искажение напряжений в точке общего присоединения, которые основаны на принципах наложения и исключения. Полученные результаты позволили сделать вывод об эквивалентности двух математических моделей и их произвольном выборе для решения задачи распределения фактических вкладов линейных источников искажений в искажение напряжений в точке общего присоединения. Библ. 8, табл. 6, рис. 3.

Ключевые слова: **качество электрической энергии, фактический вклад, точка общего присоединения, несимметрия напряжений, отклонение напряжения.**

Introduction. Non-compliance of power quality (PQ) to established standards are the reasons the marriage of products, equipment damage, and additional power losses both in consumers and electrical energy (EE) suppliers [1]. According to some estimates [2] annual economical losses in several countries due to the low PQ arise USD 10-20 bln. For certain sectors of production decrease in PQ can cause damage to 3.800.000 EUR per event [3]. Obviously, if this happens, it becomes a question of determining those responsible for lowering the PQ and compensation of economic damages to the injured party. The answer to it is to solve the problem of the distribution of factual contributions (FC) of sources of distortion (SD) in the distortion of the voltage at the point of common coupling (PCC) [4].

Problem definition. One of the new directions of development of the FC SD distribution methods in voltage distortion at PCC involves the use of mathematical models, drawn up in phase coordinates, given the distributed nature of SD in the power supply system (PSS), which are based on the principles of superposition [5] and exclusion [6].

A mathematical model of the distribution of FC of linear SD (undistorting the sinusoidal voltage waveform) in the voltage distortion is based on the principle of superposition, involves the expansion of distorting parts of voltages in each PCC from the activities of all SD according to the following expression:

$$\sum_{i=1}^{n} \boldsymbol{U}_{dis\,i} = \boldsymbol{A}^{T} \times \boldsymbol{Y}_{undis}^{-1} \times \sum_{i=1}^{n} \boldsymbol{I}_{dis\,i}\,, \qquad (1)$$

where $\boldsymbol{A}$ is the incidence matrix; $\boldsymbol{Y}_{undis}$ is the matrix of undistorted nodal conductivities of the PSS and EE consumers; $\boldsymbol{I}_{dis\,i}$ is column matrix of distorted currents characterizing the *i*-th active or passive element with SD.

A mathematical model of the distribution of FC of linear SD in the voltage distortion is based on the principle of exclusion, involves determining the distorting of the voltage in each PCC, introduced by the *i*-th SD, by the following expression:

$$\boldsymbol{U}_{dis\,i} = \boldsymbol{U}_{dis} - \boldsymbol{U}_{dis}^{ex\,SD\,i}\,, \qquad (2)$$

где $\boldsymbol{U}_{dis}$ the matrix of distorted parts of voltages in the PCC from common action of all SD; $\boldsymbol{U}_{dis}^{ex\,SD\,i}$ is the matrix of distorted parts of voltages in the PCC with excluded distorted part of the *i*-th SD.

To check the adequacy and the comparison of the proposed new mathematical models of the distribution of FC of linear SD in voltage distortion at PCC it is necessary to perform the numerical analysis.

The goal of the investigation. To perform numerical analysis of mathematical models of distribution of FC of linear SD in voltage distortion in the PCC, based on the principles of superposition and exclusion.

Results of the investigation. We consider the PSS of seven EE power consumers (C) (see Fig. 1) consisting of a energy supply (ES), generalized electrical network (EN), a power transformer (T) and three overhead lines (OL).

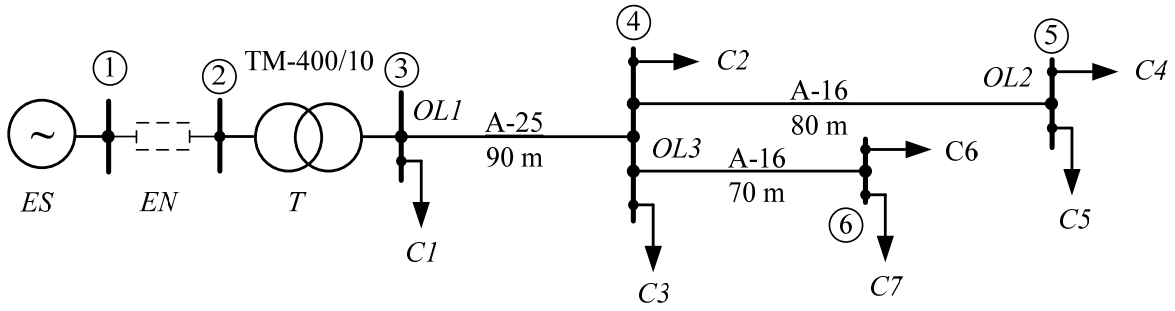

Fig. 1. Power supply system of seven consumers of EE

The parameters of equivalent circuits of the elements of the considered PSS and EE consumers reduced to the voltage of 380 V are the following. The voltage on the buses of the ES: $\underline{U}_A^{ES} = 232\angle 0°$ V; $\underline{U}_B^{ES} = 232\angle 240°$ V; $\underline{U}_C^{ES} = 232\angle 120°$ V. Equivalent resistances of the generalized EN: $\underline{Z}_A^{EN}$ = 0.008 + j0.148 Ω; $\underline{Z}_B^{EN}$ = 0.008 + j0.04 Ω; $\underline{Z}_C^{EN}$ = 0.008 + j0.056 Ω. Equivalent resistances of EE consumers:

i	$\underline{Z}_A^{Ci}$, Ω	$\underline{Z}_B^{Ci}$, Ω	$\underline{Z}_C^{Ci}$, Ω
1	7.2 + *j*3.7	6.5 + *j*3.0	6.74+ *j*3.5
2	6.9 + *j*5.2	7.7 + *j*3.7	6.87 + *j*3.9
3	13.7+ *j*5.2	15.1 + *j*4.7	14.2 + *j*4.6
4	9.7 + *j*3.2	8.9 + *j*3.1	10.5 + *j*3.5
5	6.3 + *j*1.9	6.8 + *j*1.4	7.2 + *j*1.9
6	17.2 + *j*7.1	19.8 + *j*8.1	15.6 + *j*6.5
7	13.9 + *j*3.9	14.9 + *j*4.9	15.1 + *j*4.5

Resistance of the power transformer: $\underline{Z}_{ph\,T}$ = 0.00105 + j0.0072 Ω. Conductivity of the power transformer: $\underline{Y}_{pT}$ = 0.001375 + j0.0021 S. Specific resistance of the OL: $\underline{Z}_s^{A25}$ = 1.26 + j0.34 Ω/km; $\underline{Z}_s^{A16}$ = = 1.97 + j0.345 Ω.

According to calculations carried out, the steady state operation of the considered PSS is characterized by parameters given in the Table 1. It follows from them that in the PCC No. 5, to which EE consumers C4 and C5 are connected, the coefficient of asymmetry of voltage by the zero sequence K_{0U} and steady state deviation of the voltage δU_y exceed the normal allowable values [7]. On this basis, for the PCC No. 5 we determine FC of all SD in the distortion of its voltage.

According to the mathematical models (1) and (2) in the equivalent circuit of the individual elements of the PSS and EE customers distorted part of SD must be extracted and identified [8]. If SD is a passive longitudinal element, its equivalent circuit will be determined by a series connection of two resistances, one of which describes the undistorted part ($\underline{Z}_{el}^{undis}$), and the other – distorting part ($\underline{Z}_{el}^{dis}$). If SD is a passive cross element, its equivalent circuit will be determined by the parallel connection of two conductivities $\underline{Y}_{el}^{undis}$ and $\underline{Y}_{el}^{dis}$. For SD, which is an active element the equivalent circuit is provided as a serial connection of two EMF ($\underline{E}_{ES}^{undis}$ and $\underline{E}_{ES}^{dis}$).

Determination of distorted part of any SD by voltage asymmetry is based on the deflection of its parameters from some symmetric state, for example for passive SD:

$$\begin{cases} \underline{F}_{A(B,C)el}^{undis} = \dfrac{\underline{F}_A^{el} + \underline{F}_B^{el} + \underline{F}_C^{el}}{3}; \\ \underline{F}_{ph\,el}^{dis} = \underline{F}_{ph} - \underline{F}_{ph\,el}^{undis}. \end{cases} \quad (3)$$

The basis of determination of distorted parts of the SD by the deflection voltage are the principles of compliance with the required voltage levels on the ES buses and in control nodes of the PSS voltage as well as load of the individual elements of EN and EE consumers not exceeding permissible or maximum permissible values for them.

So, in the case of excess power of consumer above the maximum permitted its distorted part will be characterized by the following conductivity:

$$\underline{Y}_{ph\,Ci}^{dis} = \Delta\underline{S}_{ph\,Ci}^{*} \Big/ U_{ph\,Ci}^{2}, \quad (4)$$

where $\Delta\underline{S}_{ph\,Ci}$ is the part of the phase power of the *i*-th EE consumer, exceeding its maximum allowed value; $\underline{U}_{ph\,Ci}$ is the phase voltage of the *i*-th EE consumer.

Distortion of the actual voltage on the ES buses ($\underline{E}_{ph\,ES}^{fact}$) from the value required by the PSS operation mode ($\underline{E}_{ph\,ES}^{undis}$) will characterize its distorted part:

$$\underline{E}_{ph\,ES}^{dis} = \underline{E}_{ph\,ES}^{undis} - \underline{E}_{ph\,ES}^{fact}. \quad (5)$$

In our case, the maximum permitted power of electrical loads of each EE consumers are listed in Table 2. On operation mode conditions of the PSS the voltage on the ES buses must be maintained as $1{,}065 \cdot U_{nom}$. Voltage regulation by the power transformer is not performed.

On the basis of the above expressions and additional information about the PSS operation, distorted and undistorted parameters of all its SD are determined (see Table 3 and Table 5). According to the mathematical models (1) and (2) the distribution of FC of linear SD in distortion of the voltage in the PCC No. 5 corresponds to the data given in Table 4 and Table 6. For a more visual representation these results are presented in Fig. 3 in graphical form.

Table 1

Parameters of operation modes of the PSS and indicator of PQ in PCC

Parameters of the operation mode of the PSS	PCC PSS					
	1*	2*	3	4	5	6
$\underline{U}_A(\underline{U}_{AB})$, V	401.84∠30	395.33∠28.67	224.09∠−1.17	210.11∠−0.88	202.01∠−0.41	206.53∠−0.85
$\underline{U}_B(\underline{U}_{BC})$, V	401.84∠−90	396.48∠−91.57	228.26∠−122.55	215.2∠−122.42	206.45∠−122.35	212.36∠−122.23
$\underline{U}_C(\underline{U}_{CA})$, V	401.84∠150	394.48∠148.4	231.05∠118.53	217.66∠118.91	210.76∠119.06	213.7∠119.14
δU_y, %	5.75	4.06	3.54	−2.59	−6.19	−4.16
K_{2U}, %	0	0.293	0.29	0.35	0.37	0.39
K_{0U}, %	0	0	1.6	1.86	2.21	1.82

** Note. For the PCC No. 1, 2 the values of the line voltages are indicated.*

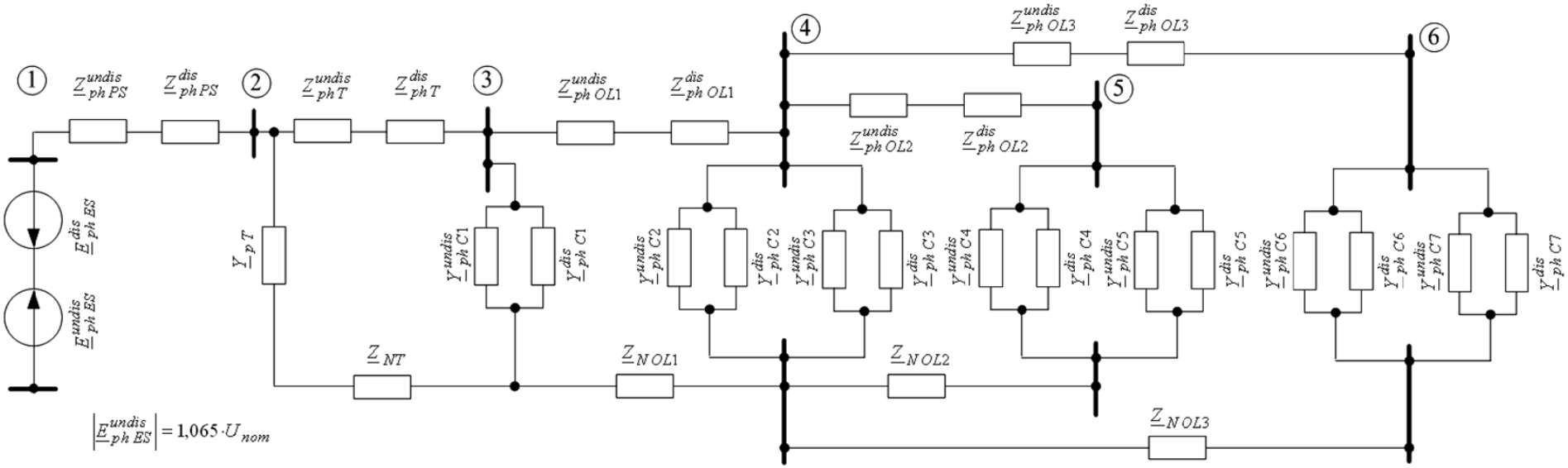

Fig. 2. Equivalent circuit of the PSS and EE consumers in the single-phase version

Table 2

Maximal permitted power of the electrical load of the EE consumers

Power	C1	C2	C3	C4	C5	C6	C7
S_{max}, kVA	8+*j*2.5	5+*j*2	3.5+*j*1.5	4+*j*1.5	7+*j*2.2	3+*j*1.3	3.5+*j*1.5

Table 3

Equivalent circuit parameters of the PSS elements and EE consumers for the FC distribution by the voltage asymmetry

Equivalent circuit	PSS element and power consumers												
	EN	T* (winding)	T* (magnetic)	OL1*	OL2*	OL3*	C1	C2	C3	C4	C5	C6	C7
$\underline{Z}_A^{undis}$, Ω ($\underline{Y}_A^{undis}$, S)	0.008 +j0.048	0.00105 +j0.0072	(0.001375 −j0.0021)	0.1134 +j0.031	0.1576 +j0.0276	0.1379 +j0.0242	(0.118 −j0.059)	(0.109 −j0.058)	(0.063 −j0.021)	(0.093 −j0.031)	(0.139 −j0.036)	(0.049 −j0.02)	(0.063 −j0.019)
$\underline{Z}_A^{dis}$, Ω ($\underline{Y}_A^{dis}$, S)	0	0	0	0	0	0	(−0.00798 +j0.0021)	(0.00227 −j0.00309)	(0.001164 −j0.00299)	(0.000011 −j0.00071)	(0.00669 −j0.00815)	(0.000488 −j0.00018)	(0.00399 −j0.00021)
$\underline{Z}_B^{undis}$, Ω ($\underline{Y}_B^{undis}$, S)	0.008 +j0.048	0.00105 +j0.0072	(0.001375 −j0.0021)	0.1134 +j0.031	0.1576 +j0.0276	0.1379 +j0.0242	(0.118 −j0.059)	(0.109 −j0.058)	(0.063 −j0.021)	(0.093 −j0.031)	(0.139 −j0.036)	(0.049 −j0.02)	(0.063 −j0.019)
$\underline{Z}_B^{dis}$, Ω ($\underline{Y}_B^{dis}$, S)	−j0.008	0	0	0	0	0	(0.008973 −j0.00029)	(−0.00342 −j0.00745)	(−0.00261 +j0.0024)	(0.007239 −j0.00352)	(0.002271 +j0.0067)	(−0.00592 +j0.0026)	(−0.00213 −j0.00099)
$\underline{Z}_C^{undis}$, Ω ($\underline{Y}_C^{undis}$, S)	0.008 +j0.048	0.00105 +j0.0072	(0.001375 −j0.0021)	0.1134 +j0.031	0.1576 +j0.0276	0.1379 +j0.0242	(0.118 −j0.059)	(0.109 −j0.058)	(0.063 −j0.021)	(0.093 −j0.031)	(0.139 −j0.036)	(0.049 −j0.02)	(0.063 −j0.019)
$\underline{Z}_C^{dis}$, Ω ($\underline{Y}_C^{dis}$, S)	j0.008	0	0	0	0	0	(−0.00099 −j0.0021)	(0.00153 −j0.00435)	(0.00109 +j0.0006)	(−0.00725 +j0.0028)	(−0.00896 +j0.0015)	(0.00543 −j0.00243)	(−0.00187 +j0.0008)
$\underline{Z}_N$, Ω	–	≈0	–	0.1134 +j0.031	0.1576 +j0.0276	0.1379 +j0.0242	≈0	≈0	≈0	≈0	≈0	≈0	≈0

* *The power transformer and OL are accepted symmetrical elements.*

Table 4

Distribution of FC of linear SD in voltage distortion by the voltage asymmetry

PCC	Indicator of PQ		Voltages of symmetrical components									
			Voltage of zero sequence, V/grad	FC of the i-th SD in voltage asymmetry								
				EN	C1	C2	C3	C4	C5	C6	C7	∑
Mathematical model based on the principle of SD superposition												
5	K_{0U}, %	2.21	$\lvert\underline{U}_0\rvert$	4.57	$4.9\cdot10^{-7}$	1.125	1.336	0.363	1.522	3.138	0.982	0.402	4.57
			$\arg(\underline{U}_0)$	142.3	2.68	49.42	−162.52	175.32	82.07	141.12	−97.23	−151.89	142.3
Mathematical model based on the principle of SD exclusion												
5	K_{0U}, %	2.21	$\lvert\underline{U}_0\rvert$	4.57	$7\cdot10^{-4}$	1.125	1.337	0.363	1.524	3.138	0.983	0.402	4.569
			$\arg(\underline{U}_0)$	142.3	167.27	49.43	−162.49	175.35	82.02	141.1	−97.21	−151.8	142.3

Table 5

Equivalent circuit parameters of the PSS elements and EE consumers for the FC distribution by the voltage deviation

Equivalent circuit	PSS element and power consumers												
	EN	T* (winding)	T* (magnetic)	OL1*	OL2*	OL3*	C1	C2	C3	C4	C5	C6	C7
$\underline{Z}_A^{undis}$, Ω ($\underline{Y}_A^{undis}$, S)	0.008 +j0.048	0.00105 +j0.0072	(0.001375 −j0.0021)	0.1134 +j0.031	0.1576 +j0.0276	0.1379 +j0.0242	(0.11 −j0.049)	(0.111 −j0.045)	(0.064 −j0.024)	(0.093 −j0.031)	(0.145 −j0.044)	(0.05 −j0.021)	(0.067 −j0.019)
$\underline{Z}_A^{dis}$, Ω ($\underline{Y}_A^{dis}$, S)	0	0	0	0	0	0	(−j0.00697)	(−j0.016)	0	0	0	0	0
$\underline{Z}_B^{undis}$, Ω ($\underline{Y}_B^{undis}$, S)	0.008 +j0.04	0.00105 +j0.0072	(0.001375 −j0.0021)	0.1134 +j0.031	0.1576 +j0.0276	0.1379 +j0.0242	0.127 −j0.048	0.106 −j0.043	0.06 −j0.019	0.094 −j0.035	0.141 −j0.029	0.043 −j0.018	0.061 −j0.02
$\underline{Z}_B^{dis}$, Ω ($\underline{Y}_B^{dis}$, S)	0	0	0	0	0	0	(−j0.01)	(−j0.0073)	0	(0.0059)	0	0	0
$\underline{Z}_C^{undis}$, Ω ($\underline{Y}_C^{undis}$, S)	0.008 +j0.056	0.00105 +j0.0072	(0.001375 −j0.0021)	0.1134 +j0.031	0.1576 +j0.0276	0.1379 +j0.0242	0.117 −j0.047	0.106 −j0.042	0.064 −j0.021	0.086 −j0.029	0.13 −j0.034	0.055 −j0.023	0.061 −j0.018
$\underline{Z}_C^{dis}$, Ω ($\underline{Y}_C^{dis}$, S)	0	0	0	0	0	0	(0.014)	(0.00453 −j0.002)	0	0	0	0	0
$\underline{Z}_N$, Ω	–	≈0	–	0.1134 +j0.031	0.1576 +j0.0276	0.1379 +j0.0242	≈0	≈0	≈0	≈0	≈0	≈0	≈0

* *The power transformer and OL are accepted symmetrical elements.*

Table 6

Distribution of FC of linear SD in voltage distortion by the voltage deviation

PCC	Indicator of PQ		Voltage deviation by direct sequence										
			Voltage deviation from lower normal permitted (np) bound, V/grad		FC of the i-th excluded SD in the voltage deviation								
					ES	C1	C2	C3	C4	C5	C6	C7	∑
Mathematical model based on the principle of SD superposition													
5	δU_y, %	−6.19	$U_{\min}^{np} - \lvert\underline{U}_1\rvert$	2.615	2.051	0.12	0.423	0	0.122	0	0	0	2.575
			$-\arg(\underline{U}_1)$	178.8	178.68	166.26	129.12	0	−161.52	0	0	0	171.84
Mathematical model based on the principle of SD exclusion													
5	δU_y, %	−6.19	$U_{\min}^{np} - \lvert\underline{U}_1\rvert$	2.615	2.046	0.119	0.423	0	0.121	0	0	0	2.57
			$-\arg(\underline{U}_1)$	178.8	178.76	166.6	129.17	0	−161.68	0	0	0	171.9

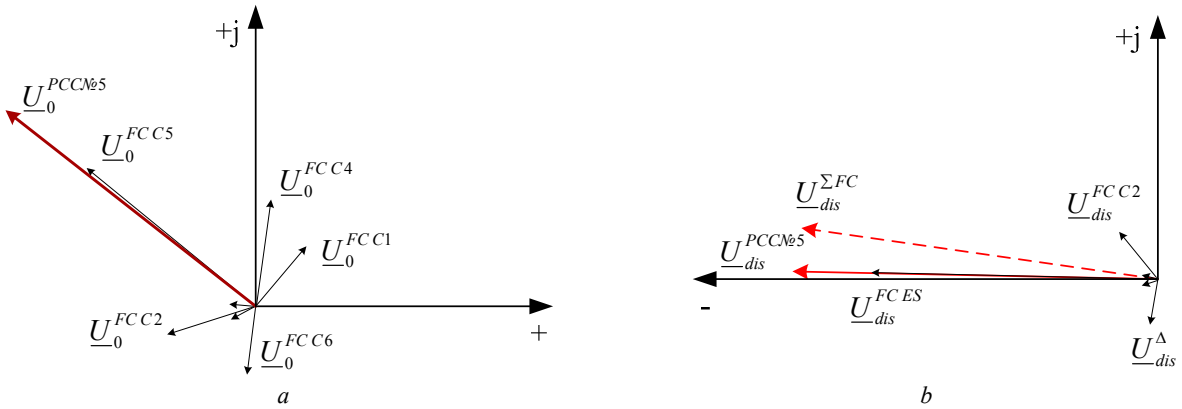

Fig. 3. Graphical representation of the distribution of FC of linear SD in voltage distortion in the PCC No. 5 on the base of the mathematical model: (1): *a*) by the voltage asymmetry; *b*) by the voltage deviation

We estimate the divergence of results for the distribution of FC of linear SD in distortion of voltages in the PCC No. 5, obtained on the basis of (1) and (2) mathematical models, by the relative root-mean-square deviation:

$$\delta = \frac{\sum_{i=1}^{n}\left\{\left[\mathrm{Re}\left(\underline{U}_{dis(1)}^{FCi}\right)-\mathrm{Re}\left(\underline{U}_{dis(2)}^{FCi}\right)\right]^2+\left[\mathrm{Im}\left(\underline{U}_{dis(1)}^{FCi}\right)-\mathrm{Im}\left(\underline{U}_{dis(2)}^{FCi}\right)\right]^2\right\}}{\sum_{i=1}^{n}\left[\mathrm{Re}\left(\underline{U}_{dis(1)}^{FCi}\right)\right]^2+\left[\mathrm{Im}\left(\underline{U}_{dis(1)}^{FCi}\right)\right]^2}\cdot 100\%, \qquad (6)$$

where n is the total number of SD; symbols 1 and 2 correspond the mathematical model (1) and (2), respectively.

In our case, δ by the voltage asymmetry is $6.4\cdot10^{-5}$ %, and by the voltage deviation – $8.1\cdot10^{-4}$ %. These values lead to the conclusion of equivalence of (1) and (2) mathematical models and, consequently, their arbitrary choice for the solution of the problem of the distribution of FC of linear SD in the voltage distortion in the PCC.

We analyze the obtained FC distributions. Firstly, FC distribution of linear SD in the voltage distortion in the PCC is a vector (two-dimensional) quantity. It is obvious that in such a form the FC can not be used for the distribution of financial compensations for the reduction of PQ and it is necessary to provide a corresponding one-dimensional criterion. We set as the basis of the one-dimensional criterion of the FC distribution the FC scalar product in vector form:

$$\alpha_i = \left\langle \underline{U}_{dis}^{FC\,DS\,i}, \underline{U}_{dis}^{PCC} \right\rangle; \; FC_{DS\,i} = \left[|\alpha_i| \Big/ \sum_{i=1}^{n} |\alpha_i| \right] \cdot 100\% \; . (7)$$

Such an approach means that this criterion assesses the FC by projections of vector FC $\underline{U}_{dis}^{FC\,DS\,i}$ on the total vector of the voltage distortion in the PCC $\underline{U}_{dis}^{PCC}$. Omitting the module in the expression (7) it is possible to additionally take into account the effect of the voltage distortion compensation introduced by separate SD. In our case, this effect is most clearly demonstrated by the vectors $\underline{U}_0^{FC\,C4}$ and $\underline{U}_0^{FC\,C6}$ (Fig. 3,*a*).

Secondly, in the voltage distortion in the PCC No. 5 all SD PSS take part. Here, FC SD outside the PCC No. 5 may be comparable to or greater than FC SD connected directly to the PCC considered.

Third, the discrepancy of the FC ($\underline{U}_{dis}^{\Delta} = \underline{U}_{dis}^{PCC№5} - \underline{U}_{dis}^{\Sigma FC}$) between all SD (Fig. 3,*b*) which is caused by not taking into account or the inaccuracy of the determination of distorted parts of some SD is possible. To eliminate it is enough to group the unknown or ill-defined SD, belonging to the same subject of the energy market, for example, the PSS, and to determine their total FC by excluding from the total distortion level voltages in the PCC:

$$\underline{U}_{dis}^{FC\,PSS} = \underline{U}_{dis}^{PCC№5} - \underline{U}_{dis}^{\Sigma FC\,Ci} \; . \qquad (8)$$

On the basis of the above, a one-dimensional distribution of the FC by the voltage asymmetry in the PCC No. 5 will be:

$FC_{DS\,i}$, %	EN	C1	C2	C3
	$8.6\cdot10^{-6}$	1.0	13.43	5.36
	П4	П5	П6	П7
	13.31	55.24	8.77	2.9

Assuming that distorted parts of the SD part from the side of the EE customers are identified accurately and distorted parts of the SD from the side of PSS elements are grouped, the one-dimensional distribution of the FC by the voltage deviation in the considered PCC will be:

$FC_{DS\,i}$, %	PSS	C1	C2	C3
	80.64	4.46	10.56	0
	П4	П5	П6	П7
	4.34	0	0	0

The obtained results show that most part of the payments for compensation of economic losses for the subjects of the energy market in the PCC No. 5 from the voltage asymmetry falls on EE customers C5 (55.24 %) and C2 (13.43 %), and from the voltage deviations – on the PSS (80.64 %) and EE C2 customer (10.56 %).

Conclusions. Mathematical models of determination of FC of linear sources of SD in the voltage distortion in the PCC, based on the principles of superposition and exclusion, are equivalent. To assess the degree of participation of each SD in the voltage distortion in the PCC and the distribution of financial compensation to the injured

party between all SD, a one-dimensional criterion of FC distribution based on the scalar product of vectors is developed. Not accounting the group of SD, belonging to one subject of the energy market, permits to determine their total FC as the discrepancy of the distribution of FC between all SD.

REFERENCES

1. Shidlovskiy A.K., Kuznetsov V.G., Nikolaenko V.G. *Ekonomicheskaia otsenka posledstviy s nizheniia kachestva elektricheskoy energii v sovremennukh sistemakh elektrosnabzheniia* [Economic evaluation of the effects of reducing the quality of electricity in modern power supply systems]. Kiev, IED AN USSR Publ., 1981. 49 p. (Rus).

2. Zhezhelenko I.V., Saenko Yu.L. *Kachestvo elektroenergii na promushlennukh predpriiatiiakh* [Power quality in industrial plants]. Moscow, Energoatomizdat Publ., 2005. 261 p. (Rus).

3. Chepmen D. Price of low power quality. *Energosberezhenie - Energy Saving*, 2004, no.1, pp. 66-69. (Rus).

4. Sayenko Yu., Kalyuzhniy D. Analytical methods for determination of the factual contributions impact of the objects connected to power system on the distortion of symmetry and sinusoidal waveform of voltages. *Przeglad Elektrotechniczny*, 2015, vol.11, pp. 81-85. **doi: 10.15199/48.2015.11.23**.

5. Saenko Yu.L., Kalyuzhnyiy D.N. Superposition principle in mathematical models of the factual contribution distribution of linear sources of distortion in voltage distortion at the point of common coupling. *Elektrifikatsiya transporta - Electrification of transport*, 2015, no.10, pp. 123-133. (Rus).

6. Saenko Yu. L., Kalyuzhnyiy D. N. Exclusion principle in mathematical models of distribution of the factual contribution of the linear source of distortion in voltage distortion at the point of common coupling. *Visnik Harkivskogo natsionalnogo tehnichnogo universitetu silskogo gospodarstva imeni Petra Vasilenka - Bulletin of Kharkiv Petro Vasylenko National Technical University of Agriculture*, 2015, no.167, pp. 31-33. (Rus).

7. *GOST 13109-97. Elektricheskaya energiya. Trebovaniya k kachestvu elektricheskoy energii v elektricheskih setyah obschego naznacheniya* [State Standard 13109-97. Electric Energy. Requirements for the power quality in electric networks of general purpose]. Kiev, Gosstandart Ukrainy Publ., 1999. 33 p. (Rus).

8. Kalyuzhniy D.N. Presentation of linear sources of distortion in the mathematical models of their factual contribution distribution in voltage distortion at the point of common coupling. *Energosberezhenie. Energetika. Energoaudit – Energy saving. Power engineering. Energy audit*, 2015, no.11, pp. 19-25. (Rus).

Received 13.01.2016

Yu.L. Sayenko[1], *Doctor of Technical Science, Professor,*
D.N. Kalyuzhniy[2], *Candidate of Technical Science, Associate Professor,*
[1] Pryazovskyi State Technical University,
7, Universytets'ka Str., Mariupol, 87500, Ukraine,
phone +380 629 446551, e-mail: YuriSayenko@mail.ru.
[2] O.M. Beketov National University of Urban Economy in Kharkiv,
12, Revolution Str., Kharkiv, 61002, Ukraine,
phone +380 50 5606835, e-mail: KalyuzhniyDN@mail.ru

How to cite this article:
Sayenko Yu.L., Kalyuzhniy D.N. Numerical analysis of mathematical models of the factual contribution distribution in asymmetry and deviation of voltage at the common coupling points of energy supply systems. *Electrical engineering & electromechanics*, 2016, no.2, pp. 47-53. doi: 10.20998/2074-272X.2016.2.09.

UDC 621.311 **doi: 10.20998/2074-272X.2016.2.10**

G.A. Senderovich, A.V. Diachenko

THE RELEVANCE OF DETERMINING RESPONSIBILITY FOR VIOLATION OF POWER QUALITY IN TERMS OF VOLTAGE FLUCTUATIONS

Purpose. The purpose of work is the analysis of scientific and technical information for determination of expediency of researches on the determined calculations of individual share of suppliers and consumers in violation of quality of electric energy on indicators of fluctuations of voltage. Methodology. Today the indicators characterizing fluctuations of voltage aren't considered: scope of change of voltage (δU_t) and dose of a flicker (P_t). These indicators represent long changes of characteristics of tension that assumes potential opportunity for studying of regularities of their emergence and the determined distribution of responsibility for these violations between subjects. Results. As showed by results of research: fluctuations of voltage make negative impact on sight of the person and functioning of the electric equipment; in a network there is a large number of possible sources of fluctuation of tension; there are ways of identification of fluctuation of voltage; there are methods of decrease in fluctuation of voltage. The analysis of literature didn't reveal development by definition of responsibility of subjects for violation of requirements to quality of electric energy regarding fluctuations of voltage. Originality. Performance of development in this direction will make definition of responsibility for violation of quality of electric energy fuller and basic. Practical value. This research will allow to develop further the metering device which defines responsibility according to the current legislation, and has flexible algorithm for further improvement. to the legislation, also has flexible algorithm for further improvement. References 12, figures 7.

Key words: **quality of the electric power, indicators of quality of the electric power, electromagnetic compatibility, fluctuations of tension, fliker, scope of change of tension, definition of responsibility.**

В статье рассмотрены физические процессы при колебаниях напряжения, способы измерения и расчетов показателей их характеризующих, влияние колебаний напряжения на электрооборудование и мероприятия по его снижению. Сделан вывод о целесообразности проведения исследований по определению ответственности субъектов в случае превышения колебаниями напряжения допустимых значений. Библ. 12, рис. 7.

Ключевые слова: **качество электроэнергии, показатели качества электроэнергии, электромагнитная совместимость, колебания напряжения, фликер, размах изменения напряжения, определение ответственности.**

Introduction. Electrical energy as a product is used in all spheres of human activity, has a set of specific properties, and is directly involved in creating other types of products, affecting their quality. The concept of electrical energy quality (EEQ) is different from the concept of quality of other types of products. Each electrical customer (EC) is designed to operate at actual nominal parameters of electric energy, which are characterized by indicators of electrical energy quality (IEEQ). Degree of conformity of real and nominal IEEQ established by GOST characterizes EEQ.

Maintenance of requirements for EEQ on-site production does not guarantee their availability at the place of consumption, as the IEEQ influence the technical characteristics of the network and EC modes and exploitation. EEQ is also characterized by the term «electromagnetic compatibility». Under electromagnetic compatibility they mean the ability of EC to function normally in its electromagnetic environment (in the electrical network to which it is connected), without creating unacceptable interference to other EC, operating in the same environment.

Problem definition. Increase EEQ is an actual task of development of power industry, aimed at reducing electricity losses, increasing the service life of electrical equipment, ensuring the conditions of the normal process of electrical consumers. An important condition for improving the EEQ in electric networks of Ukraine is the interested the subjects of distribution and consumption of electricity. The way to improve the interest to ensure the necessary EEQ passes through the introduction of financial responsibility of suppliers and consumers for exceeding pre-admissible deviation of the IEEQ, in particular, and voltage fluctuations (VF).

Today we can say that the development of methods and techniques for determining the equity entities of the distribution of electricity in the liability for breach of EEQ in three-phase power networks for the following IEEQ and their characteristics: coefficient of asymmetry of voltage on the negative sequence and zero sequence (K_{2U}, K_{0U}), distortion factor of sinusoidal voltage curve and the coefficient of the n-th harmonic component of the voltage (K_U, $K_{U(n)}$), as well as steady state voltage deviations (δU_y). A complex technique that combines three techniques mentioned is also developed [1-4].

Not considered indicators characterizing VF: magnitude of voltage change (δU_t) and flicker dose (P_t). These indicators, like previous ones, are long-lasting changes in stress characteristics, which suggests the potential for the study of the laws of their occurrence and the determined allocation of responsibility for such violations between subjects. Implementation of development in this area will make the determination of

responsibility for violating EEQ more comprehensive and fundamental, that in the future will develop a metering device, which determines the liability according to the legislation in force, and has a flexible algorithm for further improvement. Such a device should fix the deviations of all the above parameters, and make a generalized conclusion about the responsibility of the parties.

The goal of the work is analysis of scientific and technical information to determine the feasibility studies on deterministic estimates the equity providers and consumers in violation of the EEQ in terms of voltage fluctuations.

Results of investigations. When electrical customers are working with rapidly changing shock loads, in the mains power consumption abrupt shocks arise. This causes a change in the mains voltage swings which can reach high values, for example, the inclusion of an asynchronous motor with a high starting current multiplicity. These phenomena are caused by technological installations with rapidly varying mode of operation, which is accompanied by lashing out active and reactive power, such as a drive reversing rolling mills, electric arc furnaces, welding machines, etc.

We represent the power supply of the consumer in the form of equivalent circuit (Fig. 1) in which $\underline{E}_{syst}$ is the equivalent EMF of the system; $\underline{U}$ is the voltage on the busbars of the receiving substation; $\underline{Z}_{syst}$ is the equivalent resistance of the connection with the system; $\underline{Z}_{load}$ is the equivalent resistance of the load of the enterprise.

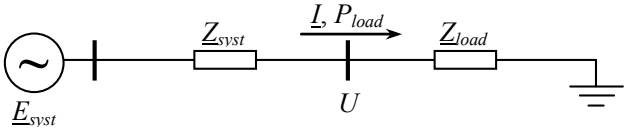

Fig. 1. Equivalent circuit of the customer's power supply

Changing of the voltage $\underline{U}$ on the busbars of the receiving substation caused by external to the electrical network of the consumer exposure, it can be seen as a consequence of changes in the EMF of the system $\underline{E}_{syst}$. On the assumption of the immutability of the load resistance ($\underline{Z}_{load}$ = const) the reduction of $\underline{E}_{syst}$ reduces the current I on the load lines and power consumer P_{load}, raising $\underline{E}_{syst}$ – to increase of I and P_{load}. In fact, when changing the voltage U the load resistance $\underline{Z}_{load}$ may vary somewhat, but in general, this change corresponds to a positive regulatory effect of active load voltage [5].

If the source of the VF is located in the electrical network of the consumer, the voltage $\underline{U}$ changes in the tire receiving substation is due to varying load at constant EMF system ($\underline{Z}_{load}$ = const). The value of voltage U is determined by the voltage drop on the resistance of the connection with the system $\underline{Z}_{syst}$. If we neglect the transverse component of the voltage drop, which is typical of the distribution network, we can write:

$$U = E_{syst} - \frac{P_{load} \cdot r_{syst} + Q_{load} \cdot x_{syst}}{U},$$

where P_{load}, Q_{load} are the powers of the customer's active and reactive load, respectively.

As mentioned above, VF is characterized by two parameters [5]:

- magnitude of the voltage fluctuation (δU_t), %;
- flicker dose (P_{st}, P_{Lt}).

The scope of the voltage δU_t is a quantity equal to the difference between the values and U_i and U_{i+1} consecutive extremes (or extremum and the horizontal portion) of the envelope of the fundamental frequency of the mean-square value of voltage values determined in each half period as a percentage of the nominal voltage.

The scale of change of voltage is calculated according to the formula, %:

$$\delta U_t = \frac{|U_i - U_{i+1}|}{U_{nom}} 100,$$

where U_i, U_{i+1} are the values of following one another extrema in accordance with Fig. 2.

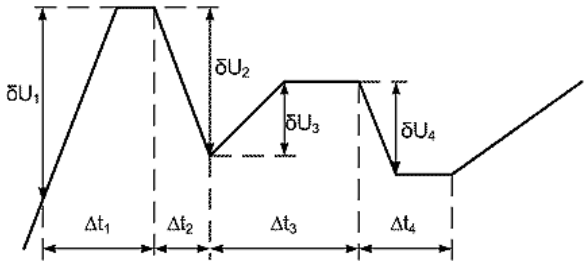

Fig. 2. Voltage fluctuations

Appearing at any point in the system VF distribute and toward the low voltage busbars substantially without attenuation, and the high-voltage bus bars - with damping amplitude. This effect is depending on the short circuit power ($S_{sc.syst}$) system. When propagating in any direction VF of the frequency spectrum is retained, and the attenuation factor or amplification ($K_{\delta Ut}$) [6] is given by:

$$K_{\delta U_t} = 1 + (S_{sc.syst} / S_{nom.t}) \cdot U_{sc},$$

where $S_{sc.syst}$ is the power of the short circuit of the system; $S_{nom.t}$ is the rated power of the transformer; U_{sc} is the voltage of the transformer short circuit.

Repetition frequency of voltage changes ($f_{\delta Ut}$), (1/s, 1/min) is determined by the expression:

$$f_{\delta U_t} = m / T,$$

where m is number of voltage changes by the time T; T is the time measuring interval taken equal to 10 minutes.

If two voltage changes are occurring at intervals less than 30 ms, then they are treated as one. The time interval between the voltage changes is:

$$\Delta t_{i,i+1} = t_{i,i+1} - t_i.$$

Assessment of the admissibility of the range of voltage changes by means of the curve of the permissible

range of fluctuations of the frequency of repetitions of voltage changes or the time interval between successive voltage changes (Fig. 3).

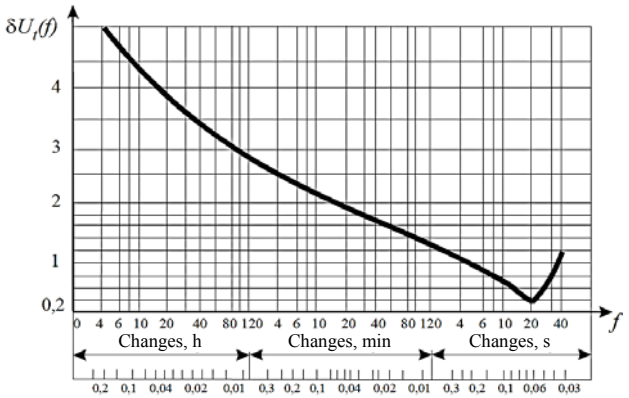

Fig. 3. Curves of permitted values $\delta U_t(f)$

EEQ at the point of common coupling with periodic VF, meander-shaped (rectangular, Fig. 4), according to the relevant requirements of the standard, if the measured amplitude of voltage changes do not exceed the values defined by the curve of Fig. 3, for relevant repetition of frequency of voltage variations ($F_{\delta Ut}$) or the interval between the voltage change ($\Delta t_{i,i+1}$).

The duration of the voltage measurement is the time interval from the start of a single measurement to its final value [5].

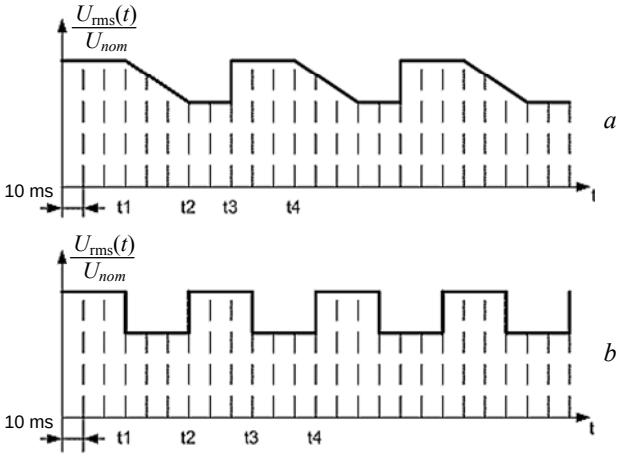

Fig. 4. Voltage fluctuations of arbitrary shape (*a*) and meander-shaped (*b*)

On the other hand based on [7] there is used the method of «partial reactions» [8], the objective and unambiguous assessment of the VF is only possible by a dose of flicker.

VF of power supply (typically of less than 1 min), including the single quick change of voltage, cause the occurrence of flicker.

Flicker is subjective human perception of the luminous flux of artificial light sources fluctuations caused by fluctuations in the mains voltage, which supplies of these sources [5].

The intensity of the voltage flicker characteristic power VF taking into account the characteristics of visual perception and brain human vibrations of the luminous flux of incandescent lamps completely like VF. Incandescent lamps are the most massive loads sensitive to the VF to a greater extent than television sets, computers, electronic and microelectronic control. Intensity Flicker is expressed in dimensionless units; ordinates of the standard curve of acceptable values VF $\delta U_t(f)$ (Fig. 3) corresponds-corresponding values flicker intensity determined over 10 minutes with a probability of 99 % $P_{St} = 1$.

Flicker dose is a measure of human susceptibility to the effects of fluctuations in the luminous flux caused by VF in the supply network for a specified period of time, which is measured by the standard flickermeter.

Time perception of flicker is the minimum time to subjective human perception of flicker, voltage fluctuations caused by certain shape.

Standard [5] determines a short-term P_{St} and long-term P_{Lt} flicker dose (determined in short term observation time interval equal to 10 minutes at a long interval – 2 hours). Initial data for calculation are the flicker levels, measured by flickermeter – a device, which is modeled sensitivity curve (frequency response) of the human organ of vision [9].

The visual perception process when VF is simulated on the basis of the theory of the passage of the composite signal through a nonlinear dynamical system. Fig. 5 shows the frequency response of the visual analyzer, adopted by the IEC. The upper limit of the frequency of the VF, affecting vision, taking into account the time constant of the filaments of incandescent lamps is about 35 Hz at δU_t $t \leq 10$ % [10].

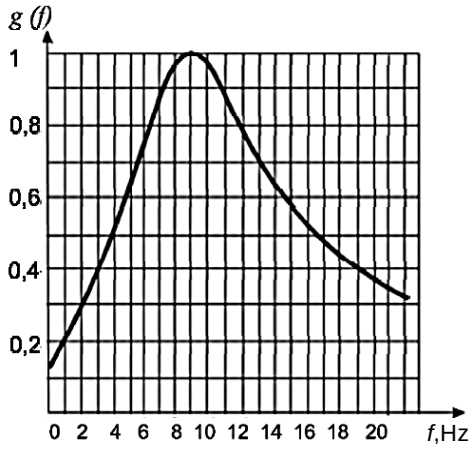

Fig. 5. Frequency response of the visual analyzer

where $g(f)$ is the variable coefficient of amplification of the inertial system (eyes), dependent on the oscillation frequency f.

The short-term flicker dose (P_{St}) can be determined by calculation making measurements on the observation interval TS = 10 min. In this case, the following formula:

$$P_{st} = \sqrt{0{,}0314\,P_{0,1} + 0{,}0525\,P_{1s} + 0{,}0657\,P_{3s} + \\ + 0{,}28\,P_{10s} + 0{,}08\,P_{50s}},$$

where $P_{0,1}$, P_{1S}, P_{3S}, P_{10S}, P_{50S} are the levels of flicker, which values have been exceeded during 0.1; 1; 3;10; and 50 % of the time interval of observation T_s. Index «*s*» in the formula indicates smoothed values P_1, P_3, P_{10}, P_{50}. Smoothed values are calculated by the following formulae [5]:

$$P_{50s} = (P_{30} + P_{50} + P_{80})/3;$$

$$P_{10s} = (P_6 + P_8 + P_{10} + P_{13} + P_{17})/5;$$

$$P_{3s} = (P_{2,2} + P_3 + P_4)/3;$$

$$P_{1s} = (P_{0,7} + P_1 + P_{1,5})/3.$$

Because the time constant of the device is 0.3 s, the $P_{0,1}$ value can not be changed quickly and for $P_{0,1}$ smoothing is not required.

Interval of 10 min of observation, used in assessing the short-term flicker, convenient to assess VF created by technical means with a short duty cycle. In cases where it is necessary to take into account the cumulative effect of several loads of interfering randomly (e.g., welding machines, electrical motors), or take into account the sources of flicker with a long and varying the duty cycle (e.g., electric arc furnace), it is necessary to assess the long-term flicker dose. For this long-term dose of flicker (P_{Lt}) is determined based on the measurement of short-term doses of flicker (P_{Lt}) with respect to the period of observation, associated with long working duty cycle or period during which the observer can perceive flicker, such as a few hours, using the expression:

$$P_{Lt} = \sqrt[3]{\frac{1}{12}\sum_{k=1}^{12}(P_{stk})^3}$$

where P_{Stk} (i = 1, 2, ... N) are the successive values of short-term flicker dose on k-th time interval T_S for a long-term observation period T_L [5].

EEQ by the flicker dose meets the requirements of the Standard, if the short-term and long-term flicker determined by measuring for 24 hours, or calculation, do not exceed the limit values: for short-term flicker – 1.38 and for long-term – 1.0 (at VF with a shape different from the meander) [11].

Voltage fluctuations in the power network lead to the following consequences:

- fluctuations in the luminous flux of lighting (flicker effect);
- deterioration of the quality of television receivers;
- violation of the x-ray equipment;
- false operation of control devices and computers;
- malfunction of converters;
- torque fluctuations on the shaft of rotating machines, causing additional power losses and increased wear and tear, as well as violations of technological processes that require a stable speed.

The degree of influence on the operation of the equipment is determined by the oscillation amplitude and frequency.

Load fluctuations of high power, for example, rolling mills, causing a moment's hesitation, active and reactive power local power generators.

Vibrations and voltage dips deeper than 10 % may result in the extinction of the discharge lamp re-ignition, depending on which type of lamp can occur only after a considerable period of time. With deep vibrations and voltage failures (more than 15 %) may fall contacts of magnetic starter, causing disruptions in production.

Sharp VF have negative impact on the dynamics of movement of trains. Current jumps and traction caused VF, reduce the reliability of the contactors and are dangerous in terms of occurrence of slipping. For electric rolling fluctuations are dangerous of the order of 4-5%.

The increase in electricity losses during in-plant networks caused by VF with amplitude of 3 %, does not exceed than 2 % of the initial value of the losses.

A the metallurgical factories VF more than 3% lead to a mismatch of speeds drives continuous stands of metal rolling, which reduces the quality (stability of thickness) of the rolled strip.

In the production of chlorine and caustic soda VF cause a sharp increase in anode wear and decrease performance.

Voltage drops when producing chemical fiber stop cause the equipment to which the restart of 15 minutes spent in the event of failure of the equipment 10 % to 24 h at 100 % of equipment failure. Reject product is from 2.2 to 800 % of the tonnage of the technological cycle. Time of the full restoration of technological process is up to 3 days.

Noticeable influence fluctuations and voltage drops at low power asynchronous motors. This poses a risk for textile, paper-making and other industries with high demands on the stability of the rotation speed of electric drives. In particular, the VF on chemical fiber plants lead to a non-stable rotation of the winding device. As a result, nylon thread, torn, or manufactured with non-uniform thickness.

GOST 32144-2013 determines the effect of VF on lighting systems that affect a person's vision. Blinking light lamps (flicker effect) causes bad psychological effect of fatigue and body as a whole. The degree of eye irritation depends on the size and frequency of blinking. The strongest impact on the human eye blinking light having a frequency of 3 ... 10 Hz, so the allowable fluctuation range of the voltage in the low: less than 0.5 %. The degree of influence depends on the type of light source. For example, under the same VF incandescent lamps have a much greater impact than discharge lamps [5].

VF with amplitudes of 10 ... 15 % can lead to failure of the capacitor, and the gate rectifier units.

In the steel mills to the number of receivers that are sensitive to the VF are continuous mills rolling.

When VF arise swing turbogenerators. For turbo-generators themselves are not dangerous swing, however, being transferred to the turbine blades, they can activate the speed controllers.

Noticeable is influence on VF asynchronous motors of small capacity. Fluctuations are unacceptable for the textile, paper-making and other industries, particularly high demands on the accuracy of maintenance of speed drives, which are mainly used asynchronous motors.

We studied in detail the effect of voltage fluctuations in the electrolysis plants. VF with amplitudes of 5 % caused a sharp increase in anode wear and reduced service life.

VFs have a significant impact on the resistance welding. This affects both the impact on the quality of the welding process, and welding control operation unreliability. On the voltage quality in resistance welding networks imposed severe restrictions on the scope of voltage changes: 5 % to weld ordinary steel, and 3 % for the welding of titanium and other high-temperature steels and alloys. Duration of admissible VF management apparatus resistance welding machines is limited to no more than 0.2 s to avoid false operation of these devices.

VF adversely affect the operation of radio equipment, disrupting their normal operation and reduces service life. Interference in television pictures appear at frequencies of 0.5 … 3 Hz and noticeable mainly in still images.

For power consumers sensitive to VF, are also computers, X-ray machines, etc. When operating in the computer control mode is sometimes only one or two scale fluctuations with 1 ... 1.5 %, so that a failure has occurred in any cell of the machine and, as a consequence, any error in control commands or in the calculations carrying out.

Measures to reduce VF. Separation of loads and static reactive power compensators (STC) are used to reduce VF.

Separation of loads. To separate rapidly changing and relaxed loads various circuits and devices can be used. The simplest is a scheme based on the use of a dual reactor: calm and rapidly changing load connected to different sections (windings) of the reactor (Fig. 6). Due to the fact that the mutual ratio between sections $M \neq 0$, the voltage drop in each of them at load currents I_1 and I_2 are represented by expressions:

$$\Delta U_1 = jx_L \cdot (I_1 - k_M \cdot I_2);$$

$$\Delta U_2 = jx_L \cdot (I_2 - k_M \cdot I_1),$$

where x_L is the inductive reactance of the reactor section; $k_M = M/L$ is the mutual inductance factor $k_M = 0.5\text{-}0.6$.

In the ideal case when $I_1 = I_2$ we have:

$$\Delta U = I_{1(2)} \cdot x_L (1 - k_M).$$

The voltage drop due to mutual inductive connection is reduced by 50-60 %. When $I_1 \neq I_2$ decrease in the value of ΔU is obviously smaller. Scale voltage changes depending on the resistance of the melting energy system to the busbars, which is connected to the reactor.

Application of this scheme to connect the electrical arc furnace (ДСП – 5МТ) and can, in some cases, to provide on the busbars «relaxed» load VF whose value does not exceed maximum permissible value.

Application of dual reactor more efficient when the coupling coefficient between the windings (sections) is equal to unity; this is possible by using reactors with iron core. In this case, you can select the parameters of the reactor so that the influence voltage drop caused by a load resistance section to an adjacent mains.

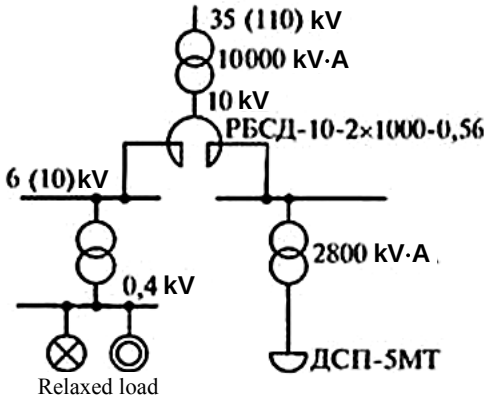

Fig. 6. A circuit using a double reactor for voltage stabilization at shock loads

For rapidly changing and relaxed loads transformer with split windings are also used. When connected to one branch of the LV transformer winding calm load, and the other – rapidly changing relationship between the values of the Range of voltage change at the respective busbars ΔU_1 and ΔU_2 and can be represented as:

$$\Delta U_1 = \Delta U_2 \cdot \frac{4 - k_s}{4 + k_s},$$

where $k_s$is the splitting factor of 3.34 – 3.64. The average value is taken $k_s = 3.5$.

When we extract rapidly changing load on a separate transformer overall resistance is reduced to the value of:

$$X = \frac{X_{T1} \cdot X_{T2}}{X_{T1} + X_{T2}} + X_C,$$

till the value X_C. Then the scope of the VF on a stable load busbars decreases X_C/X times, and on busbars of rapidly changing load it increases $X/(X_C+X_{T2})$ times [11].

When using transformers with split windings for networks 6-10 kV electric arc steelmaking furnace of small capacity VF on busbars of «relaxed» load can also be within acceptable limits.

Reducing the VF by using STC. VF compensation in this case is carried out by compensating reactive

power (RP) surges. For compensating the effect of the time lag in the generation of the RP compensator should be minimal, so as not to cause an increase in the level of the VF. For example, if compensation pounce RP rectangular shape (Fig. 7,*a*) with a certain time lag Δt instead of one there are two pounce RP (Fig. 7,*b*), and the level of the VF increases.

Equally important is the question of choosing the power of the STC. Maximum capacity compensating STC related to the maximum span VF, which can be compensated for, by the following expression:

$$Q_{k.\max} = Q_{\max} \cdot \left(1 - \frac{1}{P_{st}}\right),$$

where P_{st} is the flicker intensity.

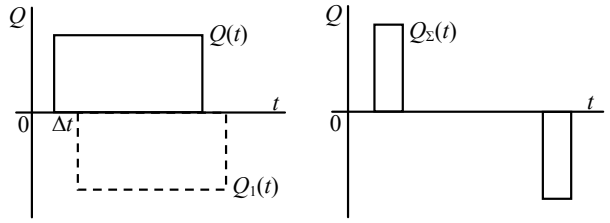

Fig. 7. Graphs of changing of load's RP: *a*) summary graph of load's RP and STC's RP (solid line) and STC's load (dotted line); *b*) summary graph of load's RP and STC's RP

The calculation of this formula gives overestimated results (the error of 5-10 % depending on the degree-fine dispersion range of the VF) [12].

In addition to the activities listed above must use the best solutions, we scheme with minimal additional power-governmental expenses, which include:

- approaching the high voltage source to large power consumers with rapidly changing load;
- reduce the induced drag of the external power supply lines (e.g., rejection of busbars, a decrease in the inductance of the reactors);
- provide power to large power consumers with rapidly changing load on individual lines coming directly from the power supply (main substations, heat-electric generating plants, and others);
- compliance with the optimal level of short-circuit power in the network feeding the power-consuming equipment with rapidly changing load within 750-10000 MVA;
- to limit the self-starting motor at VF planned to reduce, if possible, the time of action and automatic circuit reclosers and application of high-speed network security, as well as the use partial step in which the most important are only the engines, and the rest are disabled;
- use the parallel operation of power lines and transformers in the main substations (with the closed section switch);
- to limit the VF at consumers voltage loss in the line reactor in normal operation should be no more than 4-5 % of the rated voltage;
- reduction of the supply network impedances. By increasing the sectional line conductors is reduced (R), and the application of series compensation device reduces the total (X). Disadvantages are increased capital costs, and the use of a longitudinal compensation is dangerous rise in short-circuit current at ($X \to 0$).

Conclusions.

1. The problem of voltage fluctuation is relevant because:
- voltage fluctuations have a negative impact on human vision and operation of electrical equipment;
- the network has a large number of possible sources of voltage fluctuations;
- there are ways to identify and methods to reduce voltage fluctuations.

2. It is required to ensure the interest of the subjects of the distribution process and to reduce the energy consumption level of the VF to acceptable values. As an incentive to promote the interest of the authors consider the introduction of subjects of responsibility for violation of requirements for the EEQ, in particular VF.

3. Analysis of the literature revealed no developments to identify the subjects of responsibility for violation of requirements for the EEQ in terms of voltage fluctuations.

REFERENCES

1. Gryb O.G., Senderovich G.A., Senderovich P.G. The algorithm implementing the methodology of distribution of responsibility for the distortion of symmetry. *Visnyk NTU «KhPI» – Bulletin of NTU «KhPI»*, 2006, no.10, pp. 7-13. (Rus).

2. Gryb O.G., Senderovich G.A., Senderovich P.G. The algorithm implementation methodology for the allocation of responsibility harmonic distortion. *Kommunal'noe khoziaistvo gorodov – Communal economy of cities,* 2006, no.67, pp. 237-245. (Rus).

3. Senderovich P.G. The methodology and algorithm for determining the liability for exceeding the allowable voltage fluctuation. *Visnik Harkivskogo natsionalnogo tehnichnogo universitetu silskogo gospodarstva imeni Petra Vasilenka - Bulletin of Kharkiv Petro Vasylenko National Technical University of Agriculture*, 2006, no.43, vol.1, pp. 59-65. (Rus).

4. Senderovich P.G. Definition of the responsibility for quality infringement in devices of the electric power account. *Svetotekhnika ta elektroenergetika – Lighting Engineering and Power Engineering*, 2006, no.7-8, pp.48-53. (Rus).

5. *GOST 13109-97. Elektricheskaya energiya. Sovmestimost' tehnicheskih sredstv elektromagnitnaya. Normy kachestva elektricheskoi energii v sistemah elektrosnabzheniya obschego naznacheniya* [State Standard 13109-97. Electrical energy. Technical equipment electromagnetic compatibility. Quality standards for electrical energy in general use power systems]. Minsk, IPK Publishing house of standards, 1998. 30 p. (Rus).

6. Kudrin B.I. *Elektrosnabzhenie promyshlennykh predpriiatii: uchebnik dlia studentov vysshikh uchebnykh zavedenii* [Power supply of the industrial enterprises: Textbook for students of

higher educational institutions]. Moscow, Interment Inzhiniring Publ., 2006. 672 p. (Rus).

7. Kurennyi E.G., Dmitrieva, E.N., Pogrebnyak N.N. Chernikova L.V., Cigankova N.V. Analytical method of calculation of random voltage oscillations indices in power electric networks. *Nauchnye trudy Donetskogo natsional'nogo tekhnicheskogo universiteta. Seriia «Elektrotekhnika i energetika». – Scientific papers of Donetsk National Technical University. Series «Electrical Engineering and Power Engineering»,* 2000, no.21, pp. 34-37. (Rus).

8. Kurennyi E.G., Lyutyi A.P., Chernikova L.V. The partial reaction method for analyzing the processes at the output of linear filters in models for electromagnetic compatibility. *Electrichestvo – Electricity,* 2006, no.10, pp. 11-18. (Rus).

9. *GOST R 51317.4.15-99 (MEK 61000-4-15-97). Sovmestimost' tekhnicheskih sredstv ehlektromagnitnaya. Flikermetr. Tekhnicheskie trebovaniya i metody ispytanij*. [State Standard GOST R 51317.4.15-99 (IEC 61000-4-15-97). Compatibility of technical equipment. Flickermeter. Technical requirements and test methods]. Moscow, 1999. (Rus).

10. Zhezhelenko I.V, Shidlovskij A.K., Pivnyak G.G., Saenko Yu.L., Nojberger N.A. *Ehlektromagnitnaya sovmestimost' potrebitelej* [Electromagnetic compatibility of consumers]. Moscow, Mashinostroenie Publ., 2012. 351 p. (Rus).

11. *GOST R 51317.4.15-2012 (MEK 61000-4-15-2010). Sovmestimost' tekhnicheskih sredstv ehlektromagnitnaya. Flikermetr. Funkcional'nye i tekhnicheskie trebovaniya.* [State Standard GOST R 51317.4.15-2012 (IEC 61000-4-15-2010). Electromagnetic compatibility of technical equipment. Flickermeter. Functional and design specifications]. Moscow, Standartinform Publ., 2012. (Rus).

12. Zhezhelenko I.V., Saenko Yu.L. *Pokazateli kachestva elektroenergii i ikh kontrol' na promyshlennykh predpriiatiiakh: Ucheb. posobie dlia vuzov. 3-e izd* [Indicators of quality of the electric power and their control at the industrial enterprises. Educational manual for students of higher educational institutions, 3rd ed.]. Moscow, Energoatomizdat Publ., 2000. 272 p. (Rus).

G.A. Senderovich[1], *Doctor of Technical Science, Professor,*
A.V. Diachenko[1], *Postgraduate Student,*
[1] National Technical University «Kharkiv Polytechnic Institute», 21, Frunze Str., Kharkiv, 61002, Ukraine,
e-mail: senderovichg@mail.ru, alex.7491@mail.ru

How to cite this article:
Senderovich G.A., Diachenko A.V. The relevance of determining responsibility for violation of power quality in terms of voltage fluctuations. *Electrical engineering & electromechanics*, 2016, no.2, pp. 54-60. doi: 10.20998/2074-272X.2016.2.10.

UDC 621.311.171 **doi: 10.20998/2074-272X.2016.2.11**

E.I. Sokol, O.G. Gryb, S.V. Shvets

THE STRUCTURAL AND PARAMETRICAL ORGANIZATION OF ELEMENTS OF A POWER SUPPLY SYSTEM IN THE CONDITIONS OF NETWORK CENTRISM

Purpose. Development of indicators of the structural and parametrical organization of effective active and adaptive system of service of power supply systems in the conditions of ideology of Smart Grid. Methodology. In the conditions of application of ideology of Smart Grid for increase of intellectualization of electrical power system there is a need of introduction of the principle of a network centrism in the structural and parametrical organization of elements of power supply systems that involves performance of conditions on implementation of provisions of the principle of Situational Awareness. The essence of this principle consists in that, information on a condition of system has to be presented in the form convenient for the analysis, recognition, transfer, distribution and storage, to be coordinated for flexible and optimum development at the subsystem and object-by-object levels. Results. Structural and parametrical optimization of elements of power supply systems in the conditions of a network centrism and the concept of SG involves use of provisions of the theory of systems and concepts of multicriteria optimizing synthesis. It is offered to use the modified adaptive indicator of the generalizing effect of synthesis of structure of active and adaptive system of service of power supply systems in the form of a difference of the generalizing effects: the introduced option of structure of system and basic. Originality. Introduction of an adaptive indicator of synthesis of system of service of power supply systems considers the concept of «service of system on the basis of a response» in the presence of false and true refusals. Practical value. Use of the specified indicator will allow to specify procedure of selection of competitive options for the purpose of definition of a set of admissible structures which meet the requirements of criterion function. References 9.
Key words: **Smart Grid, network-centric control system, active and adaptive system of service of power supply systems, productive actual response.**

В статье рассмотрены тенденции развития и принципы организации интеллектуальных энергосистем при введении понятия сетецентризма в условиях идеологии Smart Grid. В качестве решения задач указанной проблематики предлагается создание активно-адаптивной системы, реализующей концепцию «обслуживания системы на основе отклика». Библ. 9.
Ключевые слова: **Smart Grid, сетецентрическая система управления, активно-адаптивная система обслуживания энергосистем, результативный фактический отклик.**

Introduction and problem definition. In the electric power system of the world and Ukraine is not the first year they are working on the «intellectualization of networks» – Smart Grid (SG). Currently, the ideology of building of intellectual energy networks the SG [1] (a term is introduced by Michael T. Burr in 2003 [2] – one of the most significant and developed at the modernization of the global energy industry. In the US and Western Europe, a number of large and more small-scale projects for the transition of power industry as well as housing and utilities to «smart grids» SG [3] are realized. Fundamentally new approaches are such in which the leading role is assigned to the kernel of the power system – the electrical network as a structure to ensure effectiveness of connection of the generation and consumer.

At the same time there is still no comprehensive concept of the formation of structural-parametric grid elements and the organization of information and intellectual bases of increase of efficiency of management technologies based on the SG.

Analysis of recent investigations and publications. Backgrounds of world community interest in the idea of SG concept are clear: growing indicators of resource consumption, increasing the cost of electricity production, the existing network of energy supplies rapidly respond to fluctuations in the economic sphere.

With the increasing demands of the international community used the production model and the delivery of energy resources cease to be satisfactory; for example, the current amount of electricity losses in networks of Ukraine is more than 25 % [4]. These and other factors are pushing the government and power generating enterprises of various countries for the speedy implementation of the principles of SG concept.

In general, a power supply networks, developing the concept as part of SG, you can make the following demands: adaptability, efficiency, accessibility and opportunity for feedback, safety, information security, complexity and integration functions SG [5].

At the moment, the most acute problem of power systems as an element of the Ukrainian electricity system in order to increase energy efficiency and reduce prices for consumers.

The goal of investigations is development of indicators of structural and parametric organization of effective active-adaptive service system of power systems in a Smart Grid ideology.

Main research materials. Currently, there is the evolution of energy systems – from the simplest forms, using basic networking technologies in the energy sector, to more complex forms within SG network-centric concept with elements of nature, which are based on the latest generation of Internet technologies and implement a model of energy activities.

The concept of network centrism means building and maintaining up to date common to the whole image of the real situation of the system in the most clear and simple form. Usage information field should allow to

perceive the whole image of the system as a whole at this time interval based on the system response to ongoing changes in its status under the influence of various factors.

The successful solution of management tasks within the framework of network-centric approach is to maintain this image in the most complete and reliable and able to implement the provisions of Situational Awareness principle [6] (integrated complex perception and analysis for the benefit of a single system).

The existing information infrastructure in Ukraine with its traditional practice justified solutions of information and communication problems in the difficult conditions of the territorial, technical and natural-climatic nature, it requires new approaches, taking into account the need to meet the challenges of the country's transition to an innovative path of development.

It is necessary to consider and use the new principles of active-adaptive power system on the basis of network-centric concept. The main of them is the use of all types of information, the development of traditional and new sources of information, based on the principles of adaptive structural-parametric elements of the organization of energy systems; improving the quality, safety and reliability of data collection, processing, storage and distribution of information.

The current stage of technology adoption in the SG grid of Ukraine is characterized by dependence on the processes of formation of «smart grids» of foreign technology solutions. The reason is the lack of clearly expressed in a network of information-analytical and expert-analytical support of the Ukrainian economy, namely:

- technical, organizational and legal problems of collection and processing of expert information used for management decision-making [7];
- lagging behind in the implementation of modern information tools and strategic-level control systems in the power industry [8].

When considering the performance characteristics of energy systems it is often necessary to carry out repair and maintenance works. With the introduction of the network centrism provisions it is proposed to use the concept of «service system on the basis of response» (SSR). This concept allows to increase the possibility of repair units of high-voltage transmission lines and substations for their application not distributed objects. The introduction of the SSR concept is aimed at servicing specific object (digital substation, power lines, power system status monitoring subsystem elements, etc.), located in a particular area and at a particular time, and which currently require maintenance in accordance with the response of the system. In this connection, it is possible to reduce the total number of units involved by virtue of their pitting and more efficient operation.

For real network-centric management system there are no obstacles in the number of units on the scale of action to restore the operating condition of high-voltage lines and digital substations. There are only obstacles to the effectiveness of the repair teams, that is, the ability of the selected outfit of forces and means to execute with reasonable efficiency the appointed time restore operability constituent element of the power system.

To build an effective active-adaptive power system's maintenance system (PSMS), built on the principles of network centrism it is necessary that it should based on the supremacy of communication systems, allowing real-time to receive and transmit information packets huge variety of customers, including centralized and distributed transmission. The PSMS of specified control type should be based on thorough preparation of the composition of repair crews, exploiting the system. Such an approach would greatly reduce the staff and reallocate responsibilities of team members to perform peculiar to their office tasks.

As one of the main elements of the proposed PSMS an unmanned aerial vehicle – UAV (quadrocopter, multicopter, hexacopter, etc) can act [9]. UAV operation mode is determined by the list of PSMS performed tasks within the main tasks of the power system. Among them – the control of the operator of the current events on the power system objects, control of repair when restoring a high-voltage lines, control of compliance with the requirements of labor protection and work with high voltage, remote control supply voltage after the recovery cycle uptime grid on the relevant sections of high-voltage lines, etc.

The problem of synthesis of PSMS in general formulation involves the use of a systematic approach. It is proposed to solve this problem apply the general indicator of the effectiveness of the selection options PSMS structure of the system, using the concept of the SSR.

The general formulation of the synthesis problem is as follows:

$$W = \max \{OE_v(x) - OE_b(x)\}, \quad \text{at} \quad x \in X;$$

$$C_{nz} \to \min,$$

where $OE_v(x)$ is the summarizing effect of the implementation of the introduced version of the PSMS; $OE_b(x)$ is the summarizing effect of the implementation of the basic variant of the structure of the PSMS; X is the feasible region; C_{nz} are non-productive expenditures.

This index is constructed as the difference between generalizing effects: the introduced version of the PSMS system structure and base one.

The expression for the generalizing effect of synthesized PSMS structure will look like:

$$OE_v(x) = (\sum_{i=1}^{n} P_i P_{ci} P_{wwi} k_{gi} (RO_{fi} - C_i) \times \times \prod_{j=1}^{k} \exp(-\{\lambda_{qij} + \lambda_{cij}\} t_{pij})) - C_d, \quad (1)$$

where P_i is the apriori probability requirement to perform the corresponding subsystem of the i-th problem; P_{ci} is the probability that it will not disrupt the implementation of the i-th problem due to lack of operational subsystem; P_{wwi} is the probability that it will not disrupt the implementation of the i-th problem of setting the i-th by

subsystem defective mean; κ_{gi} is the availability of the i-th subsystem; RO_{fi} is the actual cost value of the effective response in the performance of the i-th problem; C_i are the costs associated with the implementation of the selected option maintenance subsystem for the i-th subsystem and the measurement of parameters of the subsystem during operation; λ_{qij}, λ_{cij} are the intensities of sensible and latent failures of the j-th component of the i-th subsystem; t_{pij} is the time during which the explicit and latent failures are examined; C_d are costs associated with the operation of the system of the PSMS.

Using the concept of the SSR for the PSMS system expressions for RO_{fi} and C_i will be the following:

$$\begin{aligned} RO_{fi} &= RO_{bi} + RO_{ci}; \\ C_i &= C_{bi} + C_{ci}, \end{aligned} \tag{2}$$

where RO_{bi} and C_{bi} is absolute value terms the effective response of the actual costs and, depending on the decision of the i-th problem by the corresponding subsystem; RO_{ci} and C_{ci} is the actual cost value effective response and costs arising from the introduction of the concept of the SSR.

In general, for the steady operation mode of the system of the PSMS:

$$\begin{aligned} RO_{bi} &= \sum_{j=1}^{m} P_{ij} \sum_{k=1}^{m} P_{ijk} RO_{ijk}; \\ C_{bi} &= \sum_{j=1}^{m} P_{ij} \sum_{k=1}^{m} P_{ijk} C_{ijk}, \end{aligned} \tag{3}$$

where P_{ij} is the probability of finding of the i-th subsystem in each of j-th states during operation; RO_{ijk}, C_{ijk} is the actual cost value of effective response and costs derived from the proper use of the i-th subsystem in the transition from from the state j to the state k; P_{ijk} is the probability of transition of i-th subsystem from the state j to the state k in the process of solving the current problems.

Values of RO_{ci} and C_{ci} are described by expressions:

$$RO_{ci} = \sum_{j=1}^{Z} P_{ij}\left(RO_{cpij}\left(t_{sij}\right)\right) P_{ij}\left(t_{sij}\right) PO_{cpbij}\left(t_{sij}\right); \tag{4}$$

$$C_{ci} = \sum_{j=1}^{Z} P_{ij}\left(C_{cpij}\left(t_{sij}\right)\right) P_{ij}\left(t_{sij}\right) C_{cpbij}\left(t_{sij}\right), \tag{5}$$

where $RO_{cpij}(t_{sij})$ and $C_{cpij}(t_{sij})$ are the components of effective response and actual costs of the j-th component of the i-th subsystem for t_{sij}-th service time; $RO_{cpbij}(t_{sij})$ and $C_{cpbij}(t_{sij})$ are the unconditional effective components of the actual response and costs of the j-th component of the i-th subsystem for t_{sij}-th service time.

Values of RO_{ijk} and C_{ijk} will be determined by random matrices of discrete values of the size of the system in steady state operation of the PSMS:

$$\left[RO_{ijk}\right] = \begin{bmatrix} RO_{i11}\ RO_{i12} \ldots RO_{i1k} \\ RO_{i21}\ RO_{i22} \ldots RO_{i2k} \\ \ldots\ldots\ldots \\ RO_{ik1}\ RO_{ik2} \ldots RO_{ikk} \end{bmatrix}, \tag{6}$$

Values of $RO_{cpij}(t_{sij})$ and $C_{cpij}(t_{sij})$ are described by matrices, similar expressions (6). The values of these matrices are chosen for the corresponding time t_{sij}.

In the operation of the PSMS system there are situations when the j-th component of the i-th subsystem can be on service, not take into account the nature of the SSR concept, depending on the reliability of the means used, which leads to the presence of components $RO_{cpij}(t_{sij})$ and $C_{cpij}(t_{sij})$. These components are also described by matrices of the type (6).

Taking into account the expressions (2) – (5), and taking into account that the components of RO_{ijk}, C_{ijk}, $RO_{cpij}(t_{sij})$, $C_{cpij}(t_{sij})$ are described by expressions of the type (6), we obtain an expression of adaptive index summarizing the synthesis effect of PSMS structure, which has been modified for the SSR concept:

$$\begin{aligned} OE_v = &\sum_{i=1}^{n} P_i k_{gi} \times \prod_{j=1}^{N} \left(1 - \left(\beta_{ij} + \left(1 - \beta_{ij}\right) P_{1ij}\right)\right) \times \\ &\times \left(\frac{1 - P_{2ij}}{P_{1ij}\left(P_{1ij} + P_{2ij}\right)} \right) \times \left[\sum_{j=1}^{L} P_{ij} \times \sum_{k=1}^{M} P_{ijk} \left(RO_{ijk} - C_{ijk}\right) + \right. \\ &+ \sum_{j=1}^{Z} \{ P_{ij}\left(RO_{cpij}\left(t_{sij}\right)\right) P_{ij}\left(t_{sij}\right) RO_{cpbij}\left(t_{sij}\right) - \\ &\left. - P_{ij}\left(C_{cpij}\left(t_{sij}\right)\right) P_{ij}\left(t_{sij}\right) C_{cpbij}\left(t_{sij}\right) \} \right] \times \\ &\times \prod_{j=1}^{V} \exp\left(-\left(\lambda_{qij} + \lambda_{cij}\right) t_{pij}\right) - \left(P_u \left(C_u + \left(K_p + E\right) K + C_m\right)\right), \end{aligned} \tag{7}$$

where β_{ij} is the probability of latent failure of the j-th components of the i-th subsystem; P_{1ij} is the probability of finding of the j-th components of the i-th subsystem in good and working condition; P_{2ij} is the probability of finding the j-th component of the i-th subsystem in use with a latent failure; P_u is the probability of the adoption of the system of the PSMS in operation; C_u are the current annual costs of operating of the system of the PSMS; K_p is the rate of renovation of components of the system of the PSMS; K is the regulatory cost-effectiveness ratio; E are non-recurring costs during commissioning of the PSMS system operation; $P_{ij}(t_{sij})$ is the probability of service of the i-th subsystem of duration t_{sij} because of false or latent failures; C_m is the payroll staff fund.

Conclusions. In the conditions of application of «Smart Grid – opportunities» to improve the intellectualization of the Ukrainian electricity system with active-adaptive power supply network there is a need to introduce the principle of network centrism in structural-parametric organization of the elements of energy systems. This optimization of the elements of power systems under conditions of network centrism and SG concept involves the use of the theory of systems and the concepts of multi-criteria optimization synthesis. The proposed modification of the adaptive index summarizing the effect of synthesis of the PSMS structure that takes into account the concept of the SSR in the presence of false and true bounce, will clarify the competitive options selection process to determine the set of possible structures that meet the requirements of the target synthesis function.

REFERENCES

1. *SMART GRID*. Available at: http://www.oe.energy.gov/smartgrid.htm (Accessed 12 May 2014).

2. Michael T. Burr. Technology corridor: Reliability demands will drive automation. *Fortnightly Magazine*, 2003, November 1. Available at: http://www.fortnightly.com/fortnightly/2003/11/technology-corridor?page=0%2C0 (Accessed 15 June 2004).

3. Dorofeyev V.V. Intellectual network. New principles of construction. The equipment and control systems of an intellectual network. *Report at a meeting of a round table on the subject «Clever Networks – Clever Power – Clever Economy»*, Saint Petersburg, 2010. Available at: http://www.fsk-ees.ru/media/File/press_centre/speeches/Presentation_dorofeev.pdf. (Rus).

4. Bykova O., Ablyazov P. *Where the power industry moves?* Available at: http://www.bigpowernews.ru/research/document 47671 (Accessed 24 November 2015). (Rus).

5. *10 trends of the SMART Grid market in 2012*. Available at: http://www .cleandex.ru/articles/2012/08/23/10_trendov_rynka _smart_grid_v_ssha (Accessed 02 April 2013). (Rus).

6. Mica R. Endsley, Daniel J. Garland. *Situation Awareness Analysis and Measurement*. Lawrence Erlbaum Associates, Inc., Mahwah, NJ, 2000. 383 p. ISBN 08058-2134-1.

7. *Network examination. 2nd prod.* Edited by D.A. Novikov, A.N. Raykov. Moscow, Egves Publ., 2011. 166 p. (Rus).

8. Kosyanchuk T.F. Diagnosis of the competitive potential of the company. *Scientific notes. Series «Economy»*, 2013, no.23, pp. 51-54. (Ukr).

9. Available at: http://quadrocopter.ua/quadrocopters_copters (Accessed 11 July 2015).

Received 05.02.2016

E.I. Sokol[1]*, Doctor of Technical Science, Professor, Corresponding Member of the National Academy of Science of Ukraine,*
O.G. Gryb[1]*, Doctor of Technical Science, Professor,*
S.V. Shvets[2]*, Candidate of Technical Science, Associate Professor,*
[1] National Technical University «Kharkiv Polytechnic Institute», 21, Frunze Str., Kharkiv, 61002, Ukraine.
[2] O.M. Beketov National University of Urban Economy in Kharkiv,
17, Marshal Bazhanov Str., Kharkiv, 61002, Ukraine,
phone +380 67 7680838, e-mail: se_sx@bk.ru

How to cite this article:
Sokol E.I., Gryb O.G., Shvets S.V. The structural and parametrical organization of elements of a power supply system in the conditions of network centrism. *Electrical engineering & electromechanics*, 2016, no.2, pp. 61-64. doi: 10.20998/2074-272X.2016.2.11.

UDC 621.315 **doi: 10.20998/2074-272X.2016.2.12**

E.I. Sokol, M.M. Rezinkina, O.G. Gryb, V.I. Vasilchenko, A.A. Zuev, A.V. Bortnikov, E.V. Sosina

A METHOD OF COMPLEX AUTOMATED MONITORING OF UKRAINIAN POWER ENERGY SYSTEM OBJECTS TO INCREASE ITS OPERATION SAFETY

The paper describes an algorithm of the complex automated monitoring of Ukraine's power energy system, aimed at ensuring safety of its personnel and equipment. This monitoring involves usage of unmanned aerial vehicles (UAVs) for planned and unplanned registration status of power transmission lines (PTL) and high-voltage substations (HVS). It is assumed that unscheduled overflights will be made in emergency situations on power lines. With the help of the UAV, pictures of transmission and HVS will be recorded from the air in the optical and infrared ranges, as well as strength of electric (EF) and magnetic (MF) fields will be measured along the route of flight. Usage specially developed software allows to compare the recorded pictures with pre-UAV etalon patterns corresponding to normal operation of investigated transmission lines and the HVSs. Such reference pattern together with the experimentally obtained maps of HVS's protective grounding will be summarized in a single document – a passport of HVS and PTL. This passport must also contain the measured and calculated values of strength levels of EF and MF in the places where staff of power facilities stay as well as layout of equipment, the most vulnerable to the effects of electromagnetic interference. If necessary, as part of ongoing monitoring, recommendations will be given on the design and location of electromagnetic screens, reducing the levels of electromagnetic interference as well as on location of lightning rods, reducing probability lightning attachment to the objects. The paper presents analytic expressions, which formed the basis of the developed software for calculation of the EF strength in the vicinity of power lines. This software will be used as a base at UAV navigation along the transmission lines, as well as to detect violations in the transmission lines operation. Comparison of distributions of EF strength calculated with the help of the elaborated software with the known literature data has been presented also. The difference between the proposed method of monitoring and the existing methods is full automation of the complex control of a number of parameters characterizing the state of the external power grid facilities, as well as its basic electrical parameters. This will be possible due to usage of specially developed software for recognition of optical and infrared images, as well as pictures of lines of equal EF and MF strength. References 12, figures 4.

Key words: **power line, electric and magnetic fields, automated monitoring, unmanned aerial vehicles.**

Статья посвящена описанию алгоритма комплексного автоматизированного мониторинга объектов энергетической системы Украины, направленного на обеспечение безопасности функционирования ее оборудования и персонала. Данный мониторинг предполагает использование беспилотных летательных аппаратов (БПЛА) для плановой и внеплановой регистрации состояния линий электропередачи (ЛЭП) и высоковольтных подстанций (ВП). Предполагается, что внеплановые облеты будут производиться при аварийных ситуациях на ЛЭП. С помощью БПЛА будут записываться с воздуха картины ЛЭП и ВП в оптическом и инфракрасном диапазонах, а также измеряться напряженности их электрического (ЭП) и магнитного (МП) полей вдоль трассы пролета. Использование специально разработанного программного обеспечения позволит сравнить регистрируемые БПЛА картины с предварительно созданными эталонными картинами, соответствующих штатным режимам работы контролируемых ЛЭП и ВП. Такие эталонные картины в совокупности с экспериментально полученными картами защитных заземлений ВП будут сведены в единый документ – паспорт ВП и ЛЭП. Данный паспорт должен содержать также измеренные и рассчитанные значения уровней напряженностей ЭП и МП в местах пребывания персонала энергетических объектов и расположения оборудования, наиболее уязвимого к воздействию электромагнитных помех. При необходимости в рамках выполнения проводимого мониторинга будут даны рекомендации по конструкции и расположению электромагнитных экранов, снижающих уровни электромагнитных воздействий, и молниеотводов, уменьшающих вероятность поражения молнией исследуемых объектов. В работе приводятся аналитические выражения, которые легли в основу разработанного программного обеспечения для расчета напряженности ЭП в окрестности ЛЭП. Данное программное обеспечение будет использовано в качестве базового при навигации БПЛА вдоль ЛЭП, а также для распознавания нарушений в работе ЛЭП. Приведено также сравнение зависимостей напряженности ЭП, рассчитанных с помощью данного программного обеспечения, с данными, известными из литературы. Отличие предлагаемой методики мониторинга от существующих состоит в том, что комплексный контроль ряда параметров, характеризующих внешнее состояние объектов энергосистемы, а также ее основных электрических параметров будут полностью автоматизированы. Это станет возможным в результате использования специально разработанного программного обеспечения по распознаванию оптических и инфракрасных изображений, а также картин линий равной напряженности ЭП и МП. Библ. 12, рис. 4.

Ключевые слова: **линии электропередачи, электрическое и магнитное поле, автоматизированный мониторинг, беспилотные летательные аппараты.**

Introduction. Currently, the problem of guaranteeing the energetic security of Ukraine is very important. Here, the monitoring of the state of electrical energy transmission systems from producer to electrical customer is extremely important. Such a monitoring should be directed to prevent emergency switching of power transmission lines (PTL) as well as to recover as soon as possible their working capacity if such a switching takes place.

One of more perspective modern methods of the PTL state diagnosing is monitoring by using unmanned aerial vehicles (UAVs). Such a monitoring is developed in Russian Federation (RF) [1], as well as in Europe [2], China [3], Brazil [4] and other countries. Here, the PTL state check is carried out by the way of its optical registration, registration by using infrared imagers, as well as registration of partial discharges taking place in insulation.

As analysis of reasons of PTL faults in RF which power network is rather like Ukrainian one shows they take place mainly on PTL 110 kV – 86 %, 11 % – PTL 220 kV, and 3 % – PTL 330-750 kV [1]. Such a distribution of fault numbers is proportionate to the corresponding PTL length. Most number of PTL faults in RF is resulted by damage of wires and lighting guard ropes – 56 %. Other reasons of PTL faults are such damages as insulator breakdowns – 19 %, tower damage – 15 %, and damage of other PTL elements – 10 %. In the correspondence with present statistics sharp increase of PTL faults takes place in spring and summer because of bridging of insulation gaps by green plantations. There are a lot of PTL faults because of vandalism such as insulator chain damage, theft of wires and PTL tower elements, throwing over on PTL wires, etc. [1].

Problem definition. From above-stated it is following that on-line testing of the state of PTL as well as high-voltage substations which represent an integral part of the power-supply system and removal of the fault sources can be very effective. The aim of this paper is to develop an algorithm of the complex automated monitoring of objects of the power network of Ukraine directed to guarantee its safety operation.

Materials of investigations. An algorithm to carry out monitoring of objects of the power network of Ukraine. Patented engineering solutions are known which aim is to guarantee the traffic control of UAVs by using electric field (EF) strength or magnetic field (MF) strength [5, 6]. These solutions can be used to develop a method of monitoring of objects of the power network of Ukraine safety. Such a method envisages creation of passports – etalon patterns describing PTL and substations operation in normal mode. Passport data – etalons should include optical images of investigated objects and their images in infrared band obtained by infrared imagers. Besides, such passports should include distributions of electric and magnetic fields strength obtained by using calculations and measurements in determined distances over the PTL as well as in determined distances under high-voltage substations. It is supposed that UAVs with given periodicity will carry out aerophotography of investigated objects in optical and infrared bands as well as to measure their EF and MF strength. It is supposed that extraordinary flies will be carried out at PTL faults to determine place and character of damage. Comparison by the developed software of data collected during UAVs' flies with passport data as investigated object's etalon will permit to take operative decisions on its current state: to remote arose failures which presence can result in faults, or to find places of faults if it was impossible to avoid them.

Utilization of an unmanned system to compare most important parameters describing normal operation of investigated objects (PTL and high-voltage substations) will also prevent illegal power takeoff from the power network. Analysis of such parameters can be used for optimization of operation modes as well as structure of investigated energetic objects.

Besides, such passports should include maps of placement of high-voltage substations' systems of protective grounding which play a key role to guarantee safety operation of personnel and equipment. Here, such maps should be obtained as a result of MF strength measurements during the current flow by protective grounding. To obtain reliable information on actual state of the protective grounding system (PGS) it is proposed to connect a current generator to it and measure the MF density over the earth surface. The map obtained in such a way will reflect real placement of the protective grounding system's elements. It will give a possibility to assess the reliability of protection of the investigated object by the protective grounding system at various short-circuit failures and, if necessary, to develop recommendations on restoration of damaged parts of the PGS as well as on its development and modernization. Obtained in such a way data on placement of elements of the protective grounding system are used as initial data for the developed software which permits to build distributions of equipotential lines and EF strength on the earth surface, to determine levels of step voltages and touch voltages as well as impedance of the grounding system. By these distributions conclusions on the reliability of the existing protective grounding systems are done. If necessary, in the frame of the carried out monitoring recommendations on the design and placement of electromagnetic shields utilization of which permits to decrease electromagnetic exposures level will be made [7].

The next important system which secures safety operation of energetic systems is their lightning protection system. By the developed software using the method [8] distributions of probability of lightning hit on the high-voltage substations' territory will be built and, if necessary, recommendations on development and modernization of existing lightning protection system will be given.

By using maps of EF and MF strength distributions at PTL and high-voltage substations operation obtained as a result of measurements and calculations of the EF and MF strength as well as by using reliable maps of the protective grounding systems, plans of the safety movement of the high-voltage substations' technical personnel and placement of equipment especially sensitive for possible electromagnetic exposures will be prepared.

To develop the monitoring system of the energetic system objects' safety, methods for EF and MF strength calculation are necessary. Here, at the absence of the personnel in the EF exposure zone analytical methods can be used.

The main parameter which characterizes the PTL electromagnetic field and does not depend on the kind of the PTL load is the EF strength. Let's describe in detail principles of the developing the software used to realize the proposed method of the complex monitoring of energetic system's objects.

Analytical methods of PTL EF calculation.

To use analytical methods for the PTL electrical field strength calculation the following assumptions should be taken:

- it is supposed that PTL wires are parallel infinite long cylinders which charge is uniformly distributed along their axes;
- voltage in the PTL wires changes by the sinusoidal low with frequency of 50 Hz;
- phase displacement in time between PTL wires' voltages equals 120°;
- the earth surface is supposed flat, and earth proper is supposed absolutely conductive in the comparison with air and having zero potential;
- presence of towers, buildings, technical and biological objects in the PTL zone is not taken into account;
- presence of additional strands (lightning protective, compensative, etc.) is not taken into account;
- it is supposed that the PTL wires are in the air with relative dielectric capacitivity equals $\varepsilon_e = 1$;
- root-mean-square values of the electric field strength are determined near a plain which is perpendicular to the PTL wires' direction in the area of the maximal wires approaching to the earth.

At the mentioned assumptions values of potentials, specific charges and EF strength can be written in the symbolic form for complex quantities, and the electric field can be presented as a sum of the PTL wires' electric fields and their mirror images relatively the earth surface [9, p. 84, 93].

Typical cases of the PTL wires placements are shown in Fig. 1.

If PTL wires are bundle the equivalent wire's radius is calculated by the formula [9, p. 42]:

$$r = \left(M \cdot r_{ph} \cdot a^{M-1}\right)^{\frac{1}{M}},$$

where M – number of bundle wires of the PTL phases; r_{ph} – radius of the PTL phases wires' section [m]; a – radius of the circle on which PTL bundle phases are placed [m].

In the general case of the arbitrary placement of the PTL wires the capacity value per the unit of length is calculated by the formula [10, p. 96]:

$$C_S = \frac{2\pi\varepsilon_r\varepsilon_0}{\ln\left[2\frac{\sqrt[3]{h_1 \cdot h_2 \cdot h_3}}{r} \cdot \frac{\sqrt[3]{r_{12} \cdot r_{23} \cdot r_{31}}}{\sqrt[3]{r_{12'} \cdot r_{23'} \cdot r_{31'}}}\right]},$$

where h_1, h_2, h_3 – distances from the earth surface to each PTL wire; r_{12}, r_{23}, r_{31} – distances between PTL wires; $r_{12'}$, $r_{23'}$, $r_{31'}$ – distances between PTL wires and their mirror images.

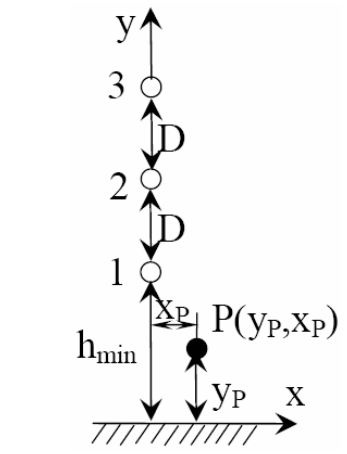

a

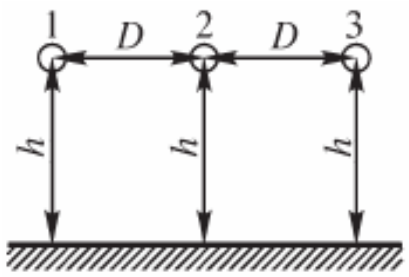

b

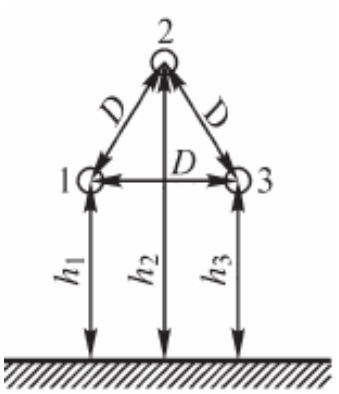

c

Fig. 1. Typical cases of the PTL wires placements

In the case of the vertical placement of PTL wires as it is shown in Fig. 1,*a* the PTL capacity per the unit of length is calculated by the formula:

$$C_S = \frac{2\pi\varepsilon_r\varepsilon_0}{\ln\left[\frac{2D\sqrt[3]{2}}{r} \cdot \sqrt[3]{\frac{h_{\min} \cdot (h_{\min} + D) \cdot (h_{\min} + 2D)}{(2h_{\min} + D) \cdot (2h_{\min} + 2D) \cdot (2h_{\min} + 3D)}}\right]}$$

where D – distance between PTL wires [m]; $h_{\min}$ – minimal distance between PTL wires and earth ($h_{\min} = \min\{h_1, h_2, h_3\}$) [м]; ε_r – relative dielectric permeability of the medium (air) in which the PTL wires are; $\varepsilon_0 = 0.885 \cdot 10^{-9}$ F/m – electrical constant.

In the case of the horizontal placement of PTL wires as it is shown in Fig. 1,*b* the PTL capacity per the unit of length is calculated by the formula [10, p. 96]:

$$C_S = \frac{2\pi\varepsilon_r\varepsilon_0}{\ln\left[\dfrac{2h_{\min}\cdot D}{r\cdot\sqrt[3]{(4h_{\min}^2+D^2)\cdot\sqrt{h_{\min}^2+D^2}}}\right]}.$$

In the case of the PTL wires placement in the apexes of the equilateral triangle as it is shown in Fig. 1,*c* the PTL capacity per the unit of length is calculated by the formula:

$$C_S = \frac{2\pi\varepsilon_r\varepsilon_0}{\ln\left[\dfrac{2D}{r}\cdot\sqrt[3]{\dfrac{h_{\min}^2\cdot(h_{\min}+D\sqrt{3}/2)}{\sqrt{(4h_{\min}^2+D^2)}\cdot[(2h_{\min}+D\sqrt{3}/2)^2+D^2/4]}}\right]}.$$

Complex values of the azimuthal and axial components of the PTL EF strength in the point $P(x_p, y_p)$ (see Fig. 1,*a*) are calculated by formulae [9, p. 68]:

$$\dot{E}_x(x_P,y_P)=\frac{U_{ph}\cdot C_S}{2\pi\varepsilon_r\varepsilon_0}\times$$
$$\times\left[\begin{array}{l}-\left[\dfrac{x_1-x_P}{(x_1-x_P)^2+(h_1+y_P)^2}-\dfrac{x_1-x_P}{(x_1-x_P)^2+(h_1-y_P)^2}\right]+\\ +\left(\dfrac{1}{2}+j\dfrac{\sqrt{3}}{2}\right)\cdot\left[\dfrac{x_2-x_P}{(x_2-x_P)^2+(h_2+y_P)^2}-\dfrac{x_2-x_P}{(x_2-x_P)^2+(h_2-y_P)^2}\right]+\\ +\left(\dfrac{1}{2}-j\dfrac{\sqrt{3}}{2}\right)\cdot\left[\dfrac{x_3-x_P}{(x_3-x_P)^2+(h_3+y_P)^2}-\dfrac{x_3-x_P}{(x_3-x_P)^2+(h_3-y_P)^2}\right]\end{array}\right];$$

$$\dot{E}_y(x_P,y_P)=\frac{U_{ph}\cdot C_S}{2\pi\varepsilon_r\varepsilon_0}\times$$
$$\times\left[\begin{array}{l}-\left[\dfrac{h_1+y_P}{(x_1-x_P)^2+(h_1+y_P)^2}+\dfrac{h_1-y_P}{(x_1-x_P)^2+(h_1-y_P)^2}\right]+\\ +\left(\dfrac{1}{2}+j\dfrac{\sqrt{3}}{2}\right)\cdot\left[\dfrac{h_2+y_P}{(x_2-x_P)^2+(h_2+y_P)^2}+\dfrac{h_2-y_P}{(x_2-x_P)^2+(h_2-y_P)^2}\right]+\\ +\left(\dfrac{1}{2}-j\dfrac{\sqrt{3}}{2}\right)\cdot\left[\dfrac{h_3+y_P}{(x_3-x_P)^2+(h_3+y_P)^2}+\dfrac{h_3-y_P}{(x_3-x_P)^2+(h_3-y_P)^2}\right]\end{array}\right].$$

Root-mean-square value of the electric field strength in the point $P(x_p, y_p)$ is calculated by the formula:

$$E(x_P,y_P)=\sqrt{\left|\dot{E}_x(x_P,y_P)\right|^2+\left|\dot{E}_y(x_P,y_P)\right|^2},$$

where $\left|\dot{E}_x(x_P,y_P)\right|$, $\left|\dot{E}_y(x_P,y_P)\right|$ – modules of the complex values of the azimuthal and axial components of the PTL EF strength in the point $P(x_p, y_p)$.

On the base of these formulae a software permitting to calculate EF strength in the PTL vicinity is developed. Comparison of root-mean-square values obtained by using this software with data from [11] are presented in Fig. 2,*a*, 3,*a* and Fig. 2,*b*, 3,*b*, respectively. In Fig. 4,*a*, 4,*b* the same comparison with data from [12] is presented.

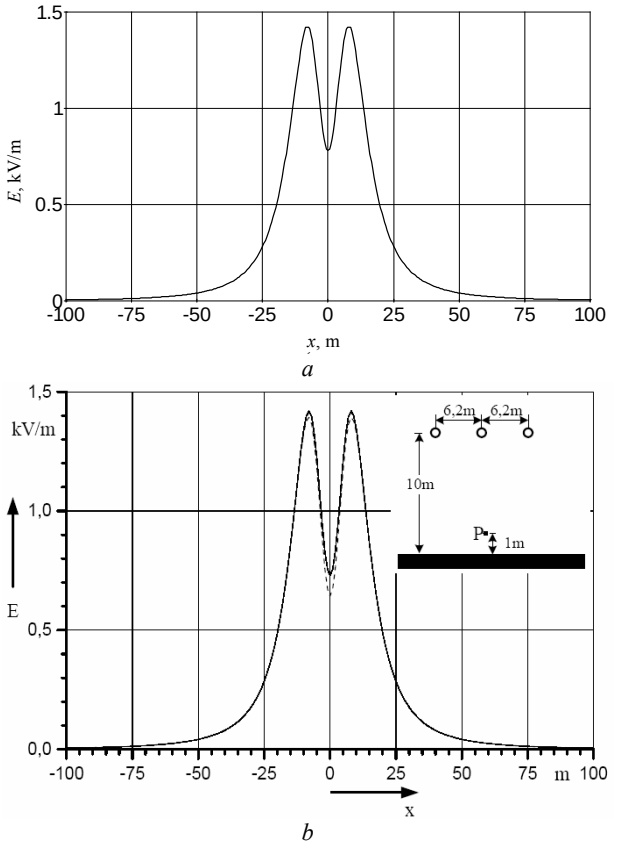

Fig. 2. Calculated dependences of the EF strength in the section perpendicular to the wires of the PTL 150 kV on the distance of 1 m from the earth surface

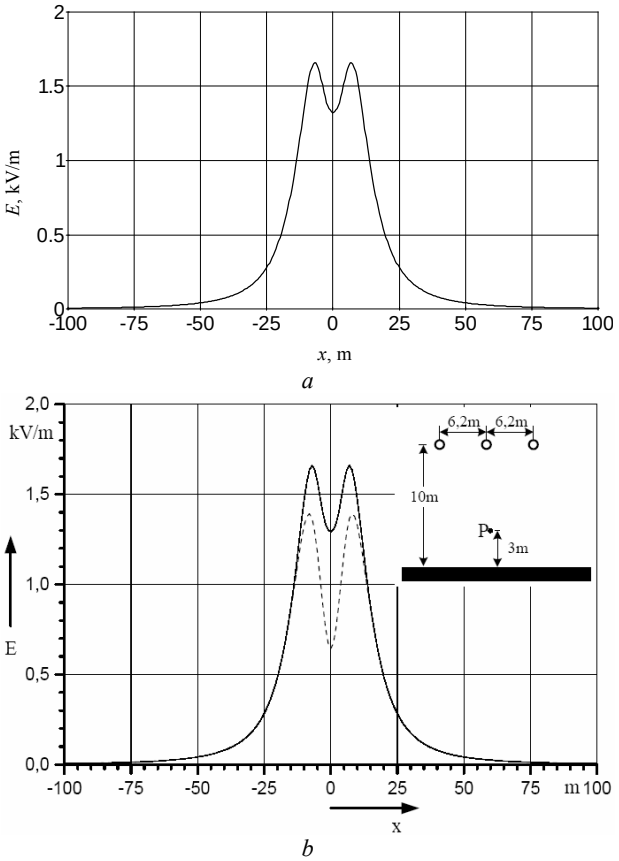

Fig. 3. Calculated dependences of the EF strength in the section perpendicular to the wires of the PTL on the distance of 3 m from the earth surface

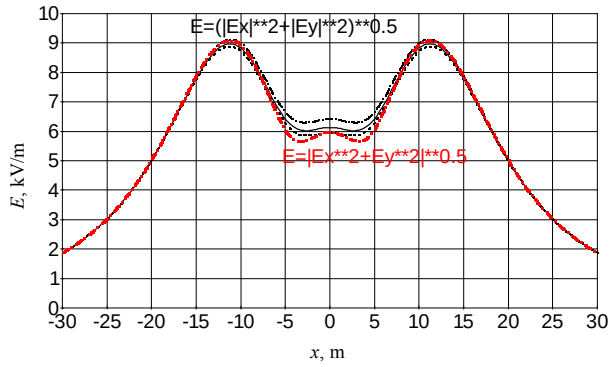

a

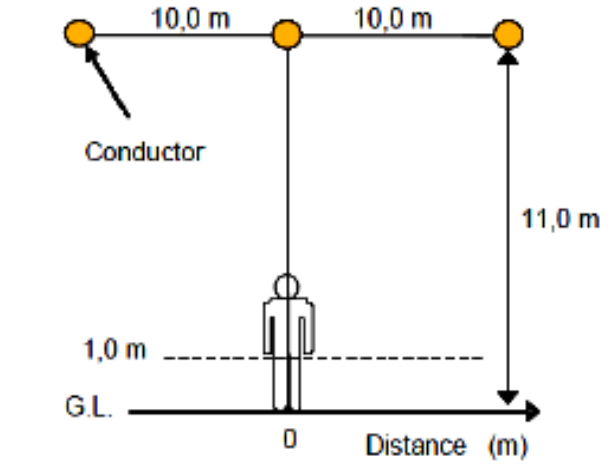

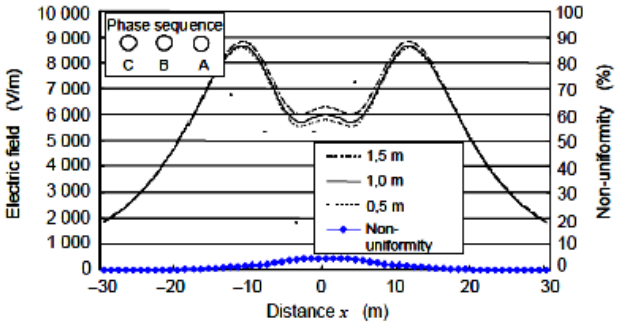

b

Fig. 4. Calculated dependences of the EF strength in the section perpendicular to the wires of the PTL 500 kV on the distances of 0.5 m, 1 m, 1.5 m from the earth surface

Conclusions.

1. A method of complex automated monitoring of PTL and high-voltage substations representing key elements of power supply system of Ukraine is developed.

2. A software for calculation of the EF in PTL vicinity is developed and tested. This software is necessary for the navigation of UAVs – the main element of the described monitoring system as well as for assessment of electrical parameters of investigated energetic objects.

REFERENCES

1. Arbuzov R.S., Ovsyannikov A.G. *Sovremennye metody diagnostiki vozdushnykh linii elektroperedachi* [Modern methods of diagnostics of overhead power lines]. Novosibirsk, Nauka Publ., 2009. 136 p. (Rus).

2. Skarbek L., Zak A., Ambroziak D. Damage detection strategies in structural health monitoring of overhead power transmission system. *7th European Workshop on Structural Health Monitoring (EWSHM)*, July 8-11, 2014. La Cité, Nantes, France. pp. 663-670.

3. Li L. The UAV intelligent inspection of transmission lines. *Proceedings of the 2015 International Conference on Advances in Mechanical Engineering and Industrial Informatics*, 2015. pp. 1542-1545. **doi: 10.2991/ameii-15.2015.285**.

4. Geraldo J. Adabo. Unmanned aircraft system for high voltage power transmission lines of Brazilian electrical system. *AUVSI Unmanned Systems*, vol.1, pp. 1556-1563, 12-15 August 2013, Washington, DC, USA. ISBN 78-1-62993-324-5.

5. Kachesov V.E., Lebedev D.E. *Sposob diagnostiki vyisokovoltnoy linii elektroperedachi* [A method for diagnosing a high-voltage power lines]. Patent Russian Federation, no. 2421746, 2011. (Rus).

6. Kachesov V.E., Lebedev D.E. *Sposob aerodiagnostiki vyisokovoltnoy linii elektroperedachi* [Air diagnostic method of high voltage transmission lines]. Patent Russian Federation, no. 2483314, 2013. (Rus).

7. Shcherba A.A., Rezinkina M.M. *Modelirovanie i analiz elektricheskih poley energeticheskih ob'ektov* [Modeling and analysis of electric field energy facilities]. Kiev, Naukova Dumka Publ., 2008. 248 p. (Rus).

8. Rezinkina M.M. Technique for predicting the number of lightning strokes to extended objects. *Technical physics*, 2008, vol.53, no.5, pp. 533-539. **doi: 10.1134/s1063784208050010**.

9. Bessonov V.A. *Elektromagnitnaya sovmestimost* [Electromagnetic compatibility]. Khabarovsk, DVGUPS Publishing house, 2000. 80 p. (Rus).

10. Demirchian K.S., Neiman L.R., Korovkin N.V., Chechurin V.L. *Teoreticheskie osnovyi elektrotehniki. Tom 3* [Theoretical foundations of electrical engineering. Vol. 3]. Moscoe, Piter Publ., 2006. 377 p. (Rus).

11. Tzinevrakis A.E., Tsanakas D.K., Mimos E.I. Analytical Calculation of the Electric Field Produced by Single-Circuit Power Lines. *IEEE Transactions on Power Delivery*, vol.23, no.3, pp. 1495-1505. **doi: 10.1109/tpwrd.2008.916748**.

12. Anamarija Juhas, Miodrag Milutinov, Neda Pekarić-Nad. Primena Monte Karlo metode za procenu merne nesigurnosti proračuna električnog i magnetskog polja nadzemnih i podzemnih vodova. Available at: http://deet.ftn.uns.ac.rs/files/tehres/TR_2012_Juhas_Milutinov_Pekaric.pdf (Accessed 12 September 2013). (Srb).

Received 16.10.2015

E.I. Sokol[1], *Doctor of Technical Science, Professor, Corresponding Member of the National Academy of Science of Ukraine,*
M.M. Rezinkina[2], *Doctor of Technical Science,*
O.G. Gryb[1], *Doctor of Technical Science, Professor,*
V.I. Vasilchenko[3],
A.A. Zuev[1], *Candidate of Technical Science, Associate Professor,*
A.V. Bortnikov[1], *Engineer,*
E.V. Sosina[1], *Postgraduate Student,*
[1] National Technical University «Kharkiv Polytechnic Institute»,
21, Frunze Str., Kharkiv, 61002, Ukraine,
e-mail: elenasosina09@gmail.com.

[2] State Institution «Institute of Technical Problems of Magnetism of the NAS of Ukraine»,
19, Industrialna Str., Kharkiv, 61106, Ukraine,
e-mail: marinar2@mail.ru.
[3] NPC «Ukrenergo»,
25, Symona Petliury Str, Kyiv, 01032, Ukraine,
phone +380 44 2383015, e-mail: kanc@nec.energy.gov.ua

How to cite this article:
Sokol E.I., Rezinkina M.M., Gryb O.G., Vasilchenko V.I., Zuev A.A., Bortnikov A.V., Sosina E.V. A method of complex automated monitoring of Ukrainian power energy system objects to increase its operation safety. *Electrical engineering & electromechanics*, 2016, no.2, pp. 65-70. doi: 10.20998/2074-272X.2016.2.12.

UDC 316 **doi: 10.20998/2074-272X.2016.2.13**

V.I. Gurevich

THE PROBLEM OF CORRECT CHOICE OF FERRITE BEADS

A ferrite bead is a passive electrical element used to suppress high-frequency noise in electric circuits. This is one of the simplest and the cheapest type of filters. Thus, such filters are widely used in electric and electronic apparatus for both domestic and industrial purposes. It would seem that such a wide application of these elements suggests that methods for their correct selection and use are well-defined. However, this is not quite true. Table 1, figures 11.
Key words: **ferrite, filters, electromagnetic pulse.**

Ферритовый фильтр – пассивный электрический компонент, использующийся для подавления высокочастотных помех в электрических цепях. Это один из самых простых и дешёвых типов фильтров. Очевидно, именно поэтому фильтры такого типа нашли самое широкое применение в электронной и электротехнической аппаратуре как бытового, так и промышленного назначения. Казалось бы, при такой широкой распространенности этих элементов методика их правильного выбора и применения должна быть хорошо всем известна. Увы, на самом деле все оказалось не так просто. Табл. 1, рис. 11.
Ключевые слова: **ферриты, фильтры, электромагнитный импульс.**

The ferrite bead is the simplest type of the filter: it is characterized by low cost and significant attenuation of short electromagnetic pulses (similar to high-frequency signal) in conductors connected to electronic apparatus. It is shaped as a ring (cylinder) filter put on the conductor (see Fig. 1).

Fig. 1. Ferrite Elements (FE) of Ferrite Bead Filters

The impedance of the winding consists of one or several turns of a control cable run through the ferrite ring and is too low both for low-frequency operating signals and for commercial frequency alternating current At the same time it is too high for high-frequency (short pulse) signals within the selected frequency range which depends on the number of turns, material and size of the ring itself. This results in significant attenuation of pulse and high-frequency noise penetrating such cables. Attenuation provided by such filters is in the range of 10-15 dB.

Numerous companies manufacture dozens of such filter types both miniature, designed to be installed on the printed circuit boards inside the apparatus (see Fig. 2), and those suitable for the installation on the conductor (cable) itself. For the sake of installation convenience such filters are often made as two matching semi-rings (semi-cylinders) located in snap-in plastic covers. This provides fast and convenient installation of the filters on the conductors (see Fig. 3).

Fig. 2. Miniature Filters Built Based on Ferrite Elements (FE) and Designed for Installation on a Printed Circuit Board

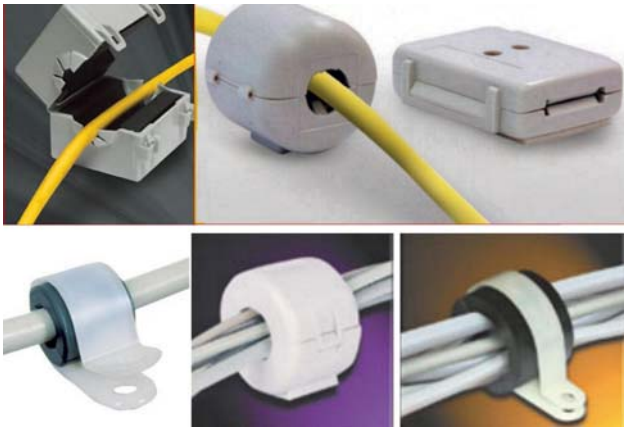

Fig. 3. Design of Ferrite Beads Providing Fast and Convenient Installation on Conductors

Such filters can be widely used in electronic equipment: in control circuits, in circuits of logical and pulse signal transmission, and in communication circuits (see Fig. 4).

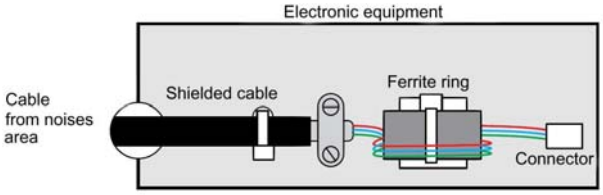

Fig. 4. Ferrite Ring Filter Installed on a Control Cable Entering the Electronic Equipment

FE-based filters are manufactured by numerous companies as given in Table 1.

Frequency ranges shown in Table 1 do not correspond to the certain filter type, but describe the frequency area provided by certain companies. Actual frequency ranges of certain filter types are much lower than shown in Table 1. Fig. 5 shows examples of frequency ranges of different types of materials used in FE manufactured by Fire-Rite Products Corp.

Table 1

Frequency Response of FE-based Filters Manufactured by Different Companies

Company name	Frequencies intervals for filters produced by companies, MHz
Fire-Rite Products Corp.	1 – 1000
Ferrishield	30 – 2450
Ferroxcube	0.2 – 200
Murata	Miniature filters for PCB mounting
NEC/Tokin	0.1 – 300
Parker Chomerics	30 – 200
Laird	30 – 2000
TDK	10 –500
Leader Tech, Inc	1 – 2450
Wurth Elektronik	Miniature filters for PCB mounting

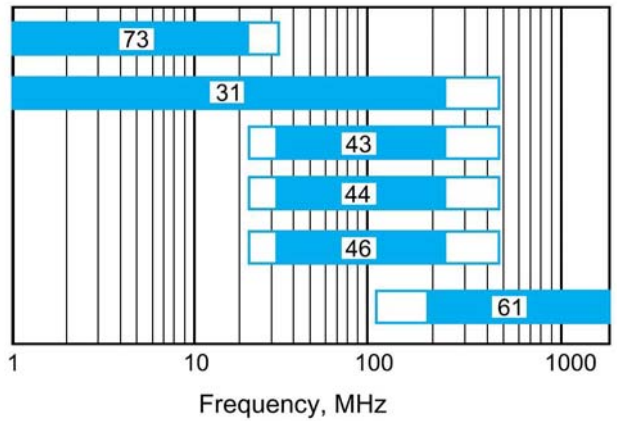

Fig. 5. Frequency Ranges of Different Material Types (designated by numbers) used in FE Manufactured by Fire-Rite Products Corp.

Despite the apparent simplicity and cheapness (1-10 USD) ferrite filters are not as simple as they seem. Their effectiveness depends on the numerous parameters, such as: material type, equivalent frequency of current pulse to be attenuated, size of FE, number of turns of the conductor passed-through the FE, the value of the DC-component in the conductor, temperature, etc.

The frequency response of the filter depends on several parameters, primarily on the FE material type. Manganese-zinc ferrites (Mn-Zn) with relative magnetic permeability (magnetic inductive capacity) $\mu = 600 – 20.000$ are usually used for frequency range of 0.1 MHz – 2 MHz, and for 1MHz – 2.45 GHz – nickel zinc ferrites (Ni – Zn) with relative magnetic permeability $\mu = 15 – 2000$ are used. Different ferrite mixes are also used during the manufacture.

Apart from the frequency response the impedance – is another very important parameter of FE-based filter. It defines the level of noise suppression.

To a large extent the impedance of FE-based filter is also determined by the type of material used and by the operating frequency (see Fig. 6).

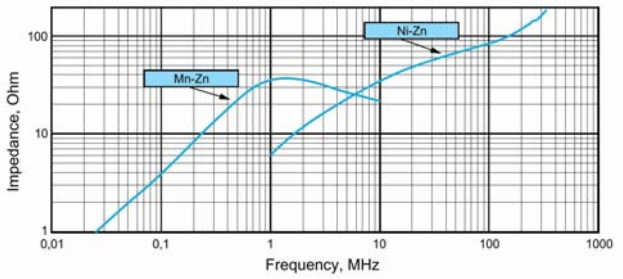

Fig. 6. Dependency of the Impedance of FE-based Filter on the Material Type and Frequency

As FE-filter has inductance, capacitance and active resistance (see Fig. 7), it is apparent that filter frequency response and impedance also depend on FE size (particularly on its length, see Fig. 8).

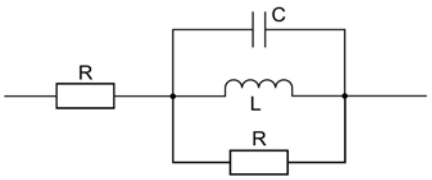

Fig. 7. Equivalent Circuit of FE-based Filter

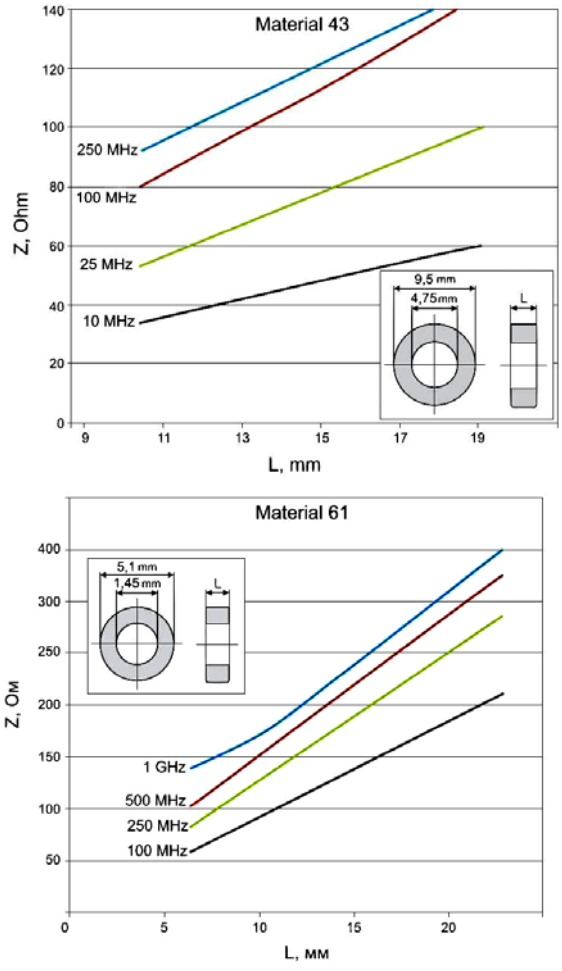

Fig. 8. Dependence of Filter Impedance Z on the Ferrite Element Length L made of two types of material (43 and 61) manufactured by the Fire-Rite Products Corp.

As shown in Fig. 8, the filters having longer FE always have higher impedance with all other parameters being equal. This results from higher inductance of filters with long FE.

To a large extent the impedance of FE-based filters also depends on the number of wire turns passed through the FE (see Fig. 9). As shown in Fig. 9 the starting impedance of the filter with several wire turns is great compared to the one-turn filter. However, the further increase in noise frequency makes filters with several turns less effective compared to filters with one turn which can result from the higher capacitance of the filter with several turns.

Also, FE-based filters have another unpleasant characteristic: their properties depend on the value of the DC-component of the passing current (see Fig. 10). This results from the change of FE magnetic properties under the existence of the DC-component of the current.

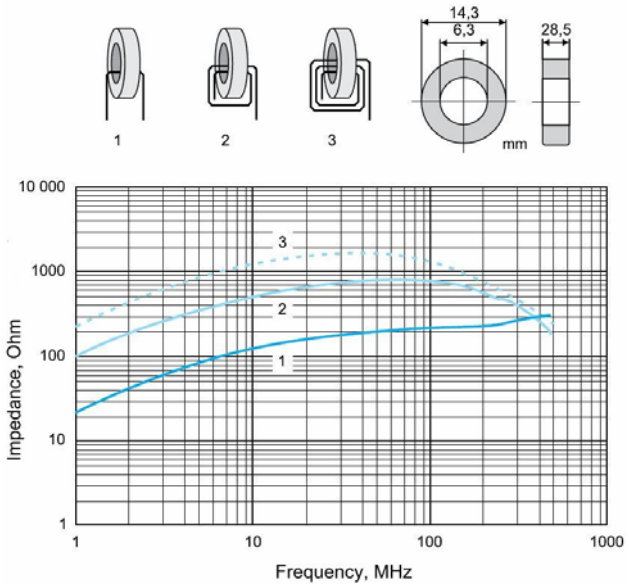

Fig. 9. Typical Dependency of Filter Impedance on the Number of Turns (designated as 1-3) Passed through the FE

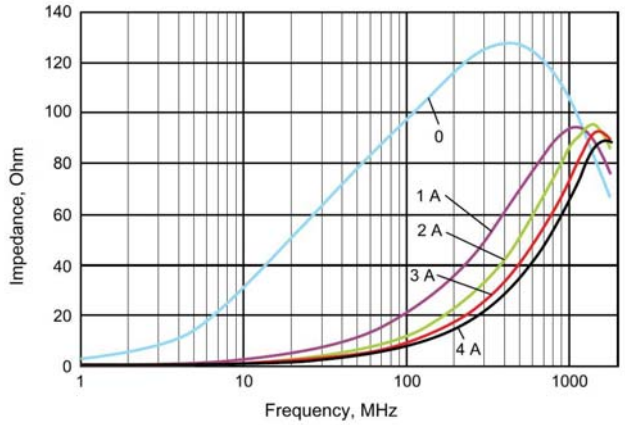

Fig. 10. Influence of the DC-component on Filter Characteristics

The presence of inductance and capacitance in the filter equivalent circuit (see Fig. 7) provokes the hazard of resonance under the certain frequencies. This can lead to another problem of such filters – such as amplification of noise instead of its attenuation.

So, if there are so many factors influencing the filter parameters, what are the basics to correctly select the filter ensuring effective protection against electromagnetic noise under a wide frequency range? It is tricky. This is especially due to 1) unavailability of standards unifying the procedure for measuring the parameters of such filters, and 2) different methods of measurement used by different manufacturers. Due to all these problems it is almost impossible to compare the parameters of filters produced by different manufacturers.

According to the above analysis the following method for the correct selection of FE-based filter can be recommended:

1. In order to ensure the effective noise suppression within the maximum frequency range it is required using at least three in-series filters installed on the same conductor (cable). Such filters should be made of different materials providing maximum filter impedance within low- (0.1 MHz), medium- (300 to 500 MHz) and high-frequency range (2 to 2.45 GHz). Three filters installed in-series on the same conductor also allows for eliminating the resonance, as they have different characteristics and thus significantly different resonant frequencies.

2. Manufacturer data can be used only for preliminary filter selection. Afterwards it is required to test the noise suppression effectiveness within the full frequency and current range needed for the customer.

This test can be done on the unit consisting of the high-frequency pulse generator simulating the noise signal within the actual frequency range, and of the receiving unit, such as oscilloscope, spectral analyzer or electronic voltmeter with the extended frequency range. The generator should be connected to the input of the receiver using the cable equipped with the filters (see Fig. 11). The measured generator output voltage within the required frequency spectrum (with and without filters installed on the cable) characterizes the value of signal attenuation on the filters and enables selecting the proper set of filters providing necessary attenuation of high-frequency signal, as well as ensuring that there is no resonance within the full frequency operating range.

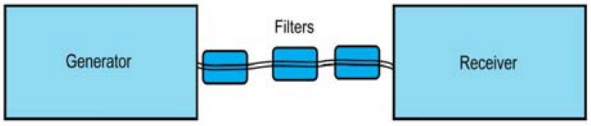

Fig. 11. Test Unit Designed to Check the FE-based filter effectiveness

Received 19.10.2015

Vladimir I. Gurevich, Ph.D, Senior specialist,
Central Electric Laboratory of Israel Electric Corp.
31000, Israel, Haifa, POB 10,
e-mail: vladimir.gurevich@gmx.net

How to cite this article:
Gurevich V.I. The problem of correct choice of ferrite beads. *Electrical engineering & electromechanics*, 2016, no.2, pp. 71-73. doi: 10.20998/2074-272X.2016.2.13.